

NORTHWEST FISHERIES CENTER
PROCESSED REPORT
JULY 1976

PHYSICAL OCEANOGRAPHY
OF THE GULF OF ALASKA

by

W. J. Ingraham, Jr., A. Bakun and F. Favorite

FINAL REPORT
RU-357

ENVIRONMENTAL ASSESSMENT of the ALASKAN CONTINENTAL SHELF

Sponsored by

UNITED STATES DEPARTMENT OF INTERIOR
Bureau of Land Management



Prepared by:
Northwest Fisheries Center
National Marine Fisheries Service
2725 Montlake Boulevard E.
Seattle, Washington 98112

NOTICE

This document is being made available in .PDF format for the convenience of users; however, the accuracy and correctness of the document can only be certified as was presented in the original hard copy format.

Inaccuracies in the OCR scanning process may influence text searches of the .PDF file. Light or faded ink in the original document may also affect the quality of the scanned document.

NORTHWEST FISHERIES CENTER

PROCESSED REPORT

JULY 1976

PHYSICAL OCEANOGRAPHY OF THE GULF OF ALASKA

by

W. J. Ingraham, Jr., A. Bakun and F. Favorite

FINAL REPORT

RU - 357

ENVIRONMENTAL ASSESSMENT of the ALASKAN CONTINENTAL SHELF

Sponsored by

UNITED STATES DEPARTMENT of INTERIOR

Bureau of Land Management

Prepared by:
Northwest Fisheries Center
National Marine Fisheries Service
2725 Montlake Boulevard E.
Seattle, Washington 98112

CONTENTS

	<u>Page</u>
I. INTRODUCTION.....	1
II. WATER PROPERTIES.....	7
A. Temperature.....	7
B. Salinity.....	19
C. Water Masses.....	27
III. CURRENTS.....	33
A. Drift Studies.....	34
B. Geostrophic Flow.....	39
C. Volume Transport.....	48
IV. WIND-STRESS TRANSPORTS.....	51
A. Pressure Fields.....	51
B. Transport Fields.....	53
C. Numerical Model.....	61
V. COASTAL SEA LEVELS.....	69
A. Sea Level Pressures.....	70
B. Mean Sea Levels.....	72
C. Relation to Transport.....	77
VI. SURFACE CONVERGENCE AND DIVERGENCE.....	83
A. Vicinity of the Coastal Boundary.....	90
B. Interior of the Gulf.....	109
C. Conditions - 1973, 1974 and 1975.....	116
VII. SUMMARY AND CONCLUSIONS.....	121
VIII. ACKNOWLEDGMENTS.....	126
IX. LITERATURE CITED.....	127

PHYSICAL OCEANOGRAPHY OF THE GULF OF ALASKA

INTRODUCTION

Although extensive oceanographic investigations have been carried out in the Gulf of Alaska in the last two decades, our knowledge of actual conditions and processes and their cause and effect is still inadequate to permit any accurate short- or long-term forecasts of oceanic conditions. However, a fairly extensive data base exists, and the purpose of this report is to summarize the state of our knowledge concerning the physical environment of offshore areas of the Gulf of Alaska prior to the commencement of present OCSEAP^{1/} investigations. The Gulf of Alaska is considered to extend southward from the coast to a line from Dixon Entrance to Unimak Pass, essentially 54°N.

It should be recognized at the outset that the ocean is a turbulent regime that can be characterized only by statistical techniques based on extensive time-series data on water properties and direct current measurements collected on appropriate space scales. Such data are not available for the Gulf of Alaska area. Physical oceanographic studies up to the present time have been limited to aperiodic, widely-spaced station data of an exploratory nature obtained primarily to provide background information on general flow and ranges of environmental conditions related to specific aspects of fisheries investigations (Favorite, 1975). The most recent and comprehensive are those of the International North Pacific Fisheries Commission (INPFC). General environmental conditions in the Subarctic Pacific Region for the years 1953 to 1971 have been summarized by Dodimead, Favorite and Hirano (1963), and Favorite, Dodimead and Nasu (1975); the latter provides an extensive bibliography that is not reproduced in this

^{1/} Outer Continental Shelf Environmental Assessment Program.

report. There is also extensive but fragmentary information available in reports of results of Soviet fishing activities (e.g. Moiseev, 1963-70)^{2/}. Although the presently available station data are extensive, they are aperiodic, non-synoptic and lack the close grid spacing, wide area coverage, repetitive observations, and direct current measurements necessary to characterize the specific nature of flow.

A general assessment of oceanographic conditions can be made from knowledge of meteorology and bathymetry. With respect to water properties, we can expect seasonal changes in both temperature and salinity. Northward flow into the gulf brings unseasonably warm water into the gulf year round. Winter cooling will gradually erode the high temperatures in surface layer, but these will quickly be restored by seasonal warming in spring and summer. The vertical extent of winter cooling or convective overturn will depend on the stability of the water column, and this is affected primarily by the distribution of salinity with depth. Because there is an excess of precipitation over evaporation and extensive dilution in spring and summer from the extensive coastal watershed, a dilute surface layer can be expected to be underlain by a halocline. The readjustment of mass as a result of the general cyclonic flow around the gulf will result in a horizontal divergence and an upward vertical transfer in the center of the gulf. This is manifested in a doming or ridging of isolines of water properties in that area resulting in high salinities and low temperatures at the surface, particularly during winter when this process is most active.

There is a general eastward surface flow across the North Pacific Ocean composed of the northern sector of the anticyclonic flow in the central North Pacific gyre driven by winds associated with the Eastern Pacific high pressure system, and the southern sector of the general cyclonic flow of

^{2/} See also Bogdanov (1961), Plakhotnik (1962), and Filatova (1973).

the Subarctic Pacific gyre, driven by interactions of the Aleutian Low pressure system. This confluence and the subsequent eastward advection of meridional admixtures of subarctic and subtropic waters is subjected to various bathymetric conditions on reaching the eastern side of the ocean: first, a gradual shoaling, reducing the water column by half (from 6,000 - 3,000 m); second, the interference of numerous seamounts, (some extending to within 500 m of the surface); and, finally, an abrupt continental shelf. This results in marked changes in the fields of acceleration, vorticity and turbulence, as well as a predominant separation of flow into northward and southward components and associated disturbances of vertical strata. The northward branch, increasing in planetary vorticity, impinges on the head of the Gulf of Alaska where it is constrained by the land mass and is forced southwestward along the Alaska Peninsula. In order to accomplish this it must displace the northeastward flow into the gulf offshore, away from the continental slope. The vorticity balance of this southwestward flow is altered not only as a result of southward displacement, but also as a result of increasing depth (5,000 - 7,000 m) on encountering the eastern end of the Aleutian Trench. Further, we can anticipate that frictional and tidal effects on the shallow continental shelf will result in considerably reduced flow over the shelf compared to flow along and seaward of the continental slope, and that flow along the edge of the shelf will be complicated by internal waves and horizontal shelf waves.

The greatest fluctuations in flow conditions will be associated with the intensification of winds in winter. The center of the Aleutian Low travels in an anticyclonic pattern; present in late spring and summer in the northern Bering Sea, it occurs in the Gulf of Alaska in late fall, and in the western Aleutian area in winter. Thus, maximum cyclonic winds occur

in the Gulf of Alaska from November to January. Maximum Ekman transport will occur at this time, piling up water along the coast and resulting in a seaward flow along the bottom. Maximum total transport also occurs at this time greatly increasing northward flow into the gulf. In summer, a northward displacement of the Eastern Pacific High results in anticyclonic winds resulting in an offshore component of Ekman transport at the surface and a compensatory onshore flow over the continental shelf. Minimum overall transport also occurs at this time.

Thus there is a potential for considerable complexity and great variability in actual conditions, and it is these time-dependent phenomena that we are most interested in. All data available will be used to define physical conditions in the gulf as accurately and completely as possible.

It is difficult to assess how representative the oceanographic data being collected or analyzed are in defining conditions in a particular area unless some measure of variability over extended time periods is available. About a century ago it was recognized that oceanic conditions in the gulf were considerably warmer than corresponding latitudes at the western side of the ocean (Dall, 1882) and this was attributed to the influence of the "Kuro Siwo" because of the known analogous effects of the Gulf Stream in the Atlantic Ocean on the climate of Europe. Although data from the "China steamers" between San Francisco, Yokohama and Hong Kong in the 1870's provided extensive data on conditions in the central Pacific Ocean, even the gold rushes and subsequent commercial traffic to Alaska failed to provide a data base documenting oceanographic conditions in the gulf. There are surface temperature data for the Gulf of Alaska from the 19th century, presumably from government and commercial vessels, but these are too

fragmentary in time and space to establish climatic trends. Nevertheless, there are historical records of monthly mean air temperatures at Sitka that began when this location, called New Archangel, was controlled by the Russian-America Company (Dall, 1879) that are fairly complete to this date. Considering all years data are available since 1828 (Fig. 1), positive annual anomalies of greater than 1.5° were recorded in 1829, 1869, 1915, 1926, 1940 and 1941; whereas, only in 1955 did a negative anomaly greater than 1.5° occur. Cycles of 4-5 year duration are apparent in the data from 1850-71. The period from 1920 to 1947 was characterized by above normal conditions; however, there was a marked decline of over 3° from 1940 to 1950. Below normal conditions have occurred from 1965 to the present. Perhaps the most significant aspect of these data is that the annual mean temperature for 1828-76 is precisely the same as the present day mean compiled and used by the National Weather Service, 6.3°C (43.3°F). Thus, both short-term fluctuations of 1-4 years and long-term trends, such as the cooling evident from 1940-55 have occurred. Although we have acquired sea level pressure data as far back as 1900, sea level data prior to 1930 are available only at Ketchikan, and oceanographic station data are generally available only since 1950. The longer records will be utilized where applicable, but most comparisons and interactions will of necessity be based on data from the 25-year period 1950-74.

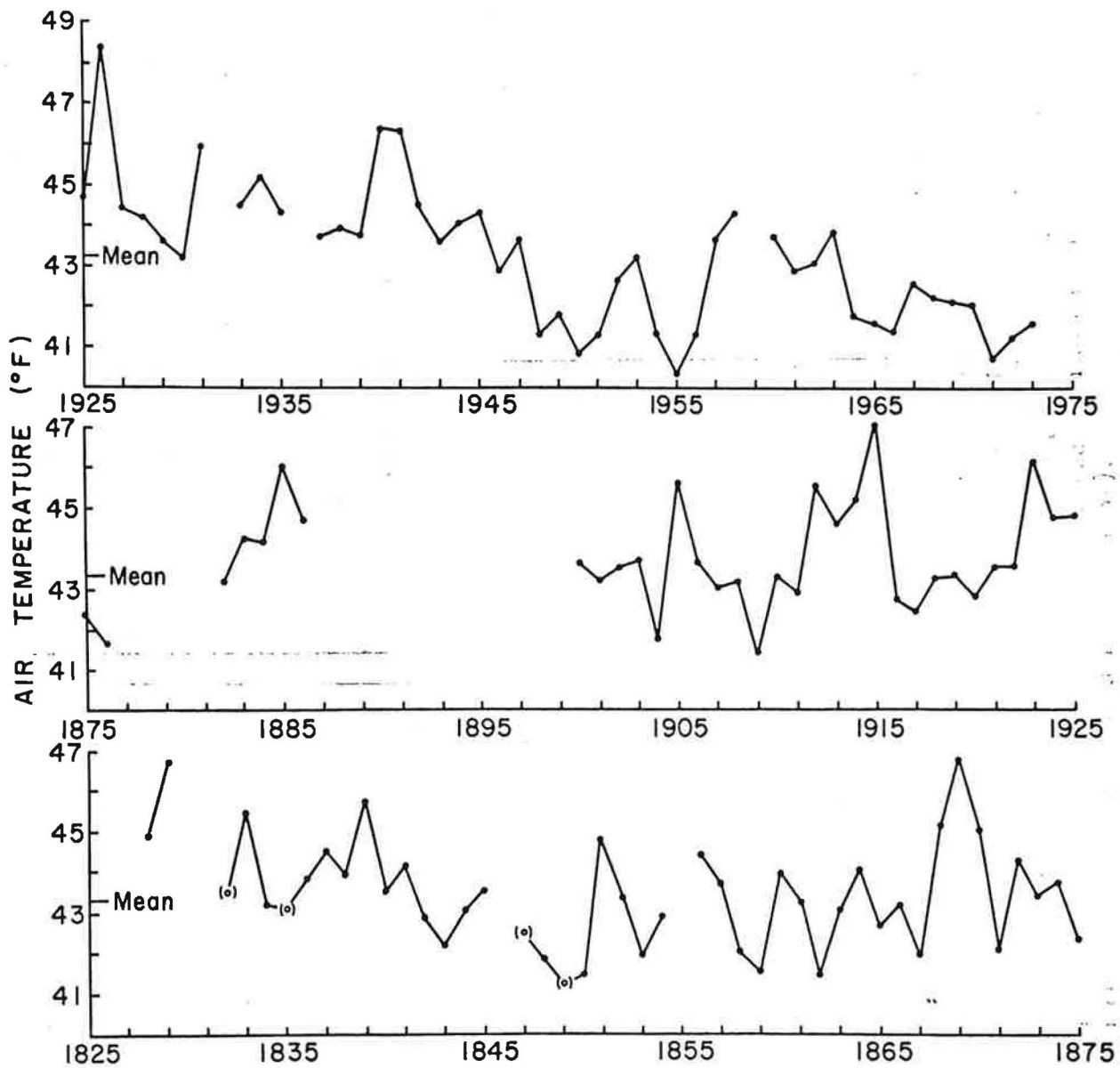


Figure 1. Air temperatures at Sitka (New Archangel) 1828-1974.

II. WATER PROPERTIES

Abrupt changes from normal conditions are usually quickly detected, but gradual changes over long periods often pass unnoticed; nevertheless, quantification of either requires an adequate data base. Reasonably complete time-series data in the gulf are available at shore stations, but none is available at specific locations in oceanic areas of the gulf^{3/}. In the latter case, in order to obtain any semblance of time-series data, observations over extensive areas must be averaged over large intervals; such data provide an indication of trends but, obviously, numerous spatial and temporal phenomena are masked by the averaging process.

A. Temperature

Although observations at shore stations are the most complete source of temperature data, only surface values are obtained. Monthly mean values (referred to 1950-74 mean, where data are available) for Ketchikan, Sitka, Yakutat, Seward, Kodiak and Dutch Harbor indicate a progressively colder regime from southeastern Alaska around the gulf to the end of the Alaska Peninsula with one exception, that temperatures in winter at Dutch Harbor are about 2 or 3 C⁰ higher than at Kodiak (Fig. 2a). In southeastern Alaska the seasonal temperature range is about 9 C⁰ (from 5 - 14°C at Ketchikan and 3 - 12° at Seward), but the range increases to 11 C⁰ at Kodiak (1 - 12°) and decreases to 8 C⁰ at Dutch Harbor. Minima occur in January at Kodiak and in February at all other locations, maxima occur in July at Seward and in August at all other locations.

There are a number of oceanographic atlases of large areas of the Pacific Ocean that permit a general assessment of mean temperatures in the offshore waters of the Gulf of Alaska (e.g. LaViolette and Seim (1969)) present monthly mean, minimum and maximum sea surface temperatures based on a

^{3/} Extensive data are available at Ocean Station "P" southward of the gulf -50°N, 145°W (e.g. Tabata 1965 and Fofonoff and Tabata 1966).

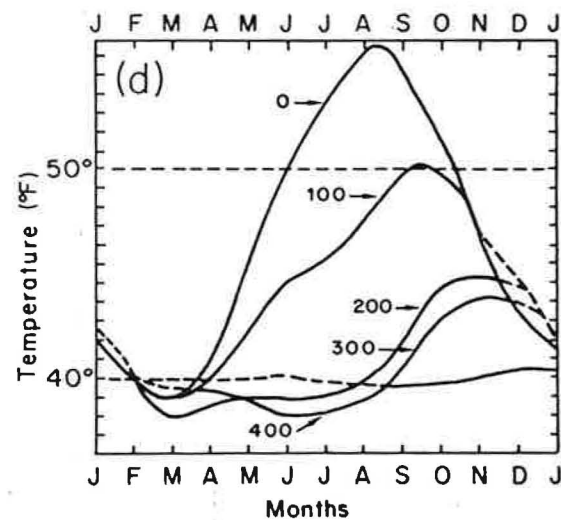
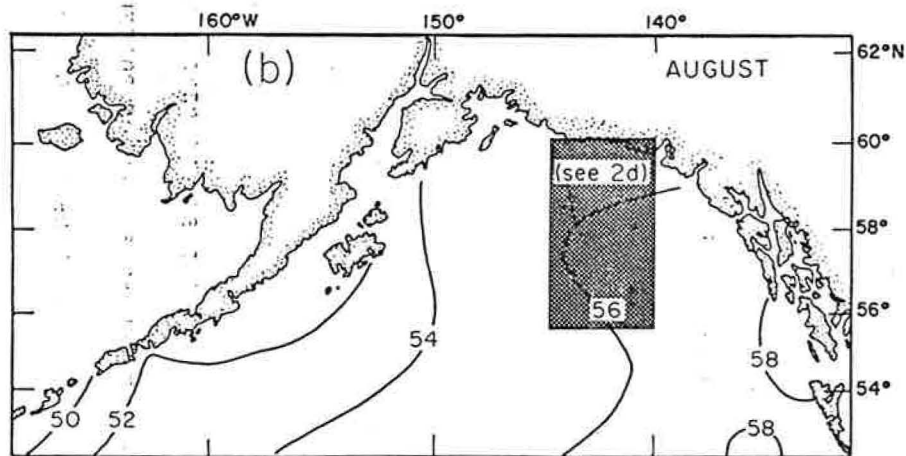
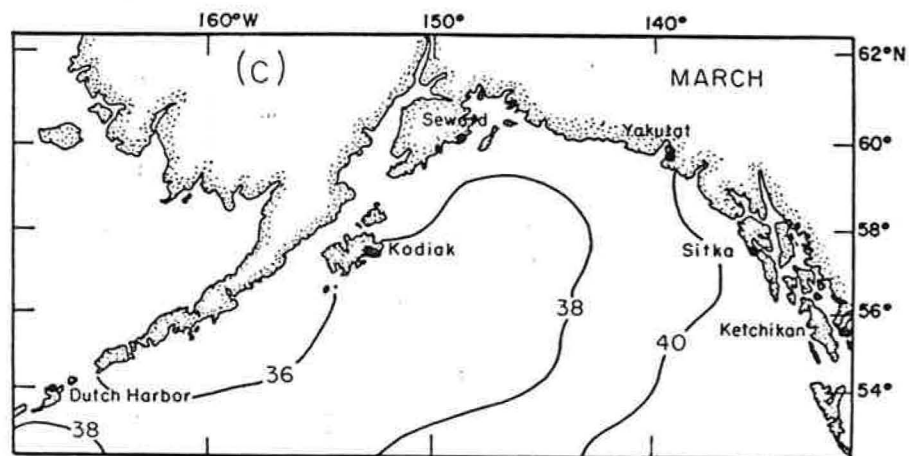
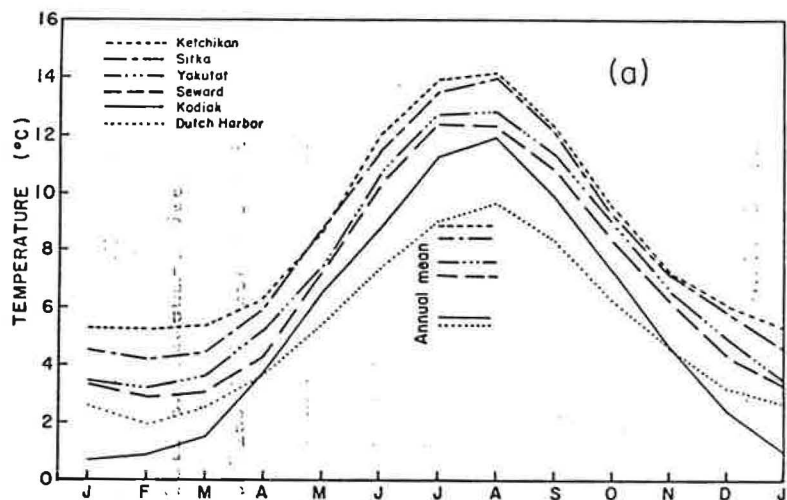


Figure 2. Sea temperature data: (a) monthly mean (1950-74) sea surface temperatures at the indicated coastal stations; (b and c) surface temperature distributions August and March (from Robinson and Bauer, 1971); and (d) monthly mean temperatures at 100 ft (30.5m) intervals to 400 ft (121.9m) in 5x5° Marsden quadrant 195-3, 55-60°N, 140-145°W (from Robinson, 1957).

1 x 1° grid), and there are also a few that are limited specifically to the gulf and adjacent area--e.g. Robinson (1957), Giovando and Robinson (1965) and Robinson and Baur (1971). These data are not only easily accessible, but adequately representative of mean conditions; thus, there is little need for an extensive summary here. It should be pointed out, however, that such atlases are representative only of offshore areas where mixing and stirring moderate the extreme conditions that occur in shallow inshore areas which are influenced by ice-melt in winter and spring, and runoff and warming over tidal shoals in spring and summer^{4/}. Maximum surface temperature, 14°C, occurs in August, but conditions are sufficiently similar in September to consider either month as representative, and minimum surface temperature, 3.5°C, occurs in March (Fig. 2b and c) - temperatures of 0°C, or lower, can be found in Prince William Sound and Cook Inlet depending on the extent of ice cover.

A representative seasonal temperature cycle to a depth of 122 m (400 ft) is afforded by a compilation of station and bathythermograph (BT) data in the 5 x 5° quadrangle from 55-60°N, 140-145°W (Fig. 2d). Near isothermal conditions are present from the surface to approximately 100 m during January-March and represent the vertical extent of convective turnover during winter. This process not only determines the extent of the surface layer in winter, but results in the formation of a temperature-minimum stratum (~3°C) at depths of 75 to 150 m when surface waters are warmed in spring and summer. Wind mixing and stirring result in the formation of a warm surface layer in summer of 20-30 m thickness that is underlain by a sharp thermocline extending to the depth of winter overturn. Subsequent downward diffusion in spring, summer and autumn gradually erodes but

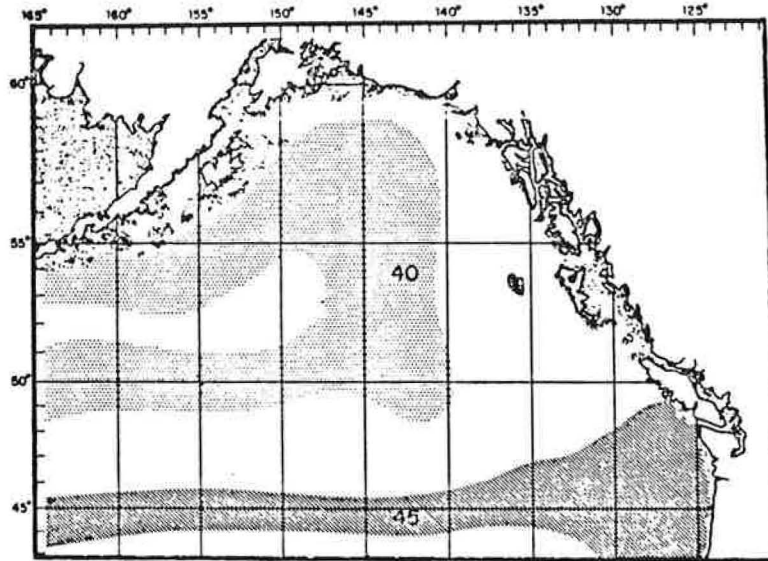
^{4/} See Muench and Schmidt (1975) for a discussion of conditions in Prince William Sound.

seldom eliminates the temperature-minimum stratum, particularly in the central part of the gulf. The effects of this process are evident until November. However, year round temperatures of 4.5 to 5.0°C occur near 122 m around the periphery of the gulf, over the continental shelf and slope. These temperatures, 1-2°C higher than those in the temperature-minimum stratum, appear as a mesothermal, or temperature-maximum, stratum, but are merely representative of conditions in the water column below the influence of local seasonal effects.

Further information on conditions at 122 m is provided by a plot of the geographical extent of selected isotherms (Fig. 3a): the zonal trends south of 50°N suggest an eastward flow toward the coast; the abrupt northward trend of the 4.4°C isotherm boundaries west of 140°W suggests a broad variable northward flow into the gulf east of 150°W; the westward continuation of this feature south of the Alaska peninsula suggests a westward return flow in that area; and, finally, the tongue-like area westward of 147°W between 51° and 54° suggests the presence of an eastward intrusion of cold water from the west or an area of upward vertical transfer of cold water from depth, or both. A vertical temperature profile along 145°W (Fig. 3b) based on long-term mean temperatures from all station data (2 x 2° grid) clearly exhibits a ridging of the 4 and 5° isotherms in the zone between 48-57°N; and the effects of temperature on geostrophic flow dictate an eastward, onshore flow to the south of this zone and a westward return flow north of the zone.

Mean temperature distributions below the range of the shallow bathythermograph (450' or 137 m) must be obtained from station data and are not

(a)



(b)

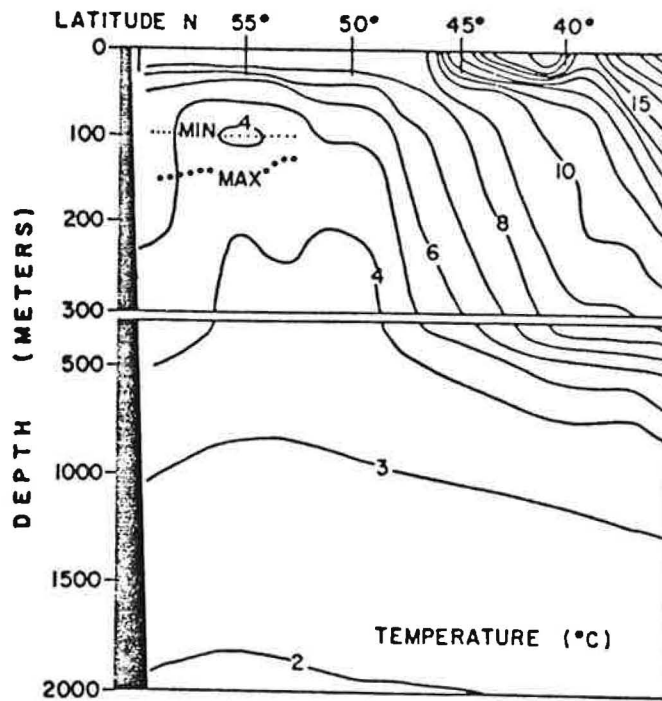


Figure 3. Geographic range of selected isotherms ($^{\circ}\text{F}$) at 400 ft (121.9m) (from Robinson, 1957), and vertical section of long-term mean temperatures (based on $2^{\circ}\times 2^{\circ}$ grid) along 145°W .

readily accessible. Plots based on long-term mean data ($2 \times 2^\circ$ grid) at depths of 200, 500, 1000 and 2000 m (Fig. 4) clearly indicate the northward sweep of warm water into the gulf on the eastern side and the permanence of the cold intrusion isolated offshore on the western side; the two features exist at all levels. It should be noted that data averaged in this manner ($2 \times 2^\circ$ grid) do not adequately represent temperature fields in the narrow boundary current at the western side of the gulf, particularly south of the Alaska Peninsula, but the gradual lowering of temperature from $5 - 4^\circ\text{C}$ in an east-west direction around the gulf at 200 m, which is considered the seaward limit of the continental shelf, is fairly representative of actual conditions as far west as Kodiak Island. A grid of less than $1/2 \times 1/2^\circ$ would be required to show continuity of isotherms west of this area, and the paucity of data prevent this. Data obtained east of Kodiak Island in spring 1972 (Fig. 5) indicate characteristics of the distribution of $4-5^\circ\text{C}$ water near 200 m in this area; and there are numerous examples of the continuity of this temperature-maximum stratum from the gulf westward out along the Aleutian Islands (e.g. Ingraham and Favorite, 1968) based on closely spaced station data from individual cruises.

At all levels from 200 to 2000 m the mean temperature distributions suggest a confluence of cold oceanic water entering the gulf in a northeasterly direction and warm water entering in a northwesterly direction. There is also a perturbation evident in isotherms in the eastern side of the gulf at 200, 500 and 1000 m that appears to suggest that flow related to the former has a blocking effect on flow related to the latter. These phenomena are discussed in later Sections on Water Properties and Currents.

Anomalies from monthly mean surface temperatures at shore stations around the gulf indicate that marked short-term deviations occur at indi-

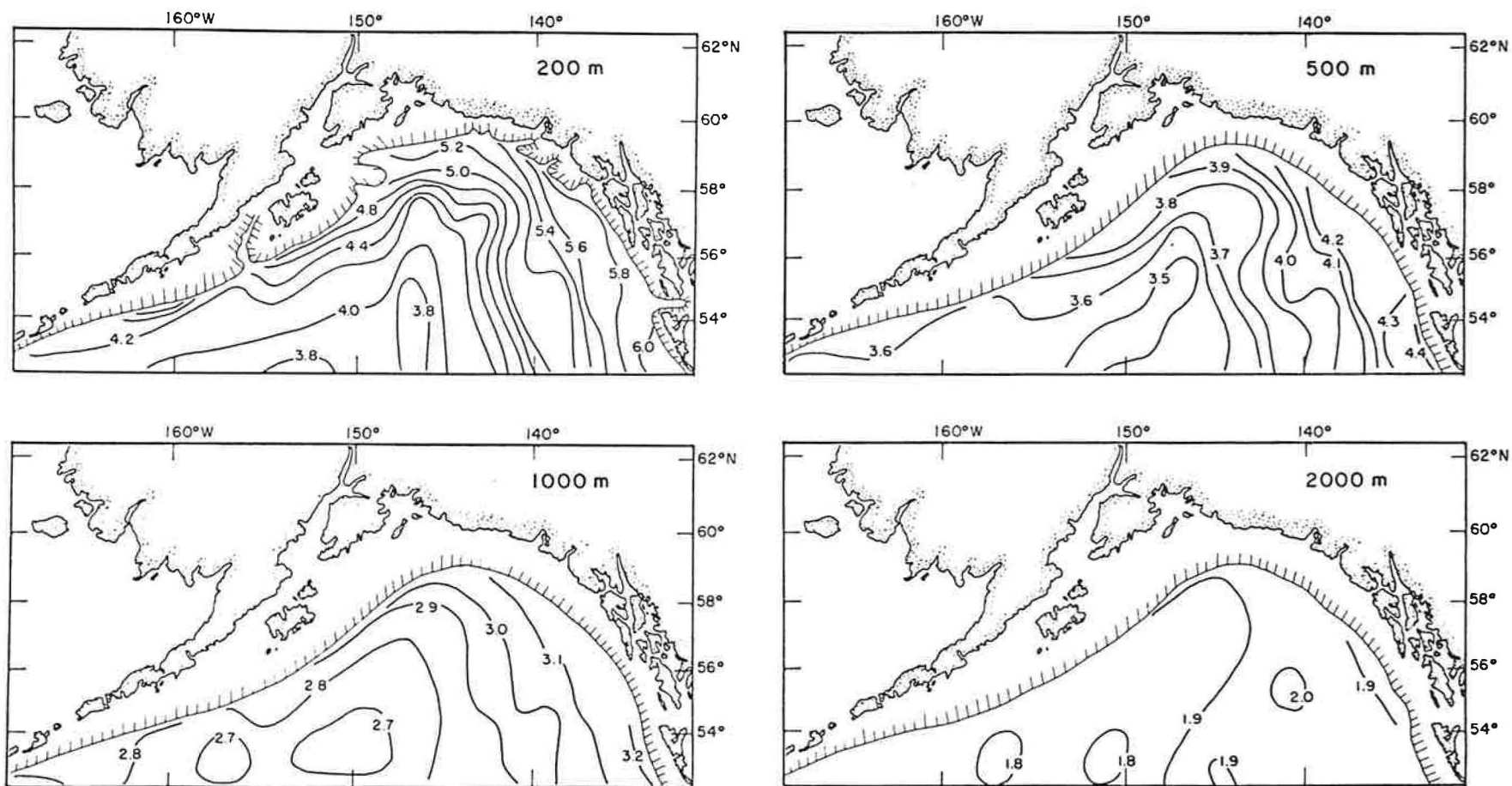


Figure 4. Long-term mean temperature distributions (based on $2 \times 2^\circ$ grid) at 200, 500, 1000 and 2000 m.

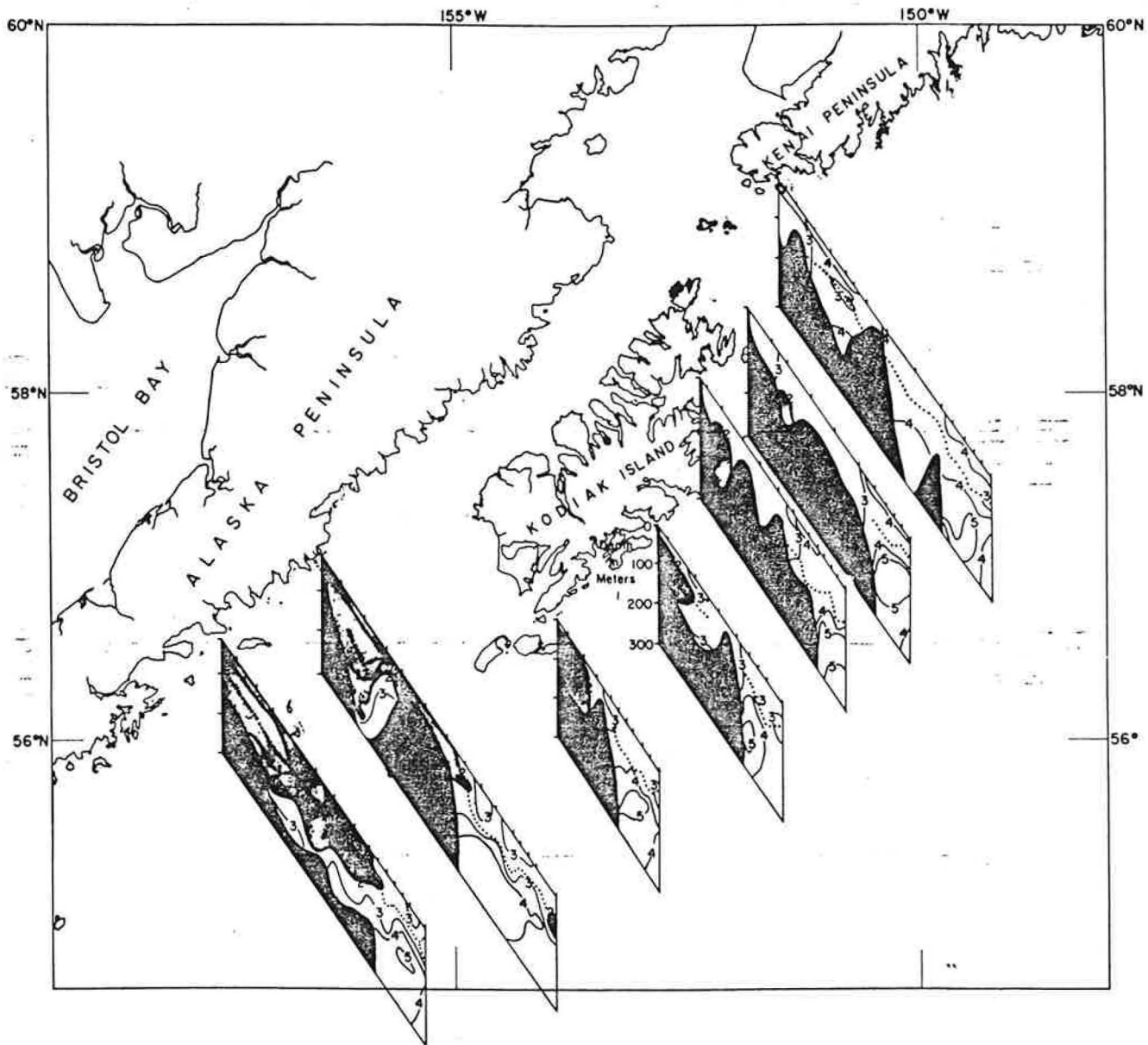


Figure 5. Vertical sections of temperature ($^{\circ}\text{C}$) along lines of stations (RV George B. Kelez, April-May 1972 - Ticks indicate station locations) normal to the shelf edge indicating temperature-minimum stratum (dotted), and temperature-maximum ($4-5^{\circ}\text{C}$) seaward of the shelf edge.

vidual stations that are not manifested at others. There is a similarity in the medium - term (1-3 years) trends, that is not apparent in the long-term trends (Fig. 6). For example, only at Dutch Harbor and Sitka is there evidence of a prolonged cooling period, 1958-73. The 12-month running mean clearly indicates cold periods centered around 1955 and 1972, and warm periods around 1958, 1963 and 1968. Similar trends in the oceanic area ($5 \times 5^\circ$ Marsden quadrant 195-3; $55-60^\circ\text{N}$, $140-145^\circ\text{W}$) are evident (Fig. 7), and the transpacific occurrence of large areas of positive and negative anomalies at periods of 5-6 years has been pointed out by (Favorite and McLain, 1973). There are sufficient station data in offshore areas during the period 1955-1963 to indicate temperature changes that can occur at depth during cold and warm periods. Comparison of data in summer 1956 and 1958 indicates that values in the temperature-minimum stratum were over 1C° lower in 1956 over a wide area in the gulf (Fig. 8). Assuming winter convective overturn to 100 m, this represents a difference of $10,000 \text{ cal/cm}^2$ (of sea surface), a significant change in the heat content of the water column and the heat budget of the area.

Temperature anomalies in the water column are related also to advective processes. It is difficult to isolate the effects of winter turnover from advection in the upper 100 m or so, but at depths below seasonal influences there are secular changes that can be detected even with fragmentary data. Favorite (1975) has shown the apparent eastward intrusion of cold water from the west into the gulf indicated by the distribution of temperature on the salinity surface = $34.0 \text{ }^\circ\text{oo}$ (which occurs at about 250 m) from 1955 to 1962. Any consideration of flow at depth in the gulf must take into

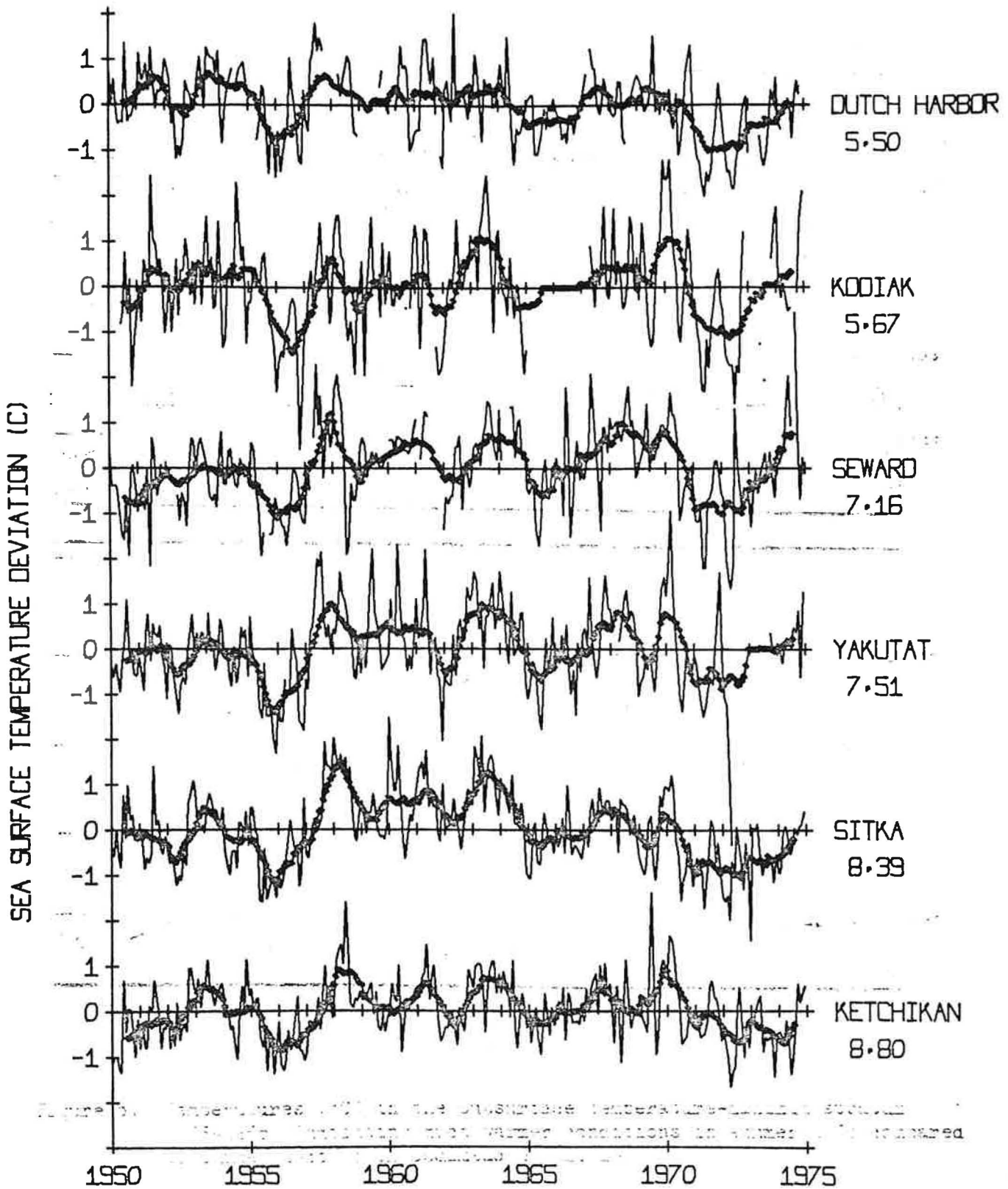


Figure 6. Deviations (C°) in sea surface temperature from monthly mean (1950-74) values at the indicated coastal stations; dotted segment indicates 12-month running mean.

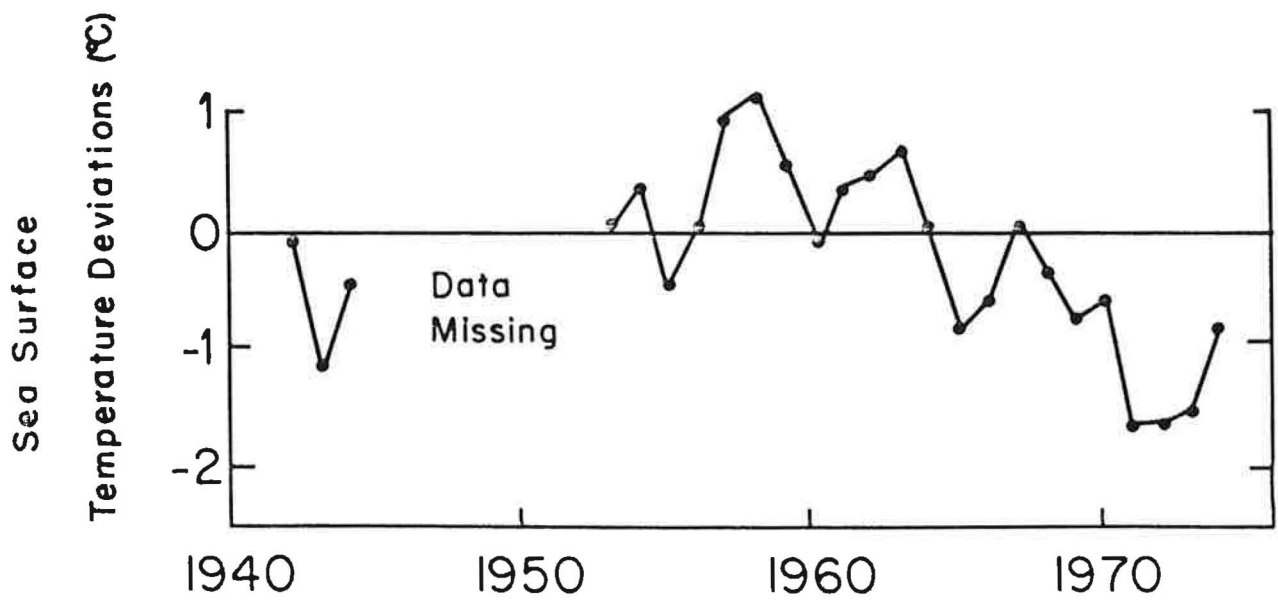


Figure 7. Deviations ($^{\circ}\text{C}$) in sea surface temperature from annual mean (1948-67) values in $5 \times 5^{\circ}$ Marsden quadrant 195-3 (see Fig. 2) reflecting a cooling trend since 1958.

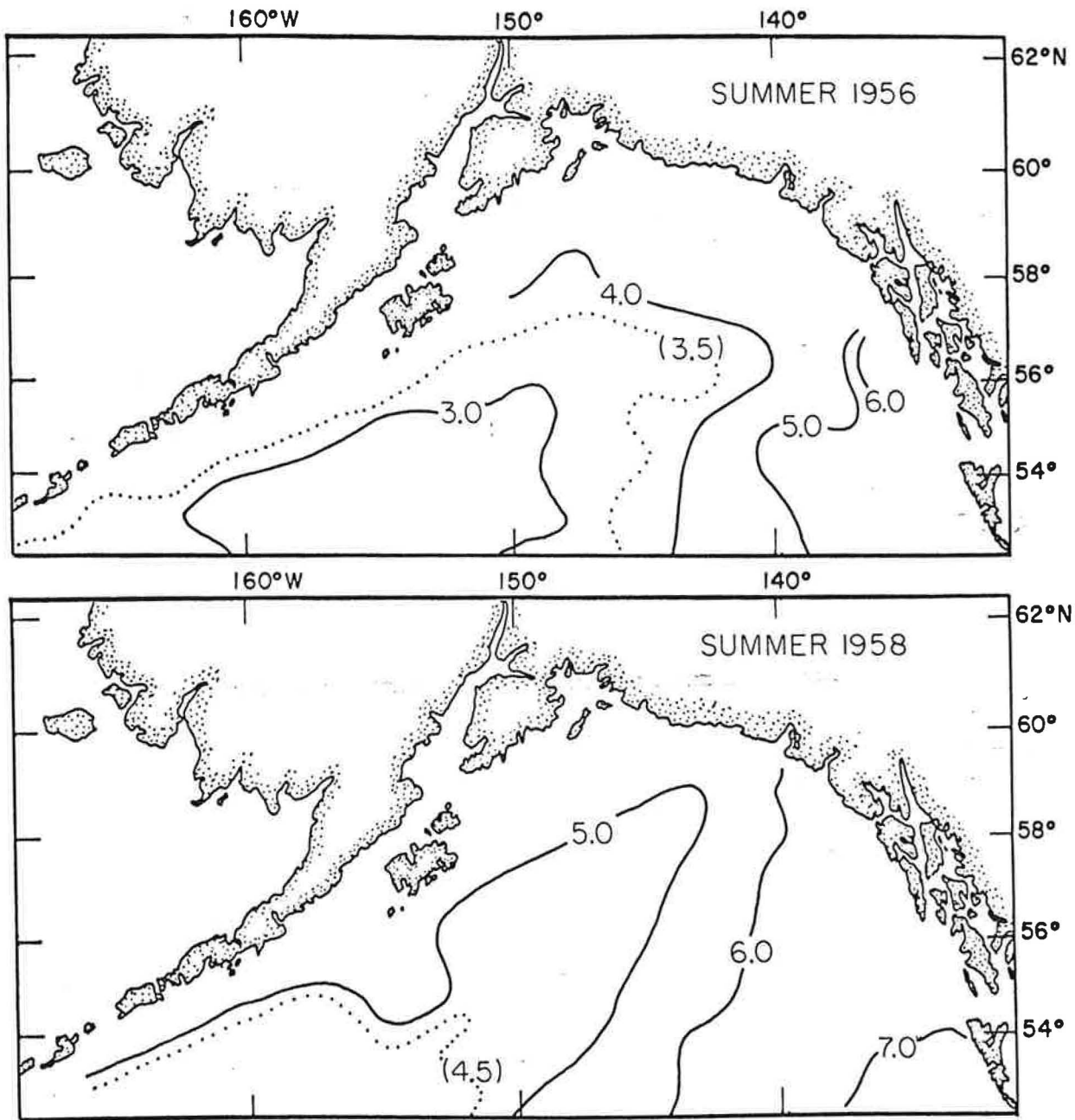


Figure 8. Temperatures ($^{\circ}\text{C}$) in the subsurface temperature-minimum stratum ($\sim 75\text{-}125\text{m}$) indicating much warmer conditions in summer 1958 compared to summer 1956 (from Dodimead et al, 1963).

consideration the fact that this anomalously cold water intruded nearly to the continental shelf in the eastern part of the gulf in 1961 (Fig. 9).

B. Salinity

Atlases depicting salinity distributions (e.g. Muromtsev, 1958; Barkley, 1968) provide limited information on actual conditions because of the paucity of these data. This is unfortunate because in many instances extensive salinity data, particularly near the surface, would provide more information concerning flow than temperature data. Because of a net excess of precipitation over evaporation (Jacobs, 1951) and extensive runoff, Tully and Barber (1960) have likened the oceanic regime to an estuarine system.

Although extensive runoff around the gulf in spring and summer dilutes coastal waters, this flow is difficult to quantify. Some clues as to the timing of this phenomenon are available from data on the monthly mean discharge from the Copper River, the dominant system in the area. Minimum discharge occurs from December to April; flow increases in May and reaches a maximum in July (Fig. 10). The effects of coastal runoff on offshore conditions is evident in station data averaged by season and $2 \times 2^\circ$ quadrangles (Fig. 11). Spring and summer data are the most complete but, although values as low as 16-18 ‰ occur in inshore areas, the $2 \times 2^\circ$ grid is too coarse to reflect precise inshore minima. Nevertheless, the seasonal offshore movement of coastal dilution is evident, specifically, the 32.0 ‰ isohaline, which moves offshore as much as 200 km in summer compared to its position in winter. Also evident is a region of high salinity in the southwestern part of the gulf reflecting vertical divergence.

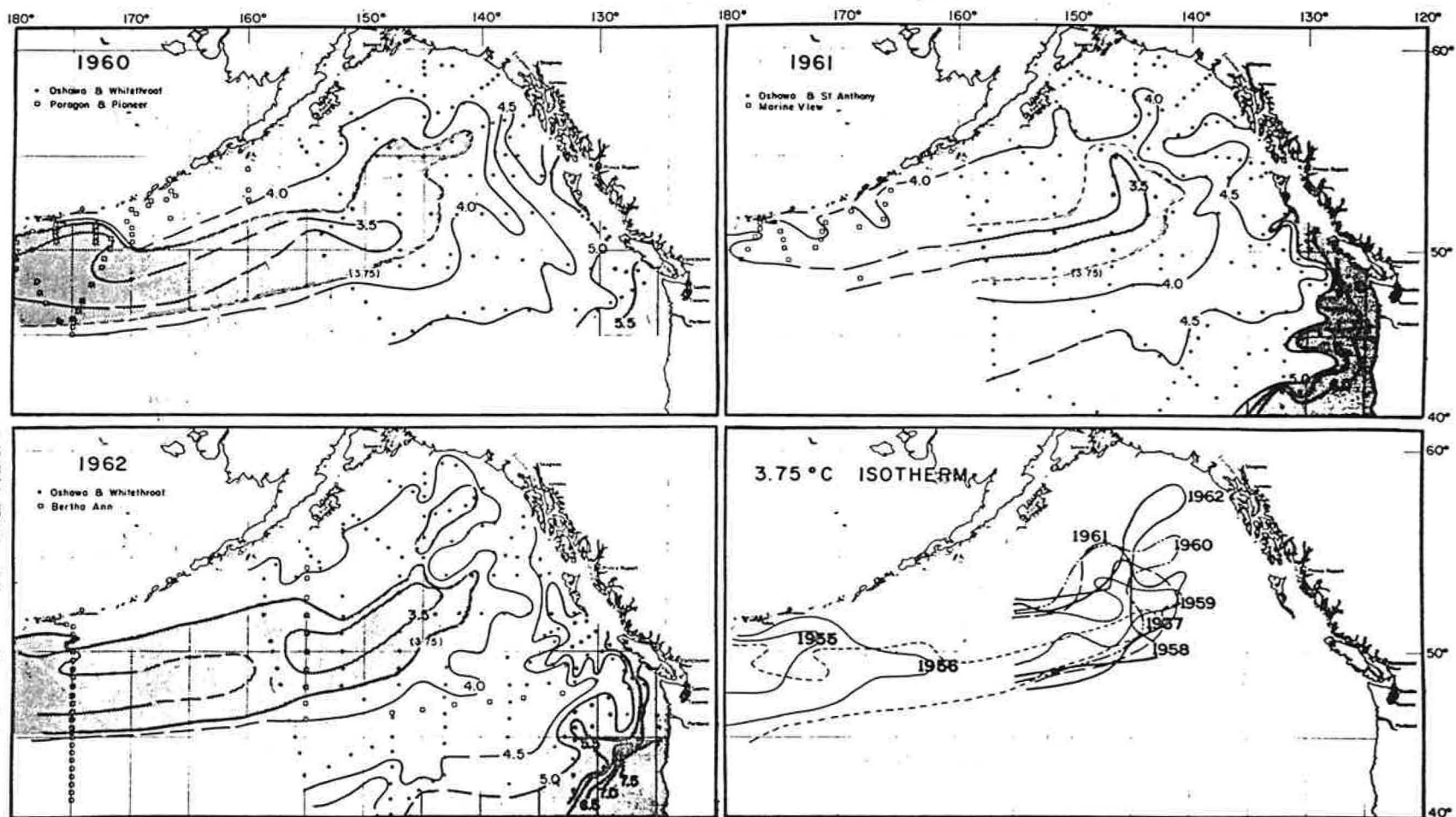


Figure 9. Temperatures ($^{\circ}\text{C}$) on surface of salinity = $34.0 \text{ }^{\circ}/\text{oo}$ ($\sim 300\text{m}$) in 1960, 61 and 62; and the configuration of the 3.75°C isotherm in 1955, 56, 57, 58, 59, 60, 61 and 1962.

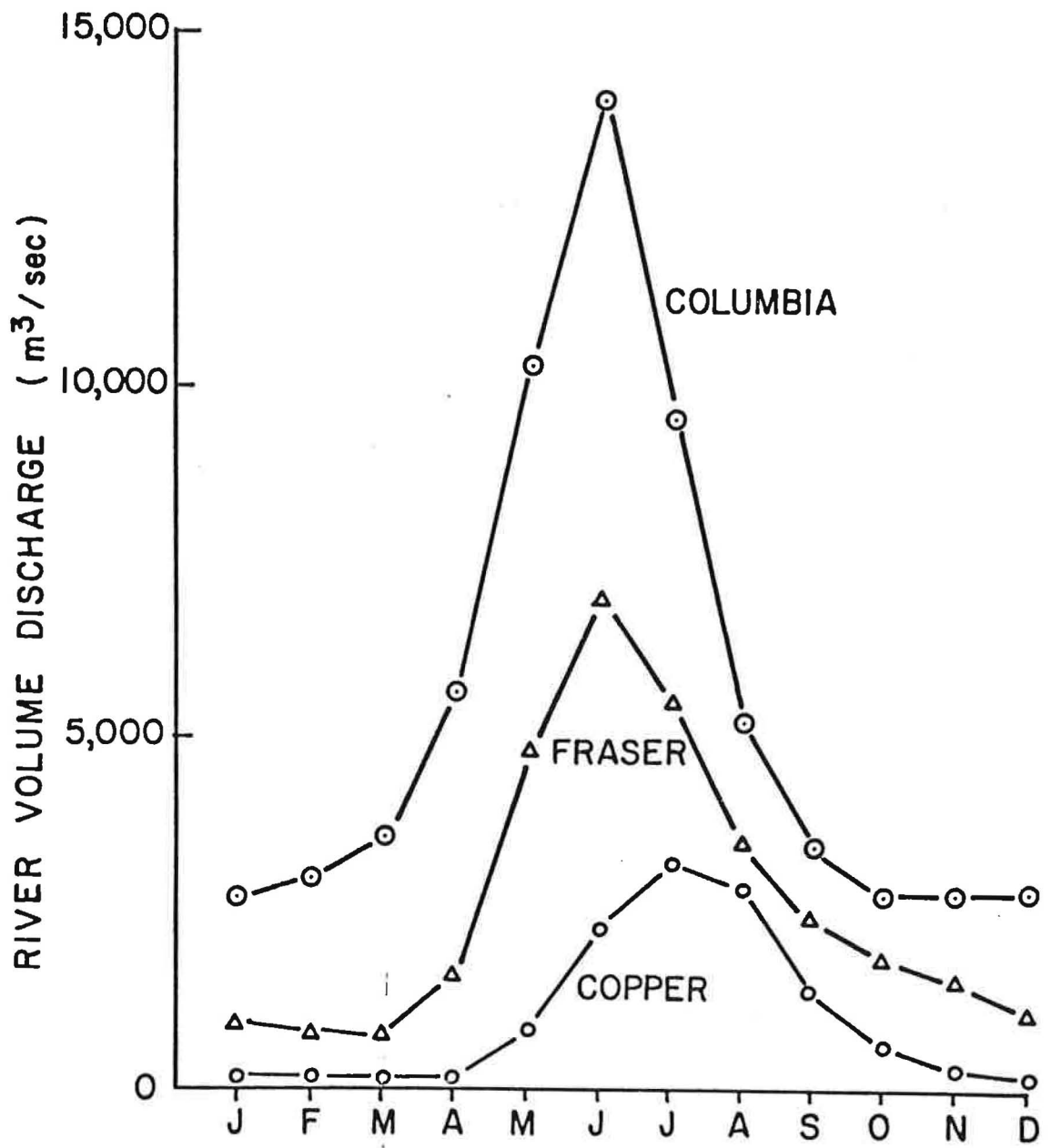


Figure 10. Monthly mean discharge (m^3/sec) from the Columbia, Fraser and Copper Rivers showing relative volume and month of peak runoff.

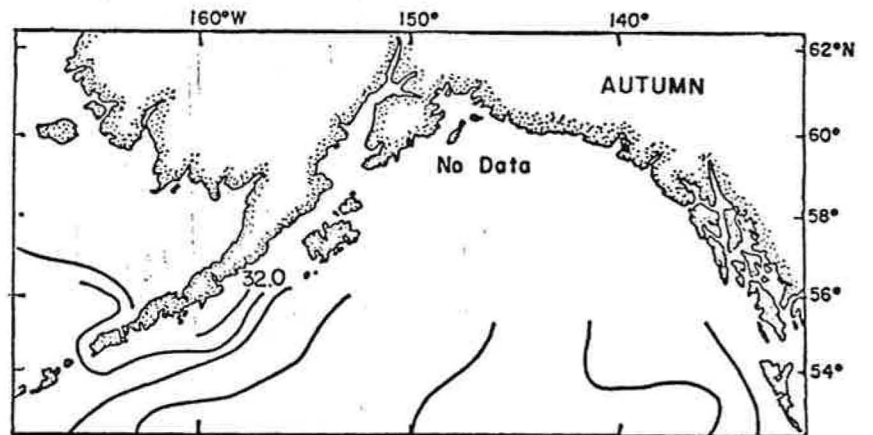
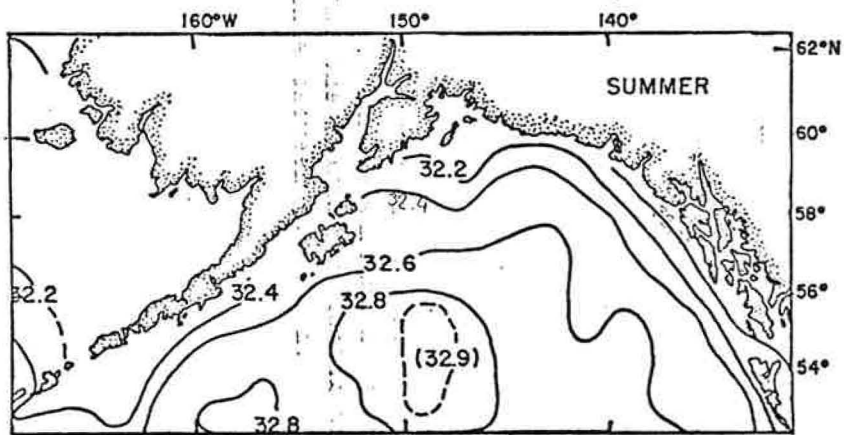
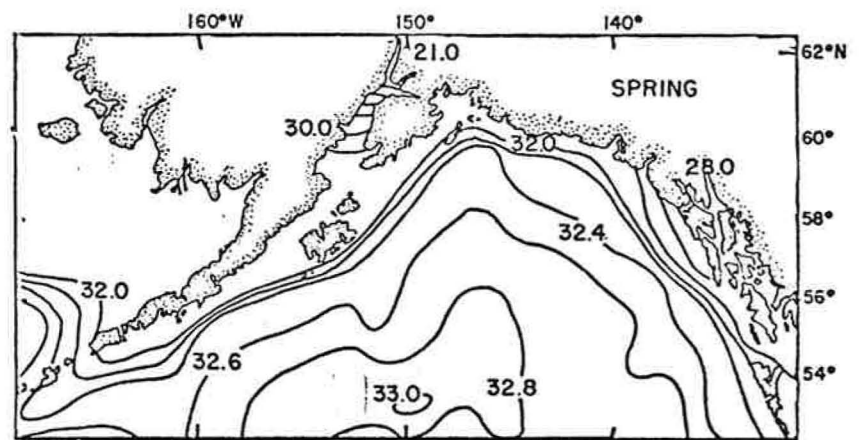
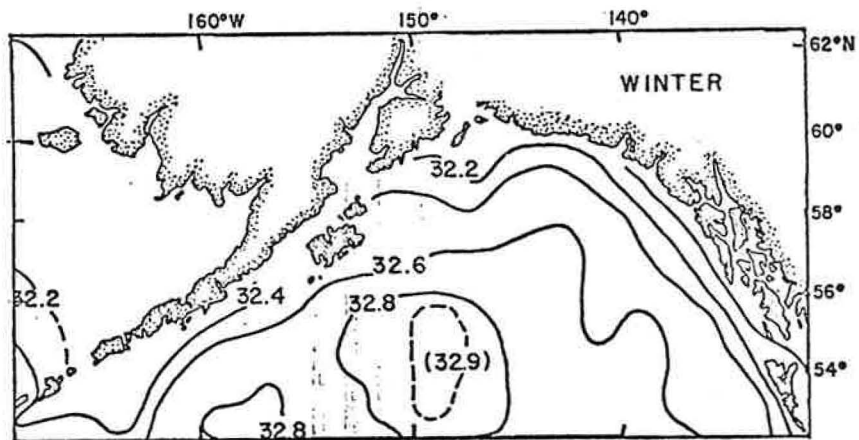


Figure 11. Long-term mean seasonal surface salinity distributions (based on a $2 \times 2^\circ$ grid) showing marked coastal dilution in summer and maximum values in southwest part of the gulf.

Maximum values (>33.0 ‰) in this area are evident in spring rather than as might be expected in winter, but this is believed due to limited data in the winter period.

Associated with the dilute surface layer is the marked halocline between 100-200 m (Fig. 12) evident in a vertical profile along 145°W . This feature gives a marked stability to the water column and greatly influences the vertical extent of winter convection and, thus, effects the vertical distribution of temperature and other water properties.

The salinity data are inadequate to show convincingly any anomalous salinity distributions in the gulf either in time or space. This does not mean that they do not occur. Considerable variability in the timing and volume discharge of coastal runoff takes place. An example of the variability possible is evident in the distributions of surface salinity off southeastern Alaska in summer 1957 and 1958 (Fig. 13). Considerable offshore dilution is evident in the 1958 distribution compared to that in 1957. However, the distributions represent mean fields over 3 month periods constructed from various data points, and it is difficult to ascertain which, if either, represents average or anomalous conditions.

There has always been speculation as to the existence of a frontal zone at the edge of the continental shelf indicating not only boundary processes such as shelf waves, but a simple separation of dilute coastal from saline oceanic water. Data from a continuously recording surface salinograph (Fig. 14) obtained during numerous transects of a short line of stations normal to the shelf edge eastward of Kodiak Island in spring 1972 (Favorite and Ingraham, 1976a) prove the existence of such a frontal

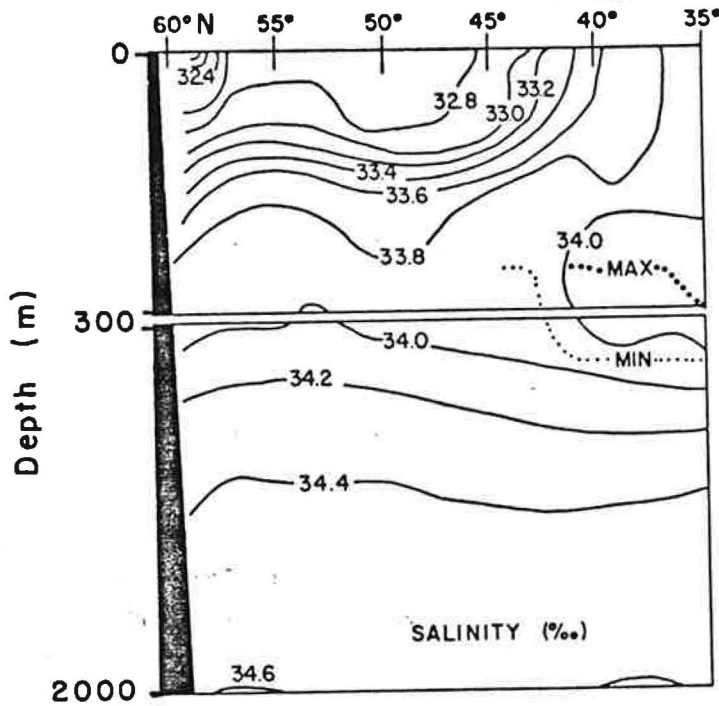


Figure 12. Vertical section of long-term mean salinities (based on $2 \times 2^\circ$ grid) along 145°W showing: the dilute surface layer north of 45°N , particularly near 60°N ; the ridging or doming of isolines at 55°N ; and, the halocline between 100-200 m.

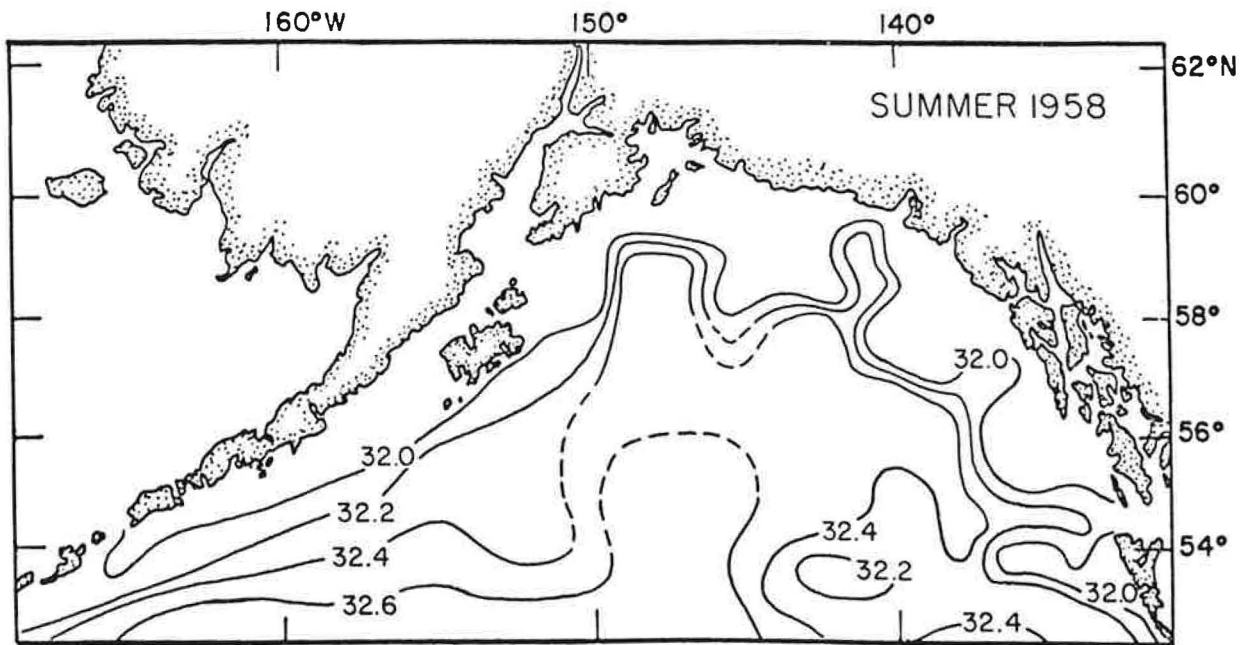
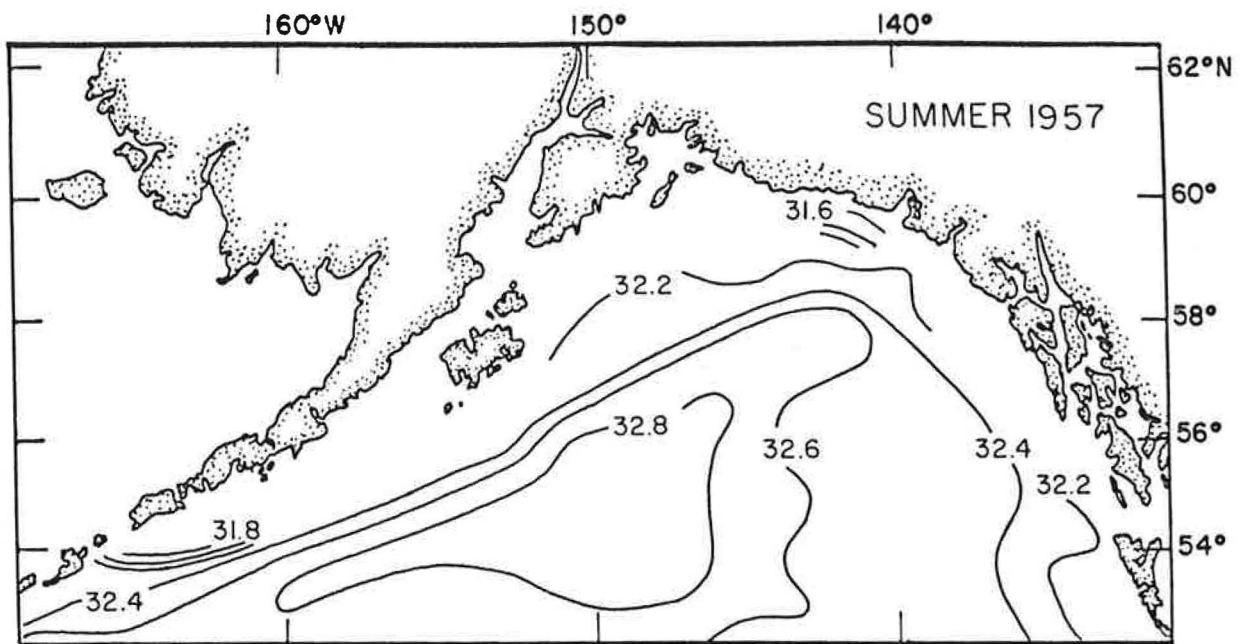


Figure 13. Surface salinity during summer 1957 and 1958 showing the extensive dilution off southeastern Alaska in the latter period reflecting the highly variable conditions that can occur in the surface layer (from Dodimead et al, 1963).

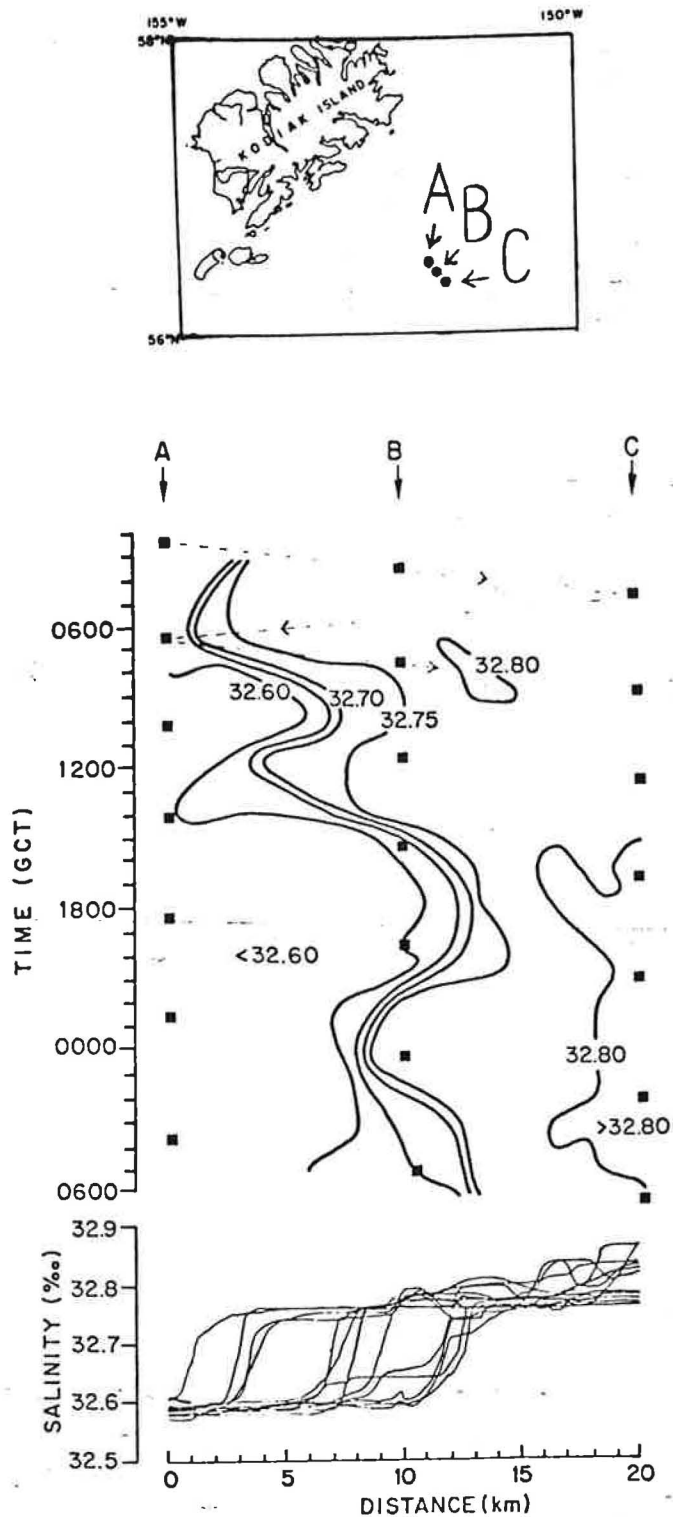


Figure 14. Surface salinity front detected seaward of Kodiak Island in the vicinity of the edge of the continental shelf (RV George B. Kelez, May 5-6, 1972) using constantly recording salinograph while occupying repetitive stations: A, B, C (dashed lines indicate vessel movement).

zone. Salinity distributions at 200, 500, 1000 and 2000 m (Fig. 15) reflect primarily the presence of the surface divergence in the offshore portion of the western gulf and the suggestion of cyclonic circulation found in the temperature distributions. There is also an obvious area of dilution off Cape Spencer in the 200 m temperature field.

C. Water Masses

All oceanic waters attain marked characteristics when they are in contact with the atmosphere and these characteristics are subsequently altered by lateral and vertical mixing. When discrete temperature and corresponding salinity values of a water parcel below the depth of seasonal influences are plotted against each other a well-defined temperature-salinity (T-S) curve results that is characteristic of a given area and defines a water mass (Sverdrup, Johnson and Fleming, 1942). Such a curve defines the Subarctic Water Mass, characteristic of the area lying generally north of 50°N in the eastern North Pacific Ocean.

The low temperatures and salinities that distinctly define this curve are due in part to the waters moving eastward at depth from the Okhotsk Sea, a general vertical movement of intermediate water due to the Ekman divergence at the surface, and an undetermined northward transport of deep water in the Pacific basin that is deflected upward in this area by the land boundaries in the gulf and the Aleutian-Commander island arc. Modifications to this basic T-S curve are caused by a northward flow of warm water on the eastern side of the gulf that originates not only from eastward flow south of 50°N, but also from northward flow in the California Undercurrent. The latter is manifested at the surface in winter, but is overridden at the surface in summer by a southward flow stemming from the southern branch of the easterly onshore flow.

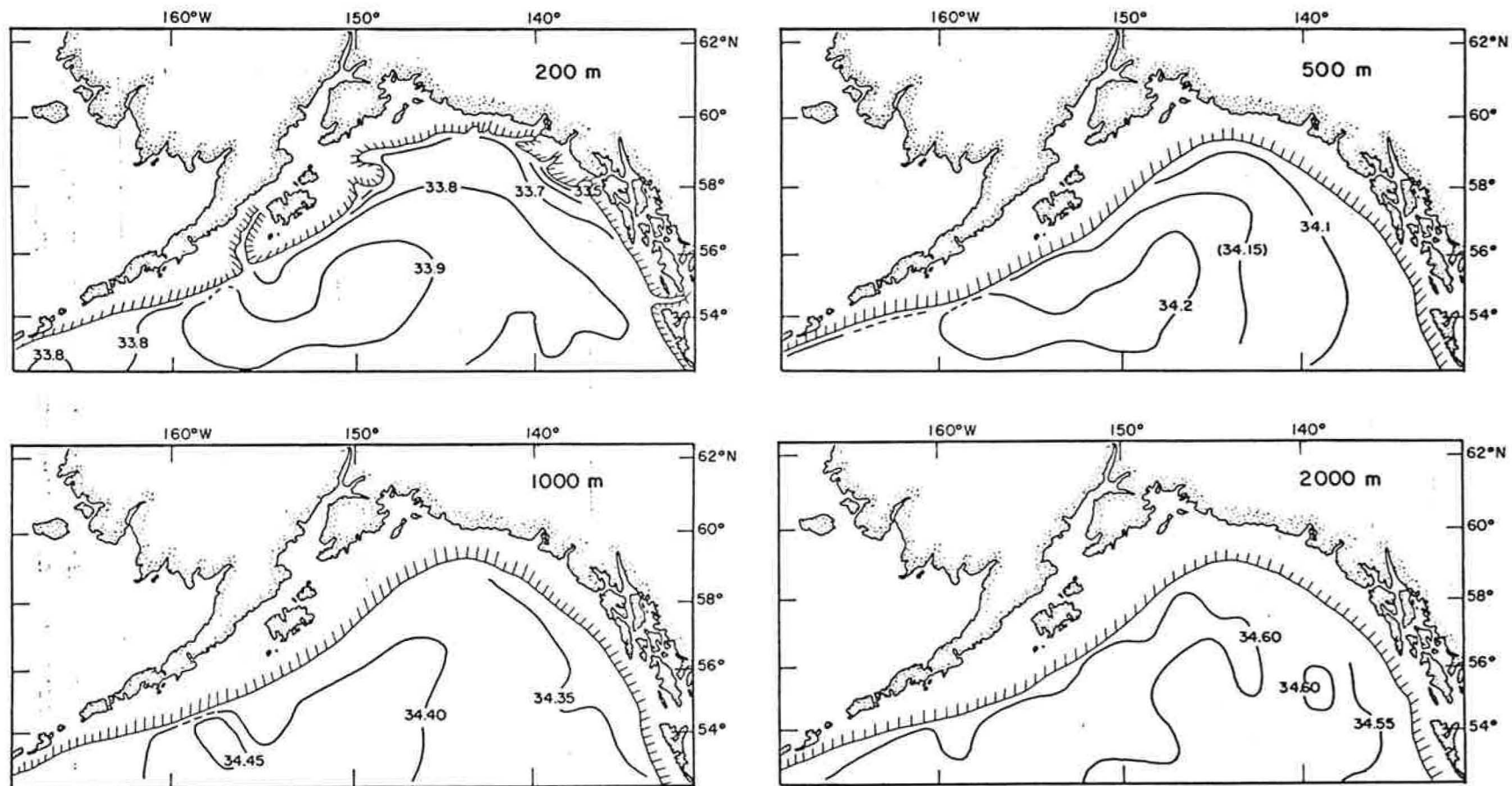


Figure 15. Long-term mean salinity distributions (based on $2 \times 2^\circ$ grid) at 200, 500, 1000 and 2000 m.

Monthly mean, as well as maximum and minimum, values of temperature and salinity at standard depths were computed from all station data by 2 x 2° quadrangles and are presented in the form of T-S curves at 4 selected locations at which winter and summer data were available (Figs. 16 and 17). Because of the paucity of data, in some instances only 3 stations, the curves and extreme values must be considered as only indicative of conditions rather than representing precise values and ranges. The water mass at the head of the gulf (area A) is formed from the merging of three major water masses moving northward into the gulf. In general, all have equivalent surface temperatures during the periods of maximum heating (summer, 13-14°C) and cooling (winter, 4-5°C), except in area B where winter temperatures of 3°C are evident, and there is a noticeable decrease in surface salinity shoreward from areas B to D, the greatest dilution occurring in area A. The elimination in winter of the temperature gradient, or thermocline, evident in the upper 50-75 m of the water column during summer is readily apparent in all areas. There are marked differences in temperatures from 100 and 300 m, about 3°C, between areas B and D; conditions at these depths in areas C and A reflect an admixture of the water masses in areas B and D, although the temperature maximum between 150 and 250 m is maintained. There is also a suggestion of a downward diffusion of summer heating below 125 m during winter. Below 300 m the T-S curves in areas A, B and C are similar and follow the trend of the general Subarctic Water Mass curve, however, there is a significant departure from this curve in area D attributed to northward flow along the coast. As might be expected, variability in temperature and salinity conditions is largely

SALINITY ‰

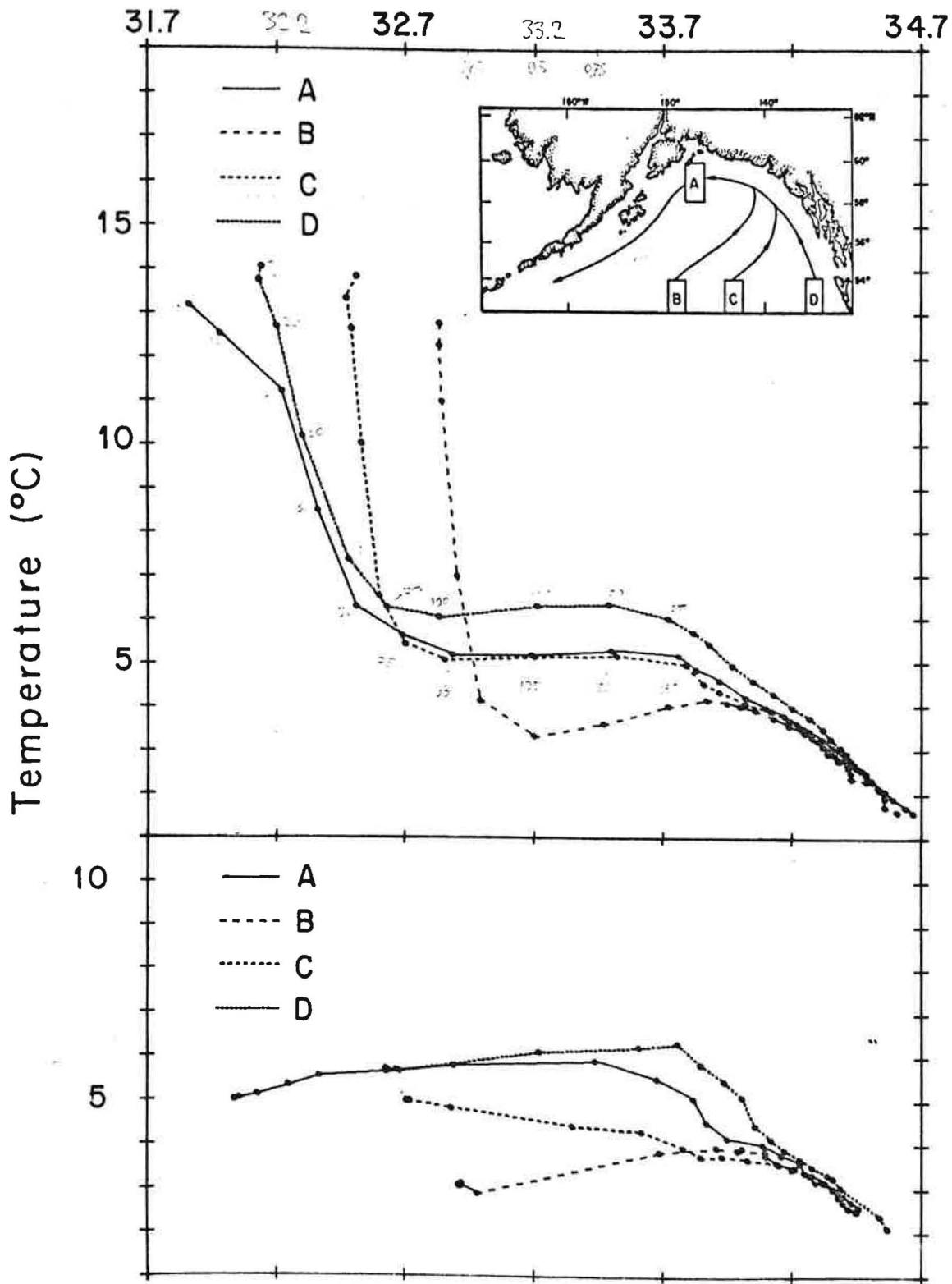


Figure 16. Long-term summer and winter mean temperature-salinity (T-S) relations at standard depths in the indicated 2x2° quadrangles showing characteristics of the various water masses funneling into the gulf.

SALINITY ‰

30.7 31.7 32.7 33.7 34.7 32.7 33.7 34.7 32.7 33.7 34.7 32.7 33.7 34.7

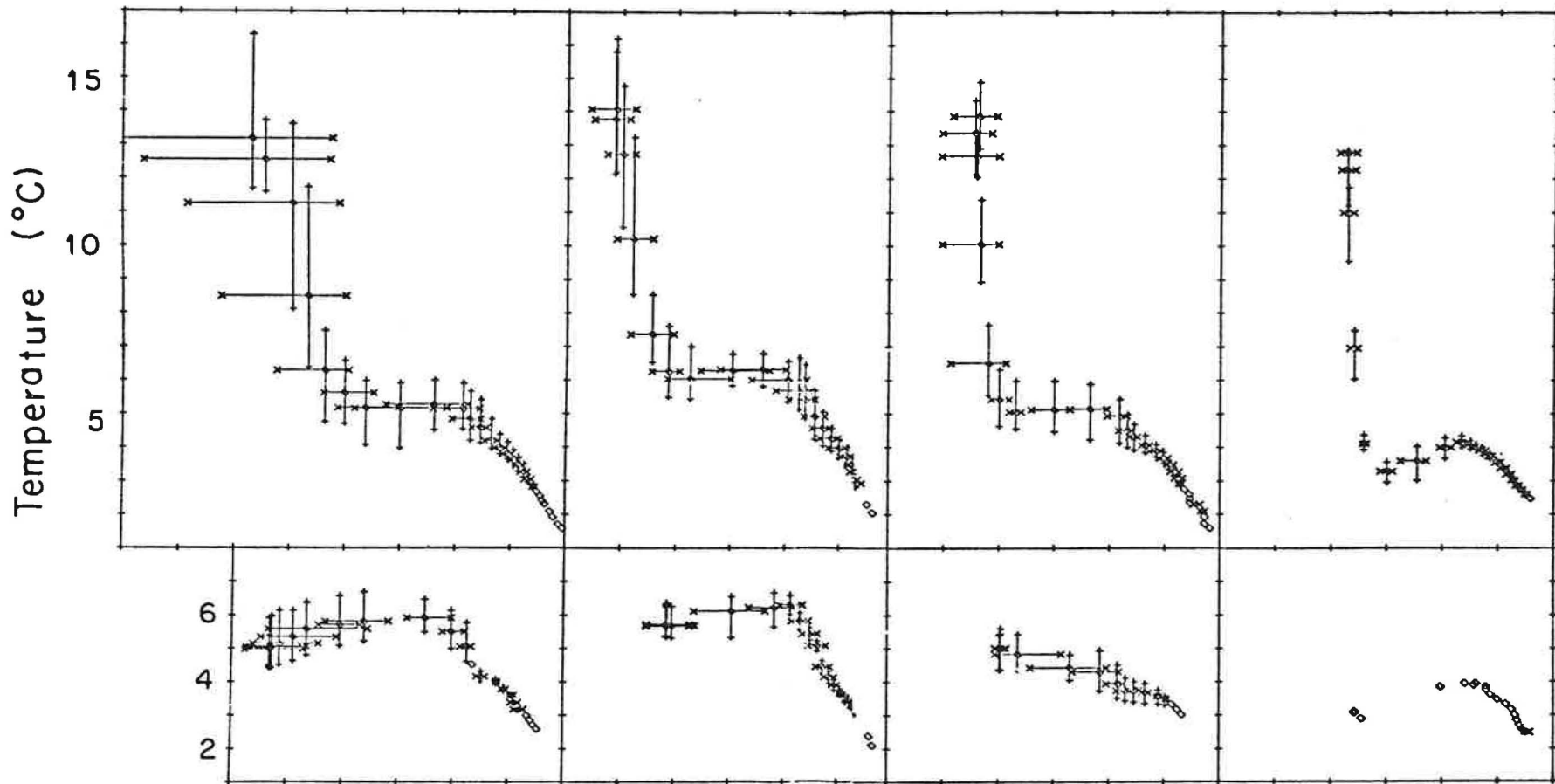


Figure 17. Maximum and minimum temperature-salinity (T-S) values at standard depths for the T-S curves shown in Figure 16.

limited to the upper 300 m of the water column and the greatest ranges occur in area A, primarily because that 2 x 2° quadrangle encompasses part of the continental shelf and is subjected to coastal runoff. Obviously conditions at the head of the gulf are dependent upon the relative components of flow in these three water masses.

III. CURRENTS

Bering, Chirikof, Cook, Clerke, Portlock, Dixon and countless other early explorers of the coastline around the gulf encountered the treacherous winds and coastal currents that exist in the area, and such information reported by mariners is constantly updated in the Alaska Coast Pilots. There are also early papers that synthesize this information. Wild (1877) presented a Current Chart of the Ocean that showed northward flow into the gulf stemming from a bifurcation of eastward onshore flow into northward and southward trending branches that occurred well seaward of Vancouver Island. Dall (1899) reported that the zone of separation was just seaward of Vancouver Island. Schultz (1911) indicated that only in summer did the separation occur at this latitude; during winter it occurred off the California coast near 41°N . Such schemes were largely based on sporadic reports and data from ship's logs, but the absence in the gulf of extensive commercial vessel traffic, whose daily observations of set and drift have provided an extensive historical data base on circulation in other areas, has resulted in a paucity of specific information concerning flow. Drift bottle studies provide information concerning gross circulation patterns, however, only the release and recovery points are known and actual trajectories are subject to various interpretations. The computation of geostrophic currents in which the relative field of currents is derived from the observed field of mass in the ocean, provides an indirect method of estimating oceanic flow. This method has several shortcomings and requires extensive synoptic observations at sea which are not possible to obtain from present platforms. Nevertheless, this method permits the calculation of relative currents and transports

that provide considerable insight into oceanic flow throughout the area observations are made. No significant direct current measurements have been made in offshore waters of the gulf prior to OCSEAP studies. However, measurements off the west coast of Vancouver Island where a similar climate occurs reveals interesting patterns of onshore and offshore flow that are probably duplicated in gulf waters (Dodimead et al. 1963).

A. Drift Studies

Long before planned drift bottle or drift float programs were instigated, the presence of debris from Japanese fishing operations and remnants of California redwood trees on the southeast Alaskan coast signaled two widely differing sources of water flowing into the gulf. Although there have been a number of recoveries of bottles or floats from a variety of experiments, there are several studies that provide most of the basic information that can be deduced by such studies.

The first extensive study was conducted by the International Fisheries Commission, (IFC)--predecessor to the International Pacific Halibut Commission (Fig. 18); over 4,000 bottles were released from 1930-34 (Thompson and Van Cleve, 1936). Those released along an east-west line across the gulf from Baranof to Kodiak Island and at several locations inshore along the Alaska Peninsula in spring 1930 indicated a broad northward flow into the head of the gulf, with recoveries only at Cape St. Elias and Cook Inlet, and a southwestward drift along the Alaska peninsula and through Unimak Pass. Releases just east of Kodiak Island were recovered only along the southern coast of the island and on the Alaska peninsula to the west and north of the island; releases from three locations inshore along the Alaska Peninsula indicated a southwestward drift along the coast. Releases off the west coast of the

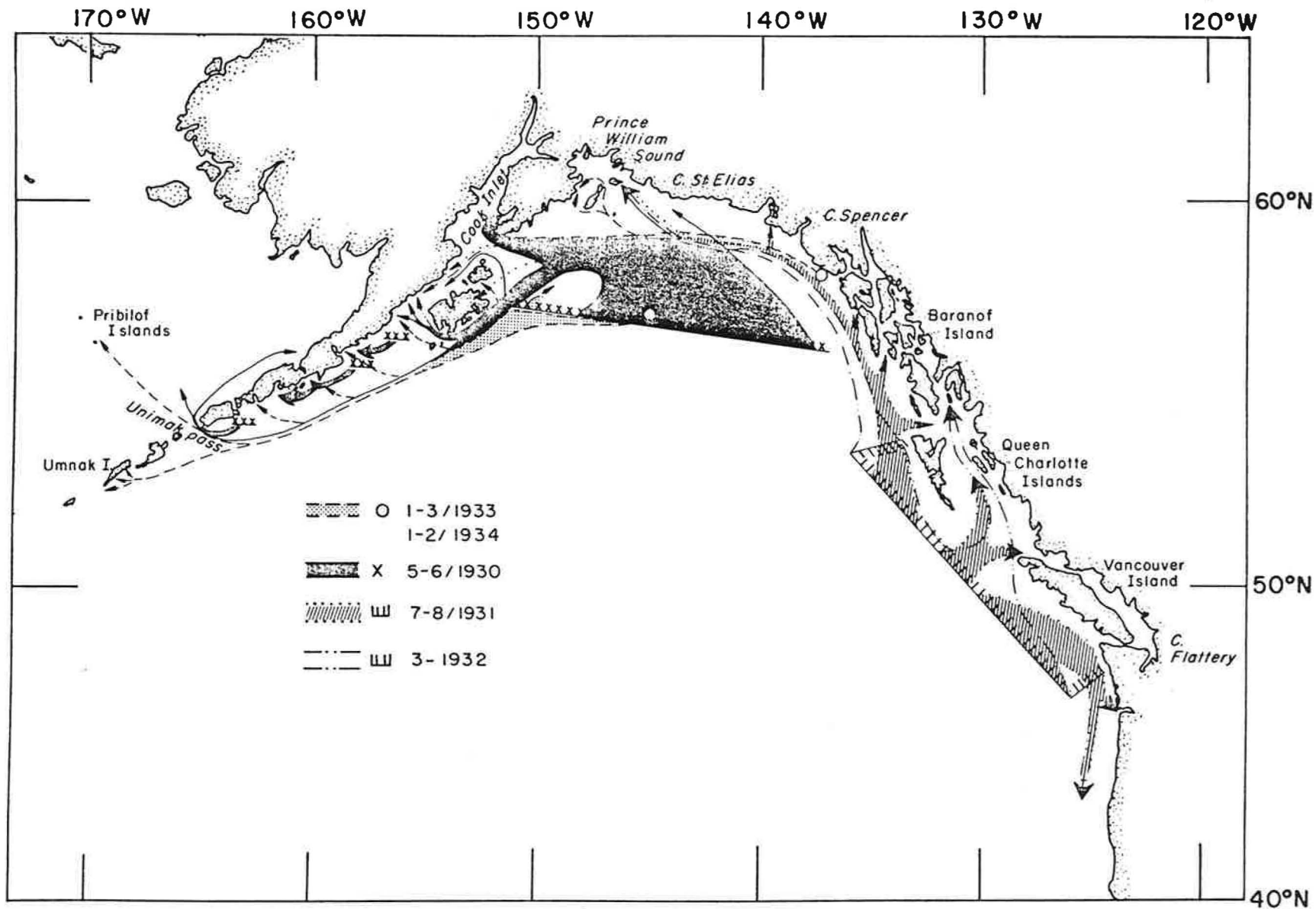


Figure 18. Schematic diagram of significant results of drift bottle studies conducted by the International Fisheries Commission (IFC) 1930-34 (adapted from Thompson and Van Cleve, 1936).

Queen Charlotte and Vancouver Islands in summer 1931 indicated a marked bifurcation of onshore flow at the northern end of Vancouver Island. Two bottles in the northern component of flow were recovered near Cape Spencer and one on Kodiak Island. In a similar experiment in spring 1932, except for one recovery at Cape Flattery (directly east of the release point), all recoveries were made northward of the release points, at various locations around the gulf. The western most recovery was made in Shelikof Strait and numerous recoveries were made in Prince William Sound where none was recovered in the 1930 and 1931 experiments. Releases north of $50^{\circ}30'N$ and recovered north of $57^{\circ}N$ were estimated to travel 9.4 miles per day. In winter 1933 and 1934, releases just north of Cape Spencer were recovered in Prince William Sound, along the west coast of the gulf, and on the Pribilof and Umnak Islands. These studies reflected a southward shift in winter of the zone of separation of the onshore flow off Vancouver Island that had been indicated earlier (Schutz, 1911). The northward branch, which moves cyclonically around the gulf, had a general drift of about 20 cm/sec and an inherent onshore component. Although a large cyclonic gyre encompassing the entire gulf at the latitude of Kodiak Island was inferred, there is no evidence other than delays between release and recovery to justify such a conclusion. The authors noted that, although westerly flow was predominant, at the head of the gulf, the currents were not regular or constant.

A subsequent experiment was conducted by the Pacific Oceanographic Group (POG), Nanaimo, from August 1956 to August 1959 (Dodimead and Hollister, 1962). Forty-two releases (33,869 bottles) were made from Ocean Station "P" ($50^{\circ}N$, $145^{\circ}W$) and surrounding locations. Twenty-three of the releases

were made at Ocean Station "P" at approximately 6-week intervals and these indicated a fairly complicated pattern in drift currents between the station and the North American coast. For example, of 998 bottles released on August 25, 1956 only one of the 114 recoveries was made north of Ketchikan and it was made on Middleton Island; whereas of 1,008 bottles released on August 24, 1957, all of the 39 recoveries were made at or west of Middleton Island. Of particular interest to the present study are the 5 releases north of Ocean Station "P", especially the 2 that were made north of 55°N . At the 3 locations south of 55°N between 155 and 160°W , an easterly set was indicated, recoveries being made throughout the head of the gulf. However, recoveries from the two releases north of 55°N (approx. 142°W) made on February 17, 1957 and August 17, 1957 were made only at the western side. Perhaps of more significance is that recoveries from the winter release (Fig. 19) were recovered as far north as the Pribilof Islands, as far west in the Aleutian area as Amchitka Island, as far east as the Washington-Oregon-California coast, and as far south as the Hawaiian Islands and Wake Islands--a tremendous dispersal that requires considerable thought when one contemplates possible oil pollution in the head of the gulf and the subsequent formation of floating tar balls.

Whereas the IFC studies were concerned with coastal drift ^{5/} and the POG studies largely with onshore drift from discrete offshore locations, the studies conducted by the National Marine Fisheries Service Northwest Fisheries Center (formerly Bureau of Commercial Fisheries Biological Laboratory) extended over a large area of the northern North Pacific Ocean.

^{5/} See Ingraham and Hastings (1974) for results of seabed drifter study off Kodiak Island in May 1972.

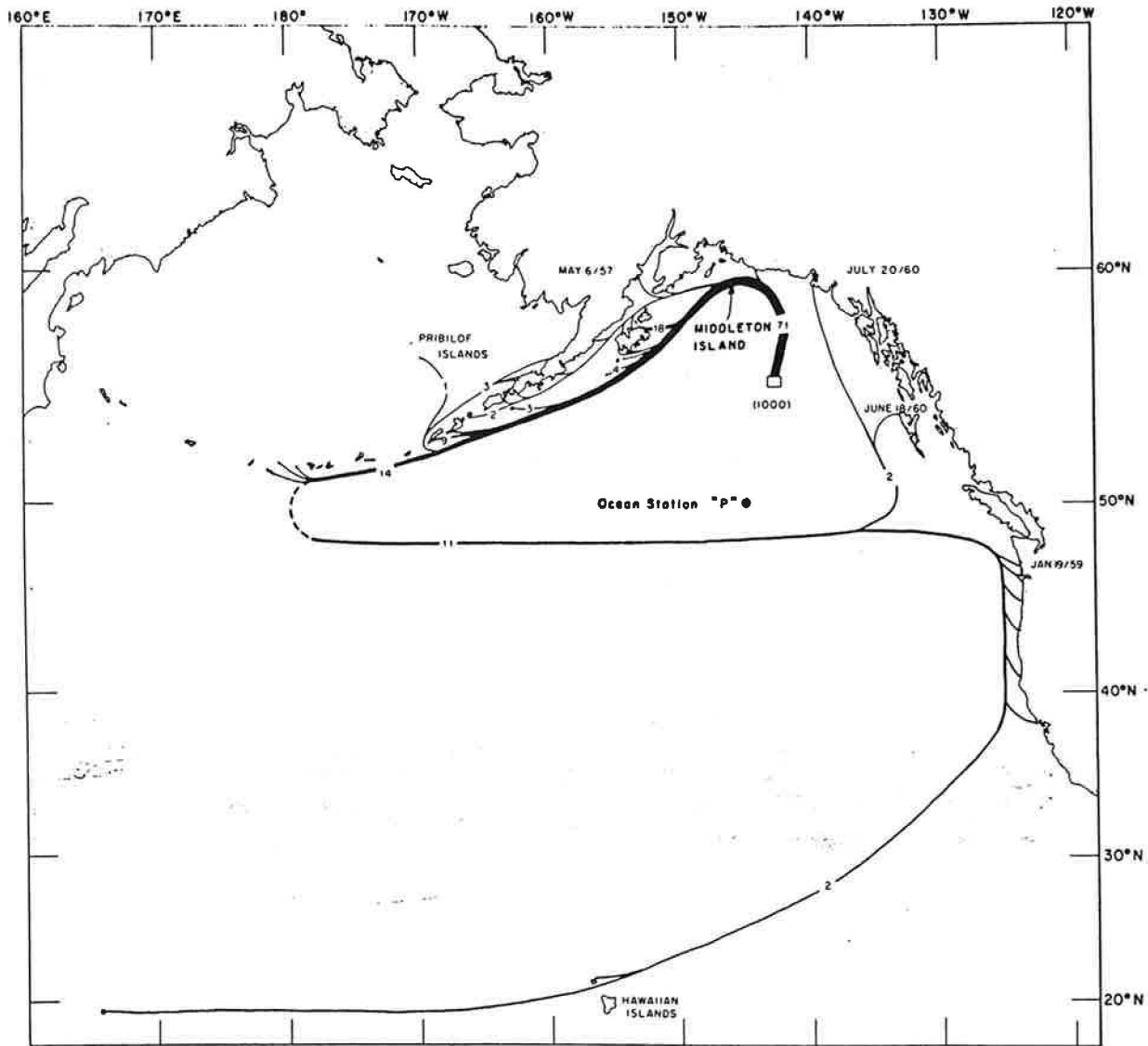


Figure 19. Release and recovery locations of drift bottles released by the Pacific Oceanographic Group (Nanaimo) in February 1957 showing the wide dispersal to the Bering Sea, the Aleutian Islands, Washington-Oregon-California coast, the Hawaiian Islands and Wake Island (from Dodimead and Hollister, 1962)

The two experiments that pertain to flow in the gulf were conducted in 1962 (Favorite, 1964) and in 1964 (Fisk, 1971); releases made along extended north-south and east-west cruise tracks (Fig. 20) indicated the broad north-south oceanic boundaries of eastward surface flow that moves directly into the gulf or toward the coasts of British Columbia, Washington, and Oregon where, in winter, a northward flow surfaces along the coast (Reid, Roden and Wyllie, 1958; Burt and Wyatt, 1964; and others).

B. Geostrophic Flow

The geostrophic (dynamic) method has been thoroughly described and evaluated (e.g. Fomin, 1964); basically, the method, which requires a balance between Coriolis and pressure gradient forces permits the computation of current relative to that at an arbitrary and perhaps fictional depth, selected in the belief that it is deep enough for isopleths of density and pressure to be parallel and thus a depth or level at which no motion exists (a zero reference level); no accelerations or physical boundaries are permitted. Fleming (1955) has presented a chart showing the locations in the northern North Pacific Ocean where the oceanographic station data required by his method had been obtained prior to 1955, and Dodimead et al (1963) showed station locations from 1955-59, as well as winter and summer fields of geopotential topography. McEwen, Thompson and Van Cleve (1930) and Thompson, McEwen and Van Cleve (1936) were the first to use this method in the Gulf of Alaska and found a westward flow in excess of 50 cm/sec at the edge of the continental shelf. The complexity of geostrophic flow in this area was evident in the closely spaced station data obtained by Doe (1955). Roden (1969) and Thomson (1972) have contributed to present knowledge of flow around the gulf.

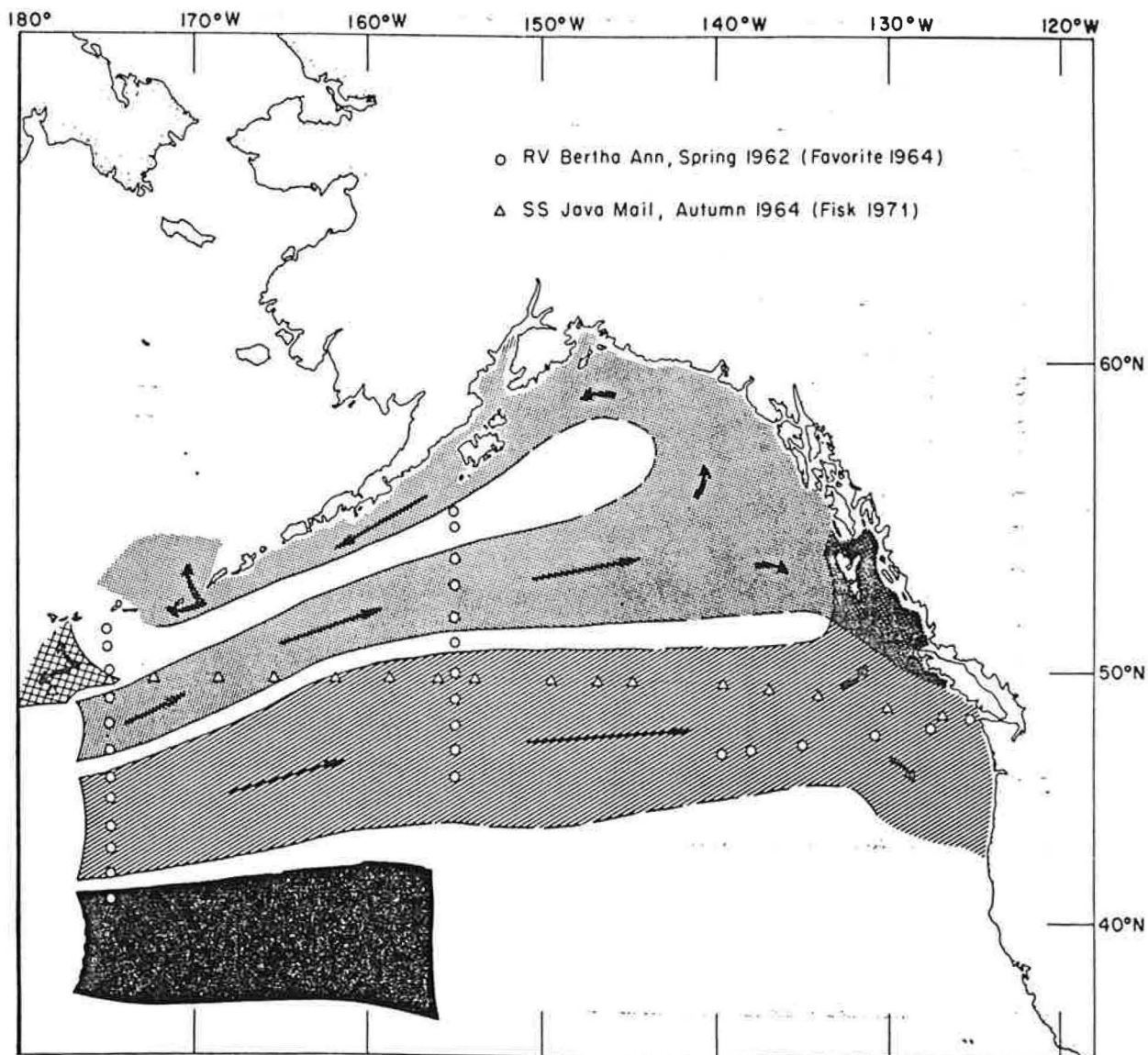


Figure 20. Schematic diagram of results of drift bottle studies by the Northwest Fisheries Center (Seattle) in 1962 and 1964 showing the general nature of easterly onshore drift.

The locations of all oceanographic station data on file at NODC (prior to OCSEAP studies) and used in this report are shown in Figure 21. Current speeds normal to a line between two oceanographic stations are obtained by the Sandstrom Helland-Hansen equation:

$$V = \frac{10}{f\Delta x} \left[\int_0^D \delta_1 dp - \int_0^D \delta_2 dp \right] \quad (1)$$

where D is the accepted depth-of-no-motion expressed in decibars; δ , the geopotential anomaly; x, distance between stations; f, Coriolis acceleration; and, p, pressure.

Computations of geopotential anomalies at all stations were averaged by 2 x 2° quadrangles to obtain long-term means and seasonal (winter, spring, summer and autumn) means for the depth intervals 0/300 db, considered to be the layer of seasonal influence, and 0/2000 db, where 2000 db is considered to represent a level-of-no-motion. Mean values over such large areas (over 20,000 km) cannot be expected to reflect boundary currents over the narrow continental slope but general circulation patterns are evident. Data for winter, spring and summer are sparse, from 1 to 30 or more observations per quadrangle, with an average of about 10; data for autumn are only 20% available. At Ocean Station "P", observations are more numerous and provide at least a qualitative check on surrounding data. For example, in the mean summer data there are 112 observations at the quadrangle associated with Ocean Station "P"; mean value 0.53 dyn cm; although there are only 11 observations in the quadrangle to the west, and 10 in the quadrangle to the east, the mean values are 0.52 and 0.53 dyn cm respectively.

The seasonal mean fields of geopotential topography for the depth interval 0/300 db (Fig. 22) are quite similar. The longitude of the topographic low, 149°W is the same for all seasons but the latitude shifts

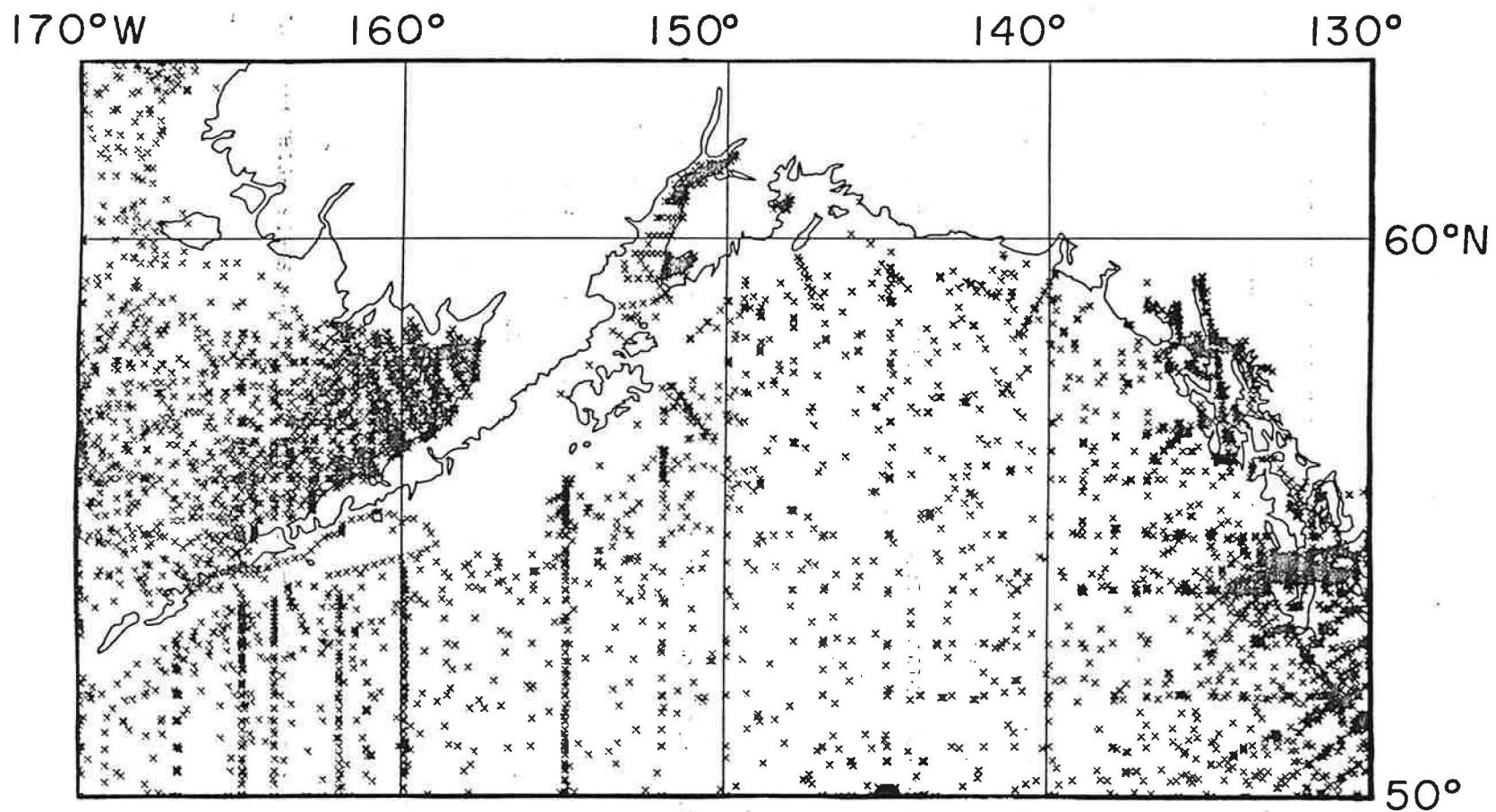


Figure 21. Locations of oceanographic stations in National Oceanographic Data Center geofile.

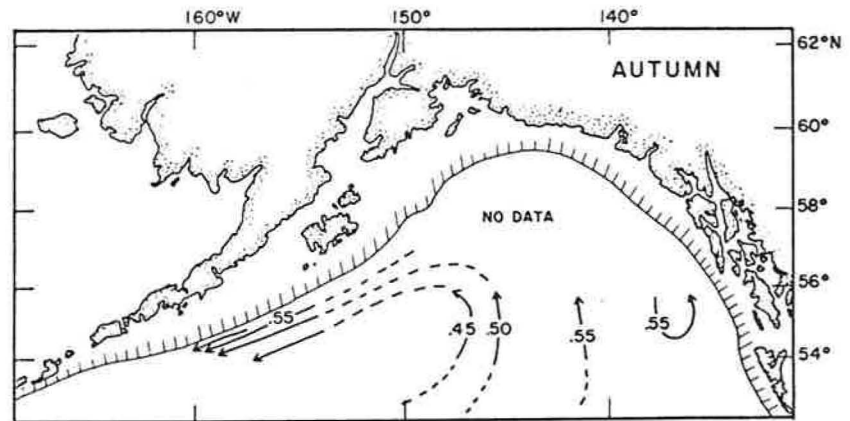
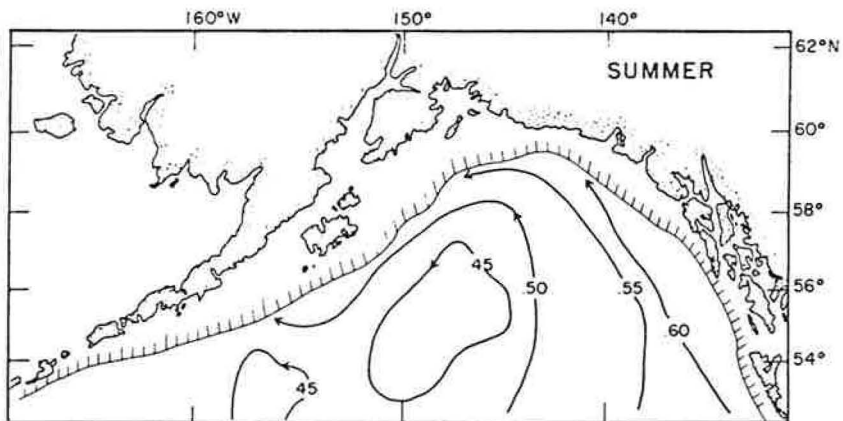
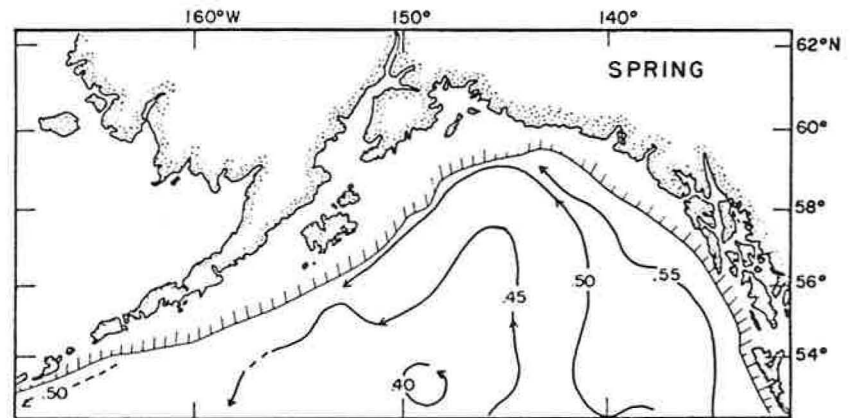
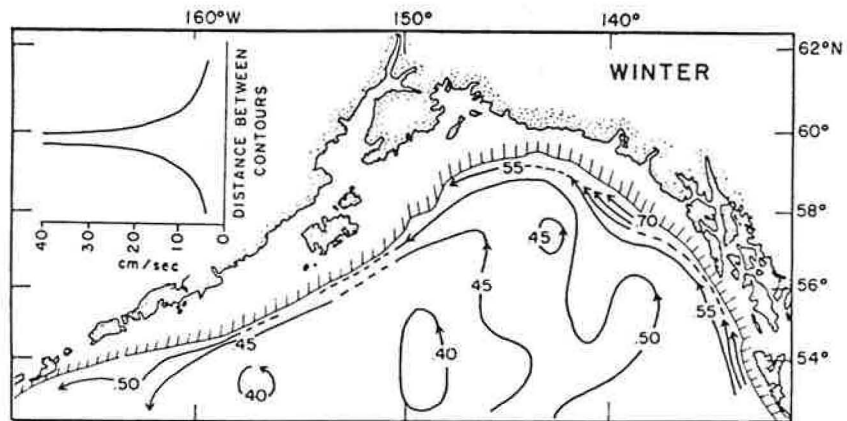


Figure 22. Long-term seasonal mean geopotential topographies, 0/300 db, (based on $2 \times 2^\circ$ grid) showing variability in geostrophic flow particularly the high velocities at the eastern side of the gulf (the broad grid spacing prevents showing the boundary current at the western side).

from 53°N in spring to 55°N in summer while winter is intermediate at 54°N (autumn data is lacking). Although numerous variations in the configurations of the respective isopleths occur, there is a difference of 15-20 dyn cm between the topographic low in the southwestern part of the gulf and the topographic high near the coast at the eastern edge of the gulf. Further, isopleths are not continuous around the gulf but, rather than representing a discontinuity in flow, as will be shown in the next section, this is primarily due to narrow width of the boundary current in the northern and western part of the gulf. Speeds of 3 - 5 miles per day and a northward transport, east of the topographic low, of 3 Sv are indicated.

The winter and summer mean fields of geopotential topography for 0/2000 db (Fig. 23) are generally similar to those for 0/300 db. The position of the topographic low remains near 55°N , 149°W . The difference in topography across the eastern side of the gulf changes from 35-40 dyn cm in summer to 50 dyn cm in winter indicating some winter acceleration; speeds are 20 and 25 cm/sec and transports are 12 and 15 Sv, respectively. Isopleths at northern and western sides of the gulf are discontinuous as before. As might be expected from the foregoing, the long-term mean field of geopotential topography for 0/2000 db is not much different from either of the above and the apparent conclusion one can draw is that in winter the baroclinic mode reflects an increase in flow of about 20 percent, and this increase stems largely from adjustment in the mass field below 300 m.

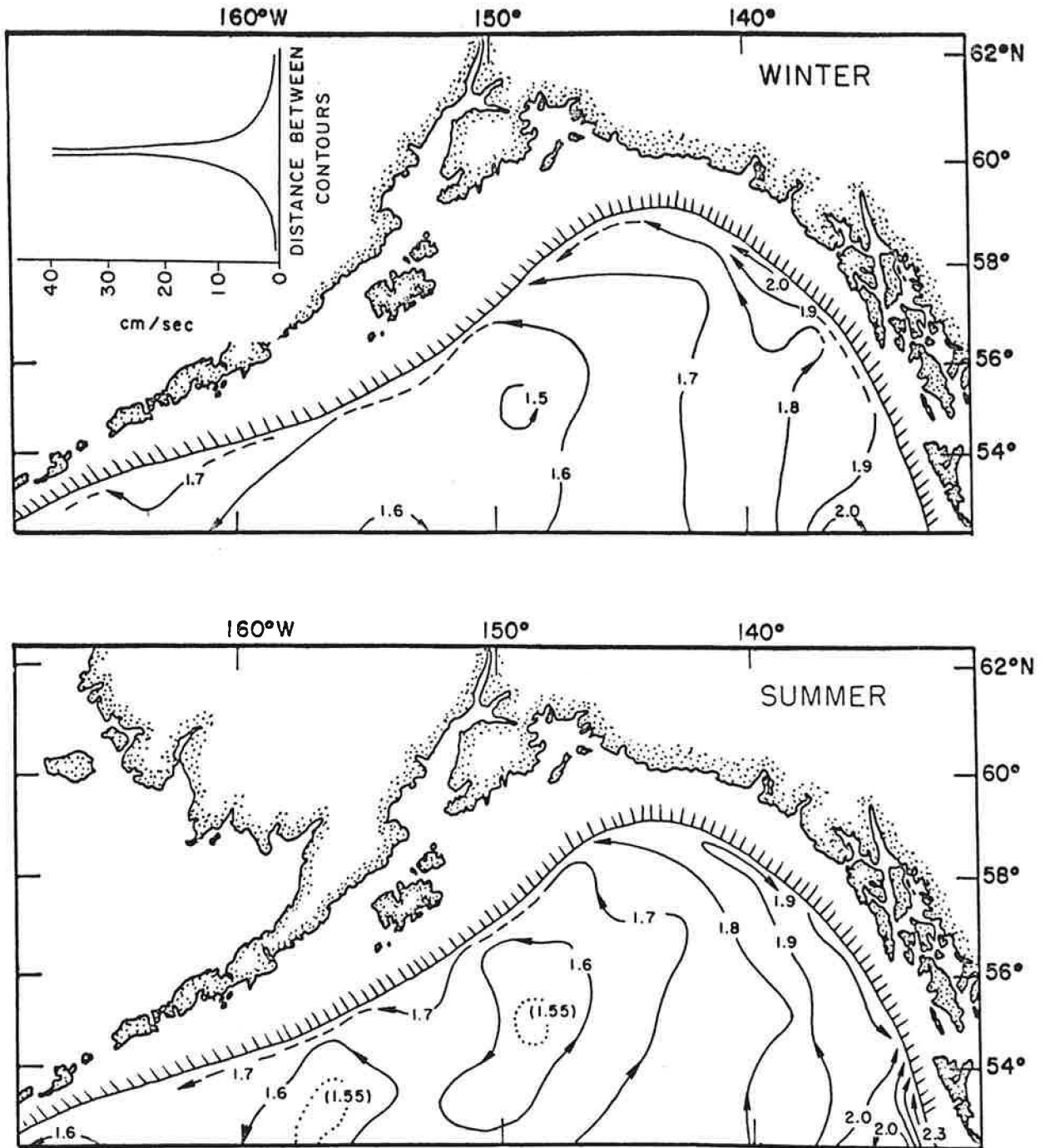


Figure 23. Long-term seasonal geopotential topographies 0/2000 db (based on $2 \times 2^\circ$ grid) showing generally similar features of cyclonic flow.

Because of the paucity and non-synoptic nature of the station data in the gulf, it is difficult to ascertain if irregularities in geopotential topographies are real or caused by the lack of synoptic data. However, there are three aspects that can be explored: are there patterns in individual years that are not obvious in the mean flow; what are the apparent fluctuations in transport, and do accelerations in the boundary current result in discontinuities in geostrophic flow on the western side of the gulf? Because most of the data that permit answering these questions were obtained in the period 1955-63 and many of the observations were limited to 1000 m at that time (even though this was not considered a realistic level-of-no-motion), some comparisons must be made in reference to this level.

One pattern that is represented in one form or another is an extensive perturbation in the northward flow at the eastern side of the gulf. Examples of this are found in the geopotential topography (0/1000 db) for winter and summer 1957 (Fig. 24). The configuration of the isopleths suggests a possible blockage of westward flow at the head of the gulf resulting in a seaward plume that extends over 500 km in a southwesterly direction. The apparent effect of this phenomenon is a convergence of isopleths, and thus an acceleration of northward flow, at the eastern side of the gulf. Unfortunately neither closely spaced or repetitive stations have ever been made in this area so the actually physical nature or cause of this feature cannot be ascertained. This is also true of features at the western side of the gulf. At times there is an

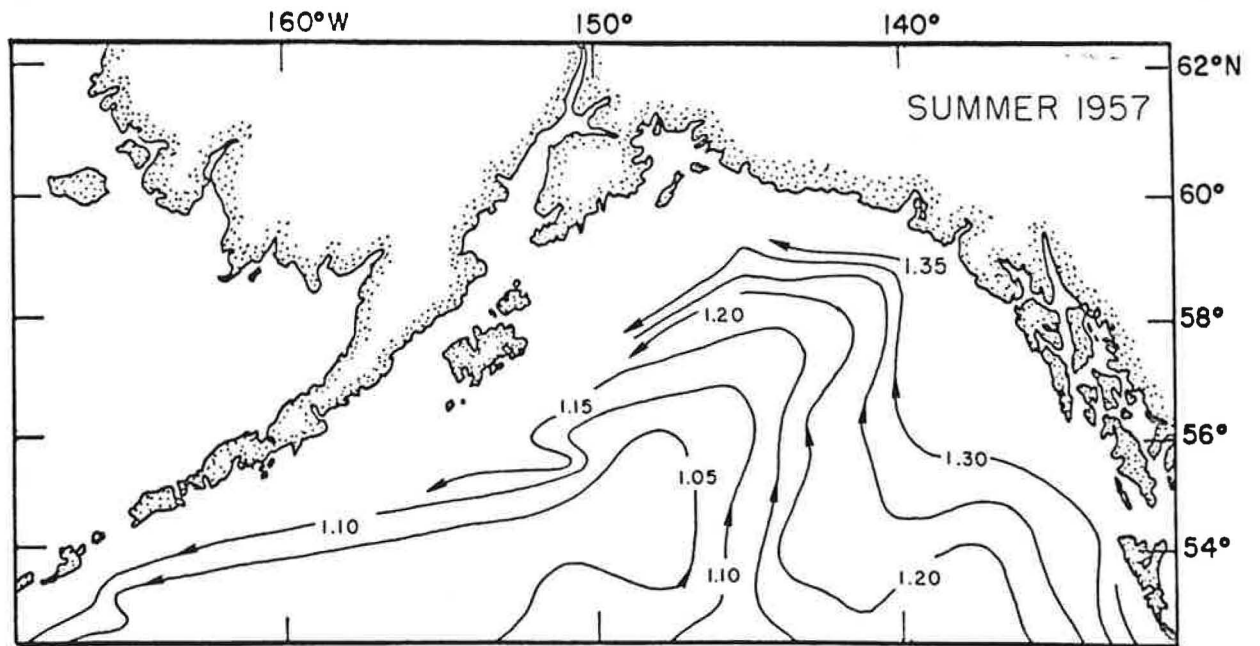
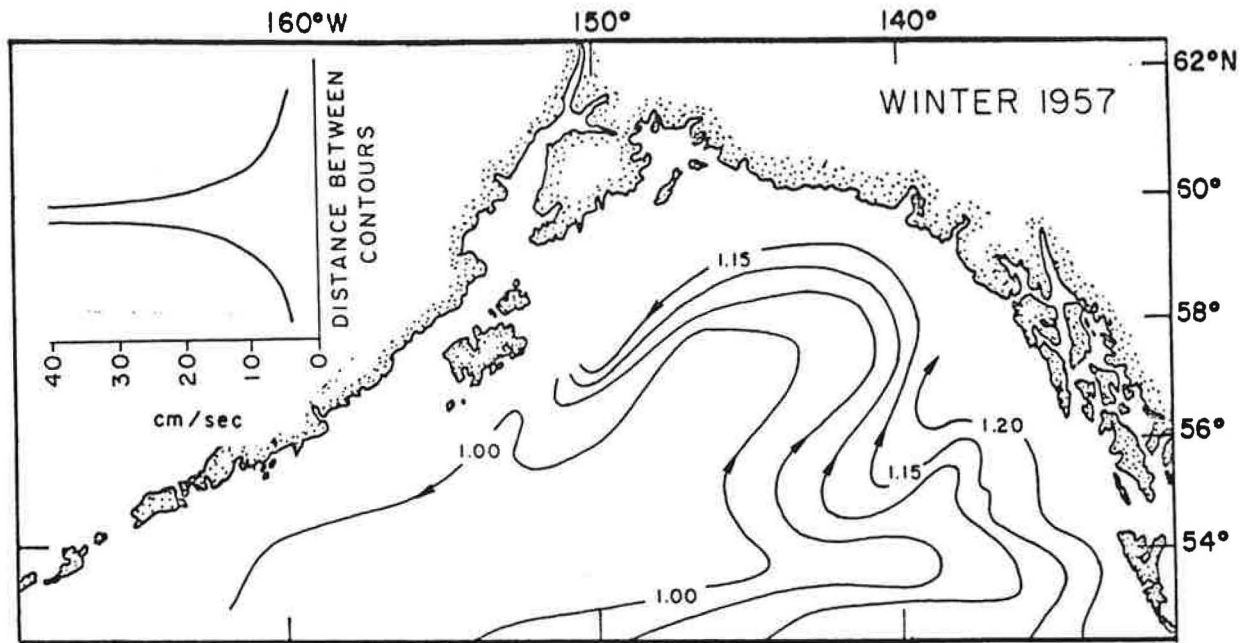


Figure 24. Geopotential topographies, 0/1000 db, winter and summer 1957 showing perturbation in flow at eastern side of the gulf.

indication of eddies breaking off to the east of the boundary current seaward of Kodiak Island (Dodimead et al, 1963), but there is also evidence that this is not a permanent feature of flow in this area.

The question as to whether or not there is continuity of geostrophic flow around the gulf would require extensive observations and extensive direct current measurements. However, some new insight into the boundary flow was obtained in 1972 when closely spaced observations were made on transects of the continental shelf and slope approximately 100 km apart east of Kodiak Island (Favorite and Ingraham, 1976a). It was discovered that approximately 70% of the westward flow out of the gulf occurred within 50 km of the shelf. Geostrophic velocities of 50 cm/sec (referred to 1000 db) occurred in a narrow band approximately 20 km wide and in one instance, velocities of 100 cm/sec (referred to 1500 db) were estimated within a 10 km band. Little evidence of any major perturbations were evident in the nearly 600 km stretch along the continental slope in this area. Thus, it would appear that when appropriate observations are made, fairly reasonable continuity may be obtained.

C. Volume Transports

Fluctuations in transport can be estimated by the difference in geopotential topography across the eastern part of the gulf. Data from 1954-62 (Table 1) indicates that the mean transport from 0 - 1000 m is approximately 8 Sv and individual values range from about 6 - 12 Sv, with no particular pattern to winter or summer values. Bennett (1958) reported that when observations are available to 2000 m the transport nearly doubles to approximately 15 Sv, with individual values ranging

Table 1. Northward volume transport (0 to 1000 m - to the nearest 0.5 Sv) into the gulf across 55°N; computed from geopotential topography (the lowest value in the Alaskan Gyre versus the inshore value at the location of the 1000-m isobath at the eastern side of the gulf).

Period	Transport (Sv)
1954 (summer)	9.0
1955 (summer)	9.0
1956 (summer)	7.5
1957 (winter)	6.5
1957 (summer)	7.0
1959 (winter)	8.5
1959 (summer)	9.0
1960 (winter)	12.0
1960 (summer)	8.0
1961 (spring)	6.5
1962 (spring)	6.5
Mean	8.1

from 13.5 - 16 Sv, and again no particular pattern to winter and summer values is evident. Thus, it would appear that the year to year seasonal fluctuations may be as great or greater than the within year seasonal ones.

IV. WIND STRESS-TRANSPORTS

Because of the paucity of data on actual winds, the wind-stress at the sea surface is obtained from distributions of sea level pressure. It should be noted at the outset that there is an unavoidable bias in long-term sea level pressure data because of not only the varying intensity and location of reports from shipping, but because of modern devices and techniques. The establishment of Ocean Station "P" in the mid-forties, the availability of satellite imagery showing cloud patterns in the mid-sixties, and the placement of ocean data buoys in the mid-seventies, all permit an increasingly better estimate of the sea level pressure fields and associated gradients. Several grid spacings are used in this report and each will be defined as encountered.

A. Pressure Fields

In order to obtain an initial assessment of variability of pressure, the historical sea level pressure data at $5 \times 5^{\circ}$ grid points were obtained from the National Center for Atmospheric Research (NCAR) and monthly mean fields (composed of 12 hourly and in some instances 24 hourly data) from 1899-1972 were plotted to ascertain the relative frequency at which the central pressure of the Aleutian low falls within the selected low pressure intervals (Fig. 25). In 6 instances the monthly mean pressure was less than 985 mb, these occurred in either December or January; in 32 instances it was less than 990 mb, all occurred from October to March; and in 91 instances it was less than 995 mb, all occurred from September to April. Although it appears that data from 1899-1950 are fairly representative of the period 1950-1972, we are concerned with the curl of the wind-stress and therefore details of the first and second derivative fields, and not

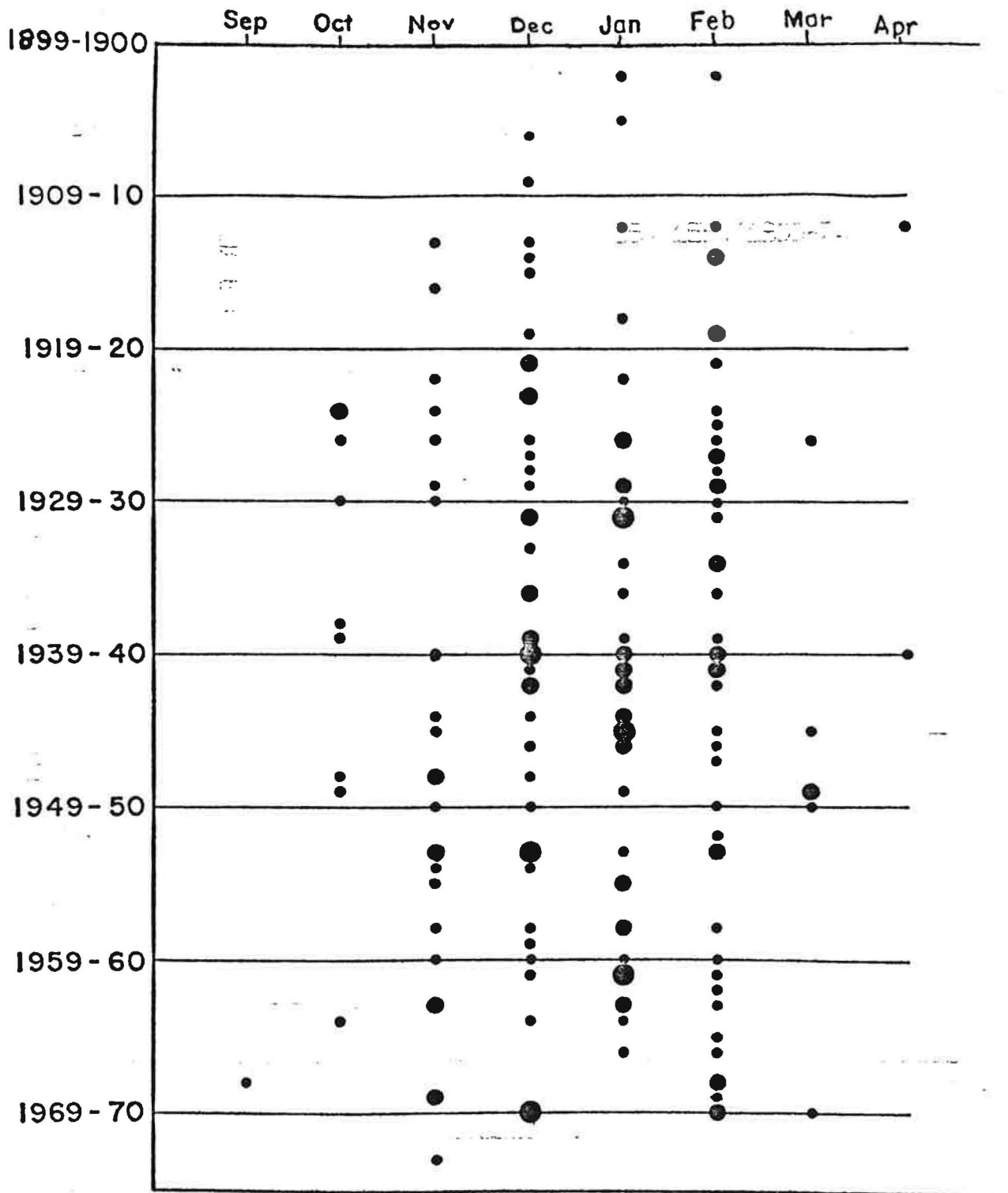


Figure 25. Frequency of monthly mean sea level pressure minima of the Aleutian low: <995 mb (●), <990 mb (●), and <985 mb (●).

merely the absolute value of pressure minima. If we choose 55°N , 155°W near the approximate center of the Alaskan Gyre, data at this grid point, deviations from monthly means, 12-month running means and power spectrum provide an indication of the general variability of sea level pressures. Deviations from monthly mean pressures do not exceed ± 5 mb and, except for the extended period, roughly 12 years, of positive deviations from 1901-1912 (which may be due to limited data), departures from normal are generally of 1-4 years duration. Particularly noticeable is the extended period of below normal pressures centered around 1940. The power spectrum (cycles less than 1.5 years not shown because of the obvious annual periodicity) based on annual mean values reflect cycles of 2.7, 6.7 and 13.3 years (Fig. 26). The 6.7 years is the approximate periodicity of oceanic temperature cycles (5.6 years) found by Favorite and McLain (1973). The 13.3 years suggests an influence of the sunspot cycle of ~~13.3~~^{11.1} years. Favorite and Ingraham (1976b) have shown that if mean pressures from October to March for the three years centered around the period of sunspot maxima and minima from 1899 - 1972 are calculated, with only one exception (1958), the center of the Aleutian low occurs in the central Aleutian area during periods of the sunspot maxima and in the Gulf of Alaska during periods of the sunspot minima; mean pressures are 2 mb lower during the latter period.

B. Transport Fields

Total integrated transports (wind-stress transports) are derived from the mean pressure fields by deriving a wind field that is transformed into a stress field. The nature of the coupling of energy between wind-stress and water transport is not precisely known and certainly varies under different conditions. When the water is warmer than the air, a

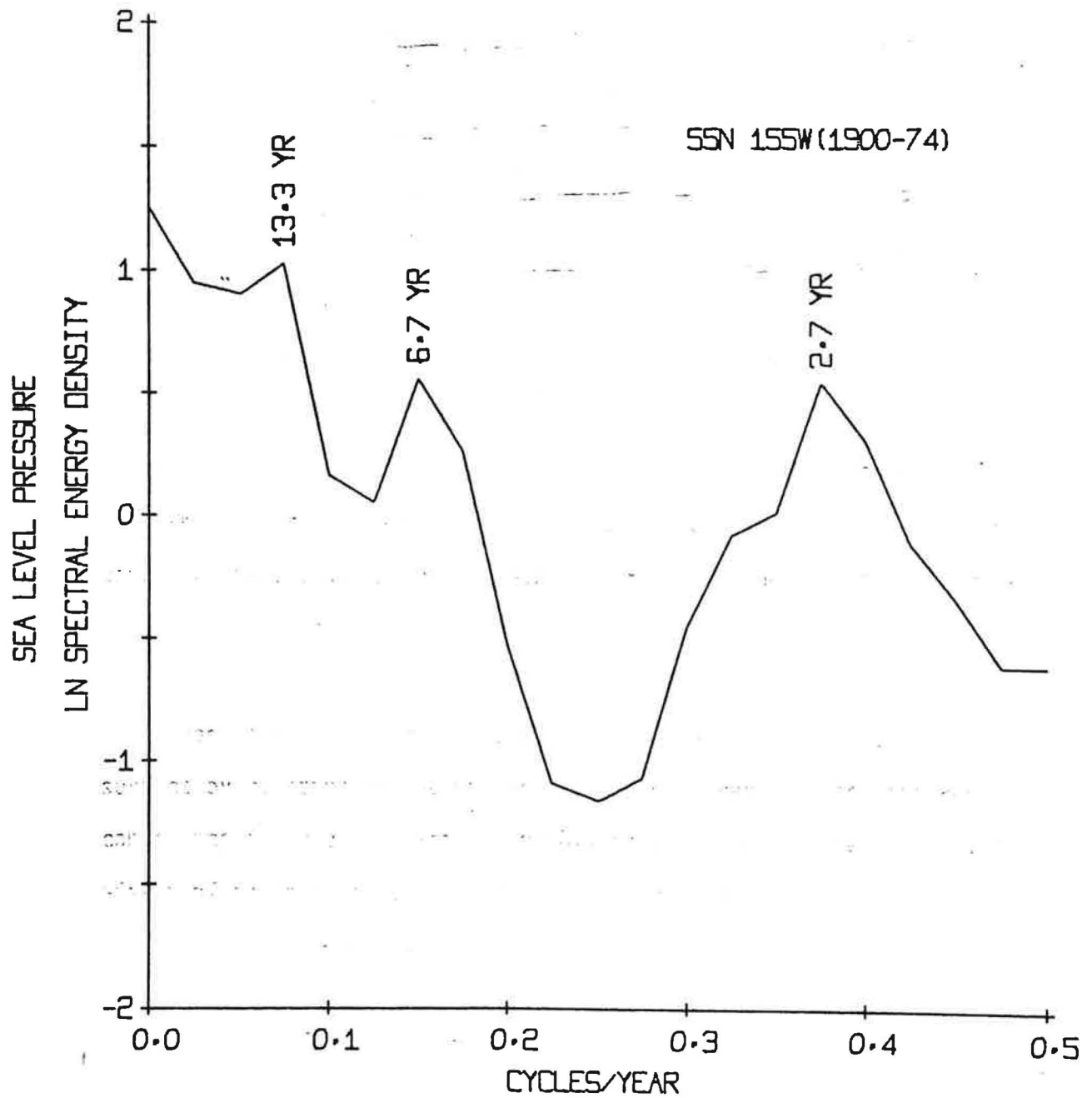


Figure 26. Spectral energy density, annual mean sea level pressure at 55°N, 155°W 1900-74 (20 lags) indicating cycles of 2.6, 6.7 and 13.3 years.

turbulent boundary layer exists and exchange of energy is more effective than when the water is colder than the air and a stable layer exists at the air-sea interface. Further, when interpolation and averaging processes are taken into account, caution must be exercised in interpreting results. However, a number of authors (e.g. Wyrтки, 1964) have indicated the usefulness of this technique in estimating flow.

Sverdrup (1947), by including the pressure gradient term in the Ekman transport equation, arrived at the following:

$$-f v = \frac{1}{\rho} \frac{\partial p}{\partial x} + \frac{\partial}{\partial z} \left(A_z \frac{\partial u}{\partial z} \right) \quad (2)$$

$$f u = -\frac{1}{\rho} \frac{\partial p}{\partial y} + \frac{\partial}{\partial z} \left(A_z \frac{\partial v}{\partial z} \right) \quad (3)$$

After cross differentiating and integrating from the surface to an unspecified depth-of-no-motion one obtains the transport equation:

$$M_y = \left(\frac{\partial \tau_y}{\partial x} - \frac{\partial \tau_x}{\partial y} \right) / \beta \quad (4)$$

where τ is the wind stress and β the variation of the Coriolis parameter with latitude $\left(\frac{\partial f}{\partial y} \right)$. This shows for steady non-divergent flow the total meridional transport, M_y , is directly related to the curl of the wind stress and independent of the details of the mass distribution as long as the pressure gradient is baroclinically compensated at depth.

Using the technique devised by Fofonoff (1962) and the program constructed by Bakun (1973), geostrophic winds were computed from sea level pressure values (interpolated from the $5 \times 5^\circ$ field) computed on an equilateral triangular grid, 222 km on a side, centered at 47°N , 170°W . Pressure data archived on magnetic tape were arranged on the computation grid surrounding each selected location using Bessel's central difference formula. Finite difference first and second derivatives were formed and the geostrophic wind field was computed in spherical

coordinates:

$$u_g = -\frac{1}{\rho R f} \frac{\partial P}{\partial \phi} \quad (5)$$

$$\frac{\partial u_g}{\partial \phi} = -\frac{1}{\rho R f} \left(\frac{\partial^2 P}{\partial \phi^2} - \frac{\partial P}{\partial \phi} \cot \phi \right) \quad (6)$$

$$\frac{\partial u_g}{\partial \lambda} = -\frac{1}{\rho R f} \frac{\partial^2 P}{\partial \lambda^2} \quad (7)$$

$$v_g = \frac{1}{\rho R f \cos \phi} \frac{\partial P}{\partial \lambda} \quad (8)$$

$$\frac{\partial v_g}{\partial \phi} = \frac{1}{\rho R f \cos \phi} \left(\frac{\partial^2 P}{\partial \phi \partial \lambda} + \frac{\partial P}{\partial \lambda} [\tan \phi - \cot \phi] \right) \quad (9)$$

$$\frac{\partial v_g}{\partial \lambda} = \frac{1}{\rho R f \cos \phi} \frac{\partial^2 P}{\partial \lambda^2} \quad (10)$$

where ϕ and λ are the latitude and longitude coordinates respectively,

u_g and v_g are the eastward and northward components of geostrophic wind, p is the atmospheric pressure, ρ is the density of air (considered to be a constant equal to 0.00122 gm/cm³), R is the mean radius of the earth and f is the Coriolis parameter.

These are transformed to estimates of the wind field near the sea surface by rotating the geostrophic wind 15 degrees to the left and contacting it by 30 percent to approximate, in a simplified manner, the effect of friction in the planetary boundary layer:

$$u = a_1 u_g + b_1 v_g \quad (11)$$

$$\frac{\partial u}{\partial \phi} = a_1 \frac{\partial u_g}{\partial \phi} + b_1 \frac{\partial v_g}{\partial \phi} \quad (12)$$

$$v = a_2 u_g + b_2 v_g \quad (13)$$

$$\frac{\partial v}{\partial \lambda} = a_2 \frac{\partial u_g}{\partial \lambda} + b_2 \frac{\partial v_g}{\partial \lambda} \quad (14)$$

where u and v are the eastward and northward components of surface wind, \vec{V} , and the transformation coefficients are: $a_1 = 0.7 \cos(15^\circ)$,

$$b_1 = 0.7 \sin(15^\circ), a_2 = -0.7 \sin(15^\circ), b_2 = 0.7 \cos(15^\circ).$$

Derivatives of surface wind speed, $|\vec{v}| = \sqrt{u^2 + v^2}$ are computed according to:

$$\frac{\partial |\vec{v}|}{\partial \phi} = \left(u \frac{\partial u}{\partial \phi} + v \frac{\partial v}{\partial \phi} \right) \frac{1}{|\vec{v}|} \quad (15)$$

$$\frac{\partial |\vec{v}|}{\partial \lambda} = \left(u \frac{\partial u}{\partial \lambda} + v \frac{\partial v}{\partial \lambda} \right) \frac{1}{|\vec{v}|} \quad (16)$$

The stress on the sea surface, $\vec{\tau}$, was computed using a relatively high value, 0.0026, of the constant drag coefficient to partially offset the effect of using mean data:

$$\vec{\tau} = \rho C_D |\vec{v}| \vec{v} \quad (17)$$

$$\frac{\partial \tau_\phi}{\partial \lambda} = \rho C_D \left(v \frac{\partial |\vec{v}|}{\partial \lambda} + |\vec{v}| \frac{\partial v}{\partial \lambda} \right) \quad (18)$$

$$\frac{\partial \tau_\lambda}{\partial \phi} = \rho C_D \left(u \frac{\partial |\vec{v}|}{\partial \phi} + |\vec{v}| \frac{\partial u}{\partial \phi} \right) \quad (19)$$

where τ_ϕ and τ_λ are the northward and eastward components of $\vec{\tau}$. The curl of the wind stress is then determined as

$$\nabla \times \vec{\tau} = \frac{1}{R} \left(\frac{1}{\cos \phi} \frac{\partial \tau_\phi}{\partial \lambda} - \frac{\partial \tau_\lambda}{\partial \phi} + \tau_\lambda \tan \phi \right) \quad (20)$$

Integration of wind-stress curl along a parallel of latitude from an eastern boundary, in this case the west coast of North America, to successive grid points results in a total transport across that parallel of latitude; and eastward flow is obtained by satisfying continuity between grid points along two parallels of latitude. Welander (1959) has shown that wind-stress transport in a semi-enclosed basin (such as the Gulf of Alaska) must flow out in the form of a western boundary jet because

eastern boundary currents are excluded, thus, northward transports across 55°N are considered to exit the gulf along the western shore.

When one considers the nature of the variability in location and frequency of ship reports that make up the bulk of these pressure data, the averaging processes involved, and the theory employed, there are severe limitations associated with this method of obtaining flow, but it provides an indication of the continuity of events that is unattainable from the fragmentary station data obtained only aboard research vessels. Mean (1950-74) seasonal integrated total transports (Fig. 27) indicate a maximum northward transport in excess of 19 Sv into the gulf in winter and an accompanying closed circulation in the gulf area. Northward transport drops to less than 5 Sv in spring and summer and is concentrated at the western side of the gulf, whereas there is a suggestion of southward flow (< 1 Sv) at the eastern side. Intense northward transport greater than 15 Sv is reestablished in autumn, but the closed circulation evident in winter east of 155°W is not developed.

There are marked departures from mean conditions and these are most readily apparent in winter. Two winter periods, in 1963 and 1969, have been selected to reflect the range in values obtained in the period 1950-74 (Fig. 28). Computed northward transport in 1963 was less than 10 Sv, whereas, in 1969 it was nearly 3 times as great, in excess of 25 Sv. Thus, considerable variability in flow is indicated not only seasonally, but annually and marked deviations from the smoothed isopleths presented must occur. One can only conclude that, although a basic cyclonic flow

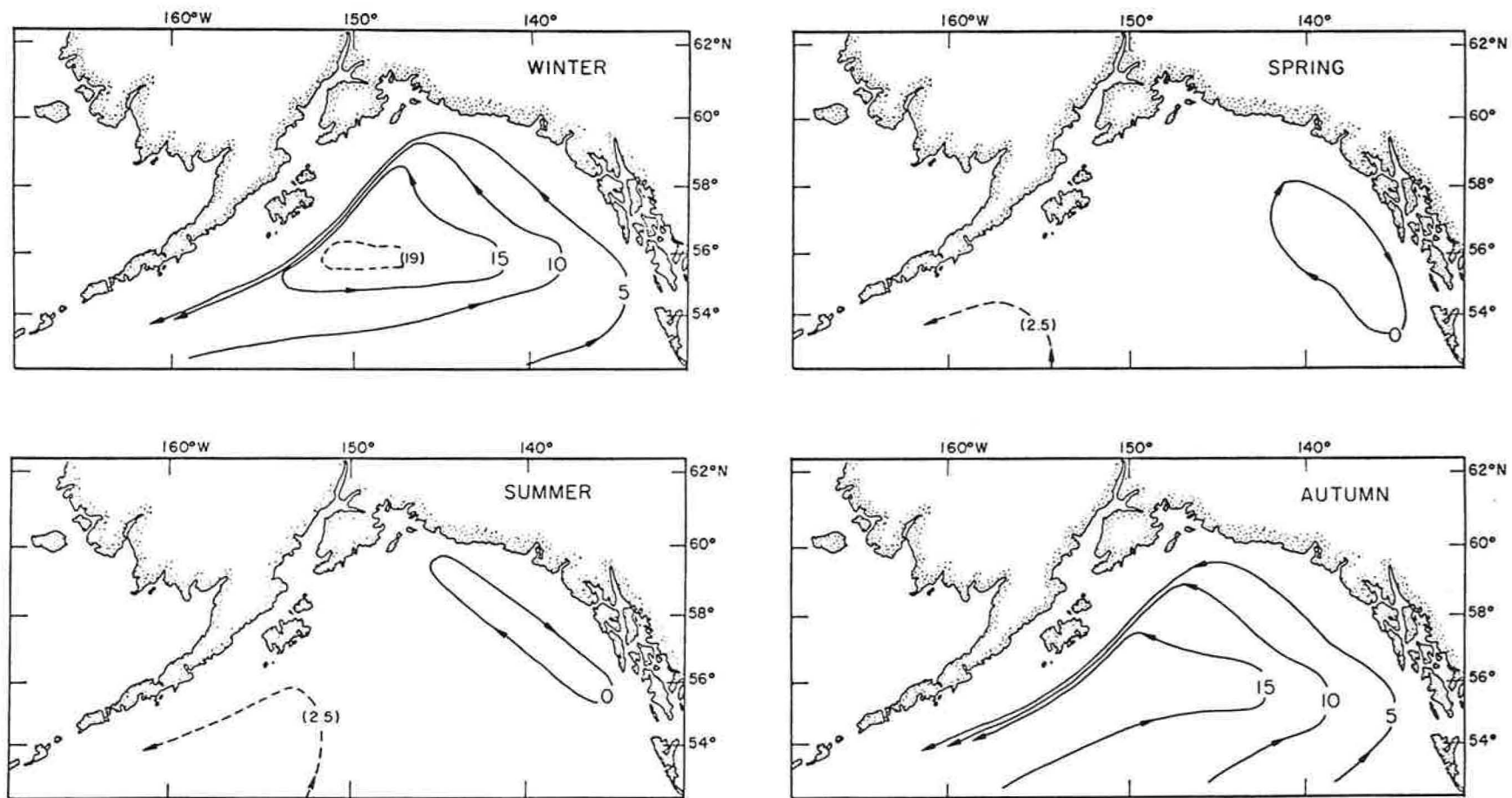


Figure 27. Seasonal mean (1950-74) integrated total transports (Sv) indicating general cyclonic flow with marked winter intensification of flow.

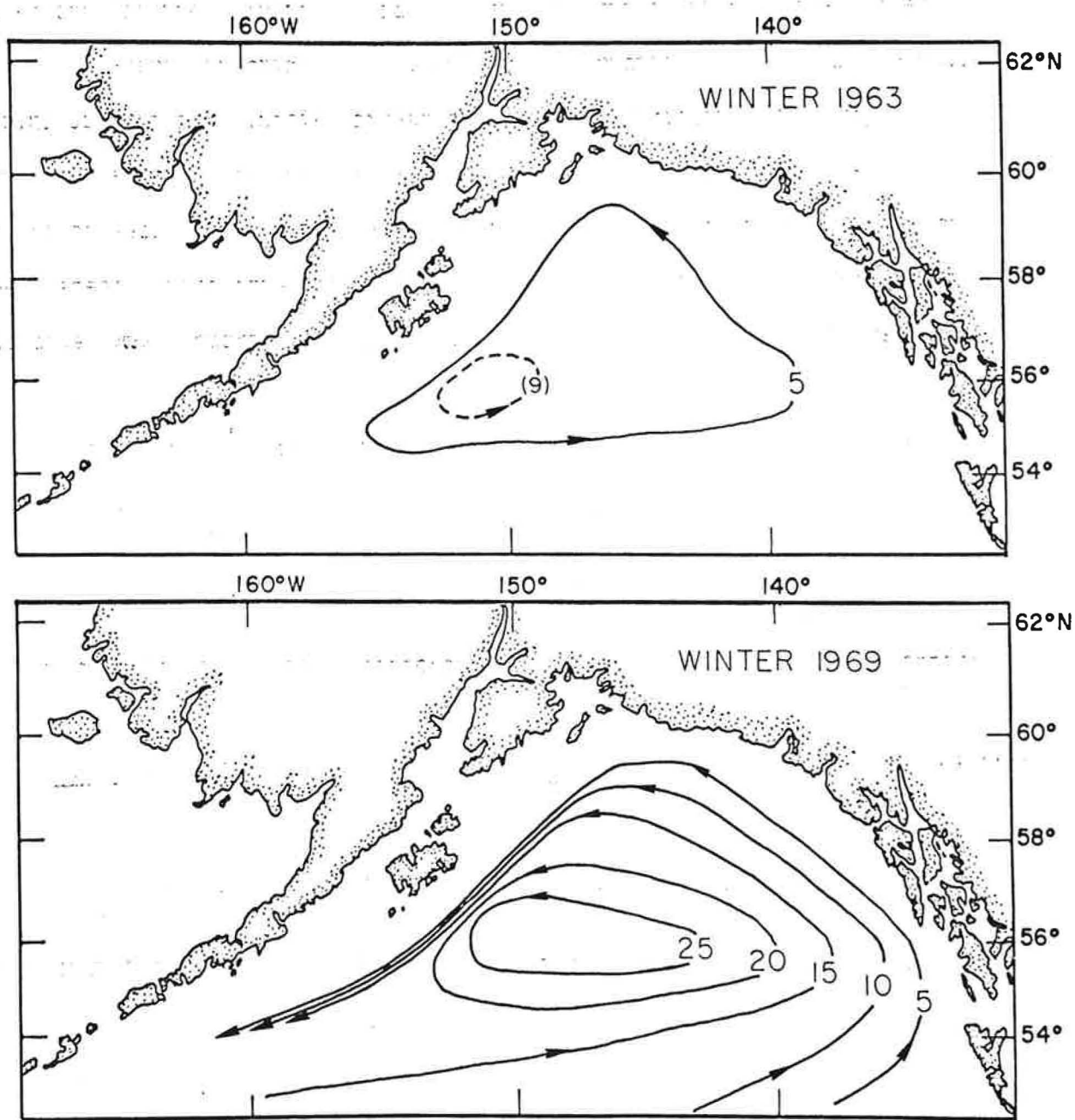


Figure 28. Total integrated transports (Sv) for winter (Jan. Feb. Mar.) 1963 and 1969 indicating variability in winter flow.

exists in the gulf, the variations and perturbations in flow due to variable wind-stresses result in a highly complex flow regime.

C. Numerical Model

Further refinements of estimates of water transport in the gulf, over those obtained by integrated total transport method, are obtained by expanding basic assumptions in the total integrated transport method to permit inclusion of variable bathymetry and to incorporate analyses in a numerical model first devised by Galt (1973) for an enclosed basin. This was configured to fit the North Pacific Ocean, Bering Sea, and Okhotsk Sea on the 222 km equilateral triangular grid mentioned in the previous section. Although limited to the barotropic flow assumption, the model provides an initial look at actual isopleths of flow considering the great increase in complexity of designing a baroclinic or multilayer model. Because of problems associated with specifying initial stream lines and vorticity on an arbitrary mid-ocean southern boundary for the Gulf of Alaska, the larger ocean area with a southern boundary far away from the area of interest was selected for the model. This exploratory version would show if a more detailed grid within the Gulf of Alaska as a subset of this large area model would be informative.

The basic model outputs are time dependent solutions of the transport stream function which, when presented in maps and contoured, give transport stream lines of flow. As before, the wind stress curl field is computed from sea level pressure; the bathymetry is scaled relative to the mean depth from flat bottom (0%) to actual bathymetry (100%) to simulate the effect of stratification; and coefficients may be selected which govern the

character of the solution by scaling the importance of nonlinear advection (α), lateral friction (β), and bottom friction (δ). As the model spins up from zero initial stream function and vorticity, maps may be obtained at any time interval which is a multiple of the time step (6 hours or less) to show the development of flow which in most cases reaches near steady state after about 60 days or 240 time steps. Caution must be taken when interpreting the results because of the barotropic assumption which allows minor changes in deep bathymetry to affect flow. Further, short (one month or less) periods of unusually intense wind stress curl patterns give unrealistically high transports if run to a steady solution a considerable time beyond their actual duration.

The model is based on a nondimensionalized vorticity equation (1) which is obtained by cross differentiation and subtraction of the vertically integrated equations of motion:

$$\frac{\partial \xi}{\partial t} = (\nabla \times \psi \bar{\kappa}) \cdot \left(\frac{\alpha \xi + f}{h} \right) + \beta \nabla^2 \xi - \frac{\delta}{h} \left[\xi + \nabla \psi \cdot \nabla \left(\frac{1}{h} \right) \right] + \nabla \times \left(\frac{\tau}{h} \right), \quad (21)$$

where ξ is the vertical component of vorticity $\left(\frac{\partial v}{\partial x} - \frac{\partial u}{\partial y} \right)$; u and v are the horizontal components of velocity; h is the depth, f is the Coriolis parameter; α , β , and δ are constants that specify the effectiveness of the nonlinear advection, horizontal and vertical frictional forces respectively; τ is the wind stress; and ψ is the transport stream function defined by $-hu = \frac{\partial \psi}{\partial y}$ and $hv = \frac{\partial \psi}{\partial x}$. The continuity equation

$$\frac{\partial (hu)}{\partial x} + \frac{\partial (hv)}{\partial y} = 0, \quad (22)$$

and finally a relationship between stream function and vorticity

$$\nabla \left(\frac{1}{h} \nabla \psi \right) = \xi , \quad (23)$$

complete the basic equations of the model. For further information on finite difference forms see Galt (1973).

A typical run of the model includes the following sequence of events throughout the 17 x 42 point array over the area from 33-61°N and 140°E-120°W. Initially the vorticity (ξ) and stream function (ψ) values are set to zero at each of the 714 grid points. Then the rate of change of vorticity ($\frac{\partial \xi}{\partial t}$) is computed at each grid point from equation (21) and integration of the rate of change over one time step interval (6 hours) gives a new vorticity value at each grid point. Using equation (23), new values for the transport stream function are computed from the new vorticity values by an over-relaxation technique, and streamfunction values at each grid point are contoured to indicate the new magnitude and direction of flow. This sequence is repeated. The model approaches steady conditions when the gradients are such that the terms on the right hand side of equation (21) approach zero indicating a balance between vorticity dissipation (by advection of potential vorticity, lateral friction, and bottom friction) and vorticity input at each grid point (the wind stress curl field).

Using the 25 year mean annual wind stress and a 10% bathymetry factor, the model after 60 days spin up shows the generally accepted features of flow around the Gulf of Alaska (Fig. 29). The cyclonic flow, western boundary intensification, and magnitude of transport (about 20 Sv) generally agree with the geostrophic calculations from field measurements

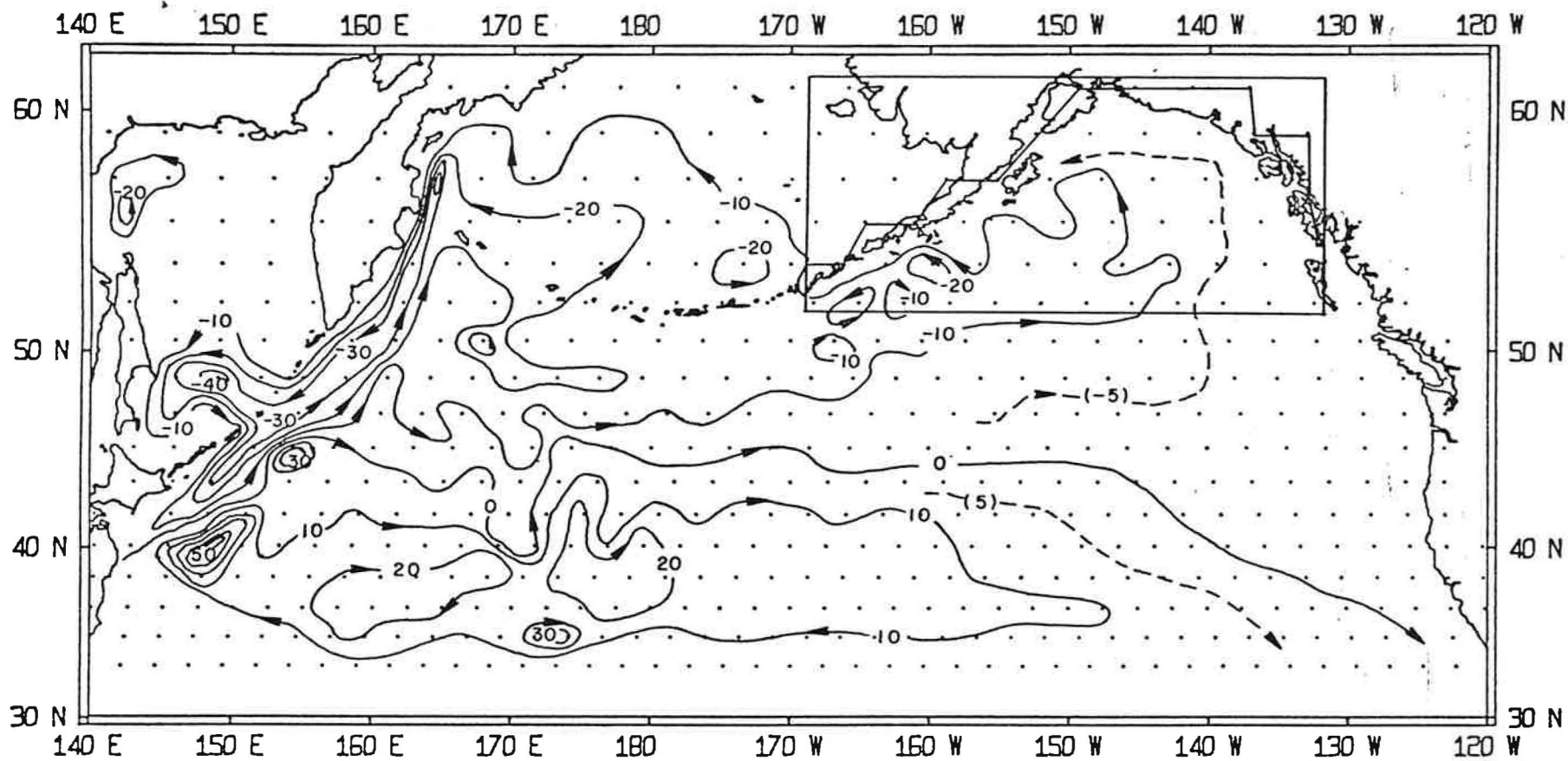
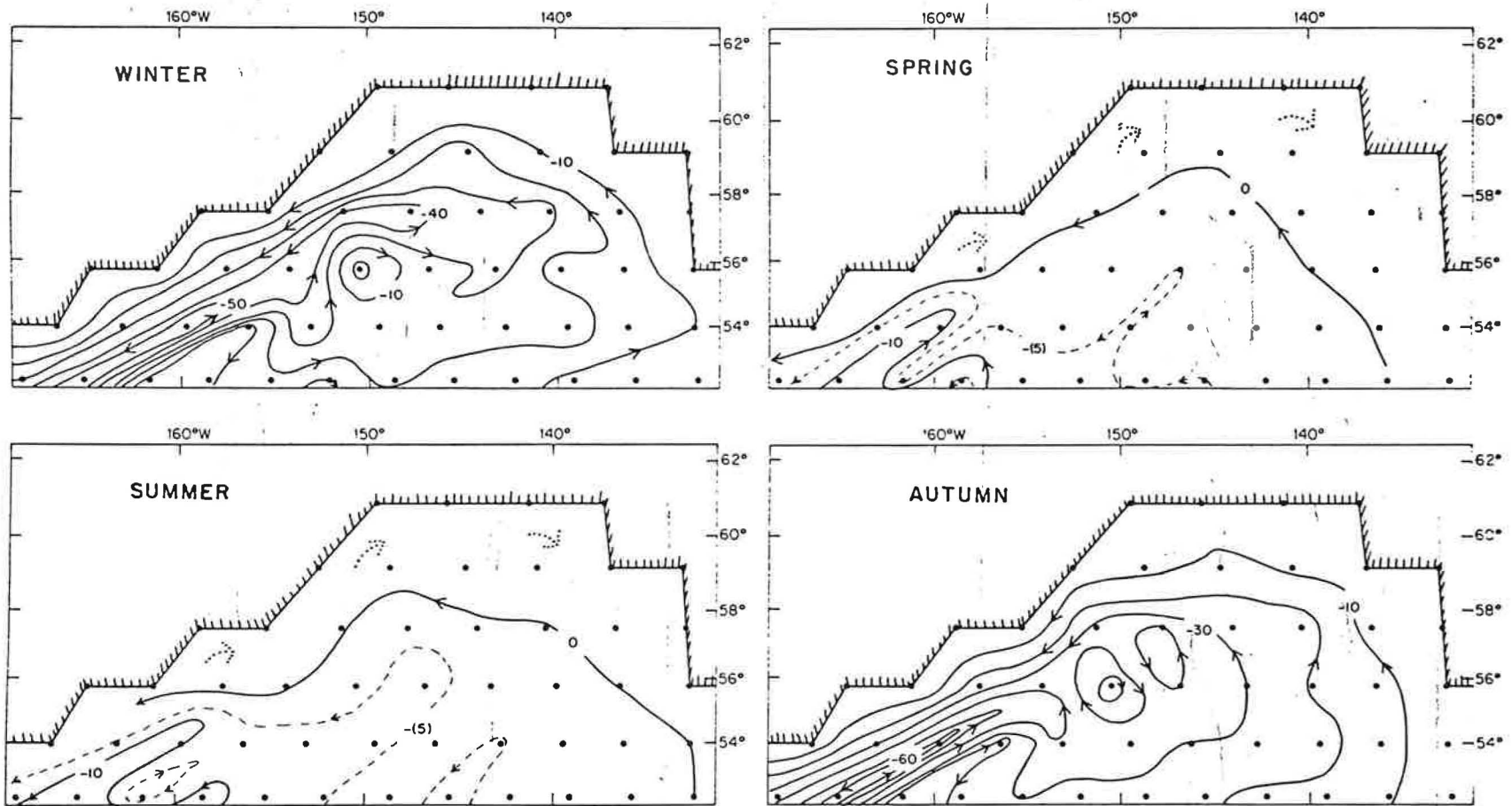


Figure 29. Numerical model of Transpacific ocean transports (Sv) using annual mean (1950-74) wind stress, 10% bathymetry factor, and α , β , γ coefficients.

of temperature and salinity if a reference level-of-no-motion of about 2000 db is used. Next the sea level pressure data were averaged by seasons to observe the effect of variable wind-stress. All factors except wind stress input were kept the same for each of the four runs which were driven by the seasonal mean (1950-74) wind-stresses, only the gulf portion of the model is presented (Fig. 30). As expected, the autumn and winter transport patterns are much more intense than the annual mean pattern, and the maximum transport of 63 Sv across 54°N (between 130° and 160°W) occurred for autumn conditions; the winter transport was 51 Sv followed by summer with 13 Sv and spring with 11 Sv. The general asymmetric cyclonic features of flow were quite similar during both of the high transport seasons and both of the low transport seasons, but details were considerably different.

During autumn and winter an intense boundary current develops on the western side of the gulf, about 2 grid lengths offshore, over the continental slope. Eddy-like features form south of the boundary current. The lack of synopticity and closely spaced stations in historical oceanographic data has precluded detecting the existence of these eddies, other than perhaps isolated instances, which have been generally overlooked. At the eastern side of the gulf, the streamlines of easterly flow converge indicating higher velocities near Yakutat. The flow remains about the same magnitude zonally across the head of the gulf and intensifies as it is forced southwestward by the land boundary off Kodiak Island and the Alaska Peninsula.

During the spring and summer low wind stress period, flow is considerably reduced in magnitude, and the center of cyclonic flow shifts southward.



66

Figure 30. Seasonal mean transports (Sv) in the gulf obtained from numerical model studies suggesting a greater complexity in flow than evident in Fig. 27.

101

A new feature appears in the form of an inshore return flow of 1-3 Sv over the shelf that is not evident in the 10 (or 5) Sv contour interval shown. This is perhaps much more significant in terms of mean velocity considering that the transport in this area is confined to within a depth interval of 200m compared to the offshore depth interval of about 4000m. Other features of spring and summer transports include weak eddies or meanders, a broad northerly flow at the east side of the gulf, and a slight intensification of the southwesterly flow at the western side of the gulf.

Computed wind-stress fields for winter 1963 and 1969 (based upon extremes in the integrated total transport (wind-stress transport) time series) were selected to show the variability that may be expected during the high wind stress period (Fig. 31). The general features of the mean winter condition are clearly present, with 1969 having a high transport value of 83 Sv compared to only 22 Sv in 1963. The greatest departure in 1969 from mean conditions occurs in the eastern gulf where the easterly flow is contained about 400 farther south than normal, resulting in a more intense northwesterly flow along the coast. This was apparently associated with unusually strong positive wind-stress curl in the eastern gulf.

These numerical model studies suggest that flow in the gulf does not appear to be of a typically uniform cyclonic nature, but rather a funneling of northward flow into the head of the gulf that exists as a narrow boundary flow at the western side. Closure may well occur in nature (see Surface Salinity section) in the surface layer, which is generally isolated from the deeper flow by the halocline at 100-300m. Future studies should take into account the stratification or baroclinic effects.

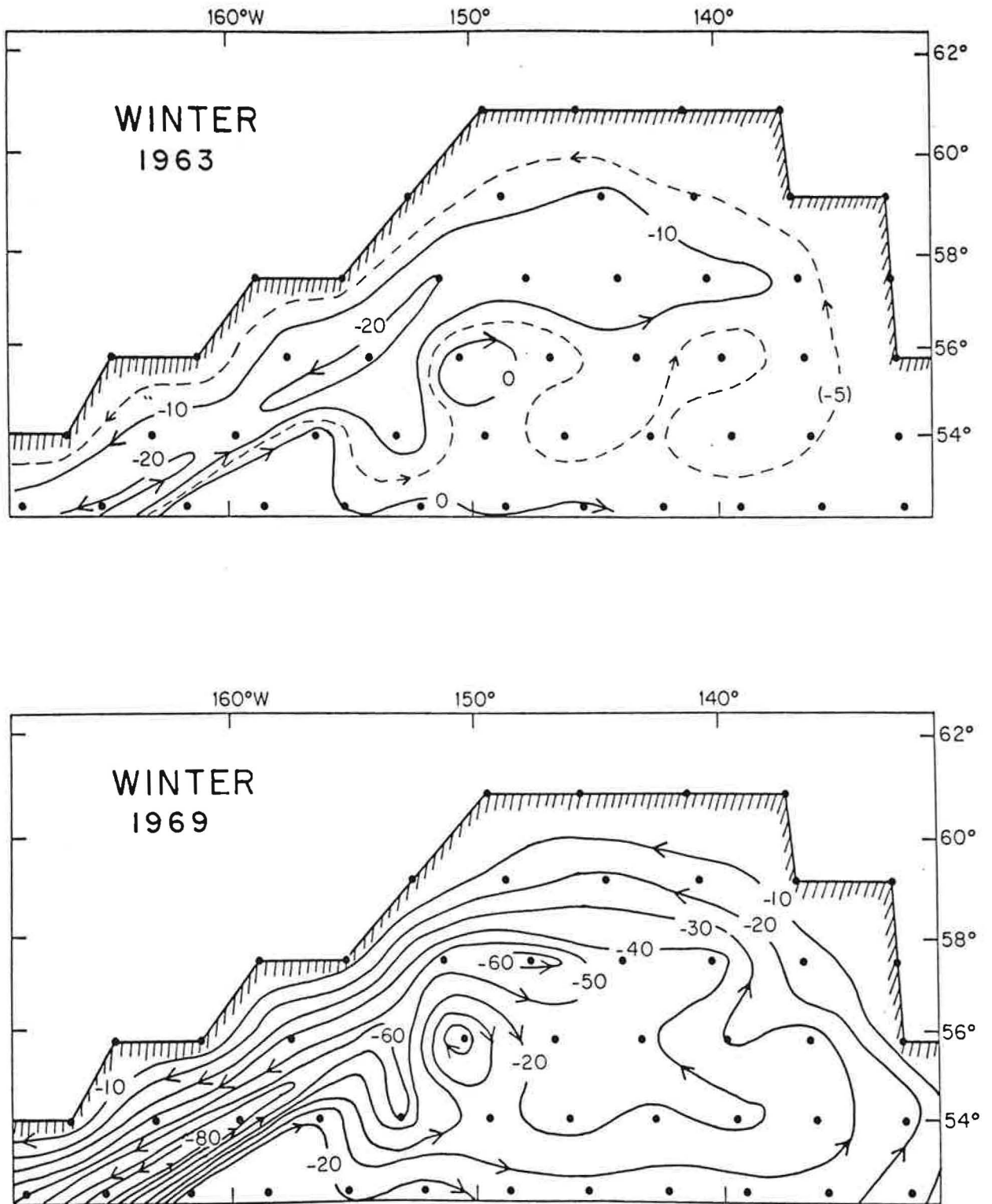


Figure 31. Numerical model transports (streamline interval 10 Sv) for winter (Jan. Feb. Mar.) 1963 and 1969 suggesting greater complexity in flow than evident in Fig. 28.

V. COASTAL SEA LEVELS

The geopotential topography computed from hydrographic data provides a relative indication of sea surface slopes but observations at shore stations are a direct measurement of actual sea level. Daily means of hourly heights referred to a local datum are recorded at selected coastal stations and the data are on file at NOAA Headquarters (Rockville). Although weekly and even daily departures from normal sea level have shown good correlations with coastal flow regimes in the Coastal Upwelling Experiments (CUE) off Oregon, monthly mean sea level data are appropriate for discussing the seasonal and longer-term variations which are the focus of this chapter. Distortions caused by changes in atmospheric pressure are corrected as follows:

$$\delta h = \frac{1}{\rho g} \delta p \quad (24)$$

where h is the change in sea level, ρ the density of water, g the acceleration of gravity and p the atmospheric pressure. Steric effects which may result in seasonal differences as great as 6 cm are not compensated for because usually only departures from monthly means are considered.

LaFond (1939) showed that nearly all variations in sea level on the west coast of the United States could be accounted for by changes in the geopotential topography of the ocean off the coast and thus, were directly related to ocean currents. Jacobs (1939) reported that such relations were not due to changes in the density of surface water but actual slopes caused by atmospheric interactions. Pattullo et al (1955) found that in

the northern North Pacific isostatic adjustments (steric and pressure effects) did not account for all seasonal departures from mean sea level, and Pattullo (1960) noted that in low latitudes sea level was high in summer but north of 40°N there was a distinct change of phase and sea levels around the Gulf of Alaska were highest in December. Local effects of river discharge on sea level at the mouth of the Columbia River were noted by Roden (1960) in a study of non-seasonal variations in sea level along the west coast of North America; only a moderate to poor coherence in relation to local sea surface temperatures were found. Sea level data south of Ketchikan were studied by Saur (1962) and deviations from isostasy were attributed to variability in ocean currents. Favorite (1974) showed that the anomalous increase in sea level at Yakutat during winter could be explained by an accompanying increase in northward wind-stress transports, and Reid and Mantyla (1975) have indicated that the winter increase in sea level along the entire coast of the northern North Pacific Ocean is due to increased flow in the overall subarctic cyclonic gyre.

A. Sea Level Pressures

A general gradual increase in monthly mean sea level pressure is evident at Ketchikan, Sitka, Yakutat, Seward, Kodiak and Dutch Harbor from February to July (Fig. 32) and this is followed by an abrupt decrease from July to October. Somewhat constant but low pressures prevail from November until January when an anomalous secondary maxima occurs that is probably caused in part by a westward shift in the center of the Aleutian low from the gulf to the central Aleutian Islands that occurs at this time.

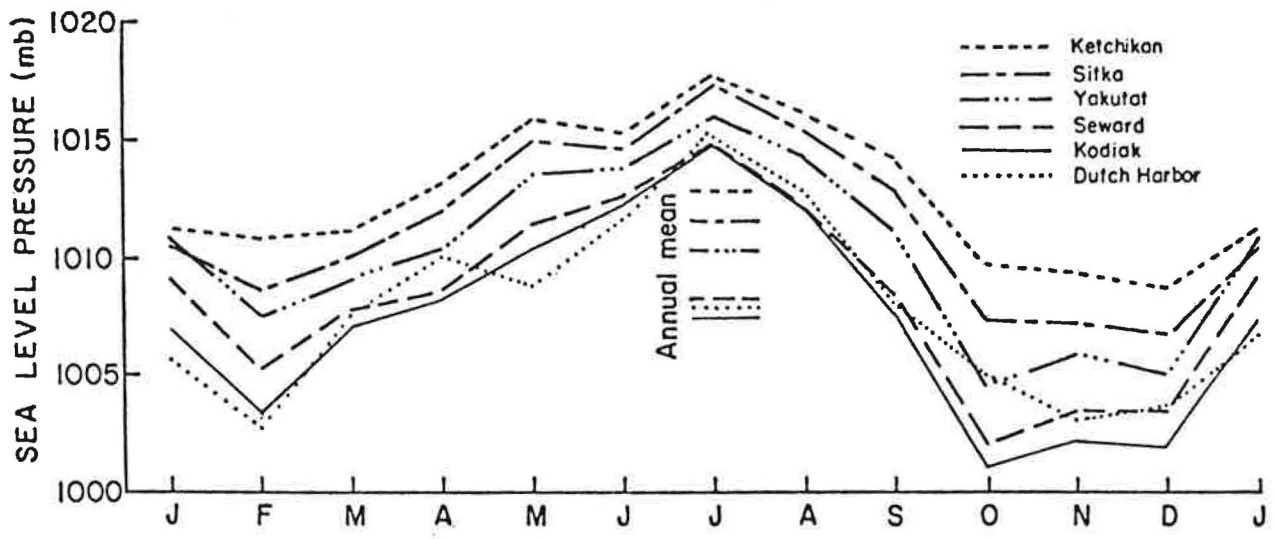


Figure 32. Monthly mean (1950-74) sea level pressure (mb) at the indicated coastal stations indicating maxima in July and minima in October.

Deviations from monthly means, and 12-month running means of sea level pressures for the 6 locations for 1950-74 (Fig. 33) indicate a marked similarity that is even reflected in abrupt anomalies of only a month or so duration. The abrupt increase in pressure in late 1950 at Dutch Harbor was evident at all stations, although decreasing in intensity to the south. In 1957 an abrupt increase and a subsequent decrease was evident at all locations and other examples are evident. Thus, there is a general response throughout the area to short or prolonged events but periods of positive or negative anomalies appear to be limited to from one month to about a year.

Spectral energy densities were computed for monthly mean values at each of the coastal stations over the period 1950-74 using a lag time of approximately 13 percent of the record length (40 lags over a continuous record of 300 data points). All locations exhibit maximum energy density at a frequency of approximately .085 cy/mo or 1 year (Fig. 34). Although the limited number of data points prohibits meaningful analysis of lower frequencies, there is an indication that the total energy distribution at these frequencies increases from Ketchikan to Dutch Harbor and a consistent indication of an energy peak at .025 cy/mo or 3.3 years. A coherency test using the coherence square technique shows a maximum coherence at a frequency of 1 year at all stations. Comparisons of data at all locations with those at Ketchikan indicates that there is also a good spatial coherence around the gulf (Fig. 35).

B. Mean Sea Levels

Monthly mean (1950-74) sea levels corrected for atmospheric pressure at Ketchikan, Sitka, Yakutat, Seward, Kodiak and Dutch Harbor (Fig. 36) reflect considerable coherence. Unfortunately there is no horizontal

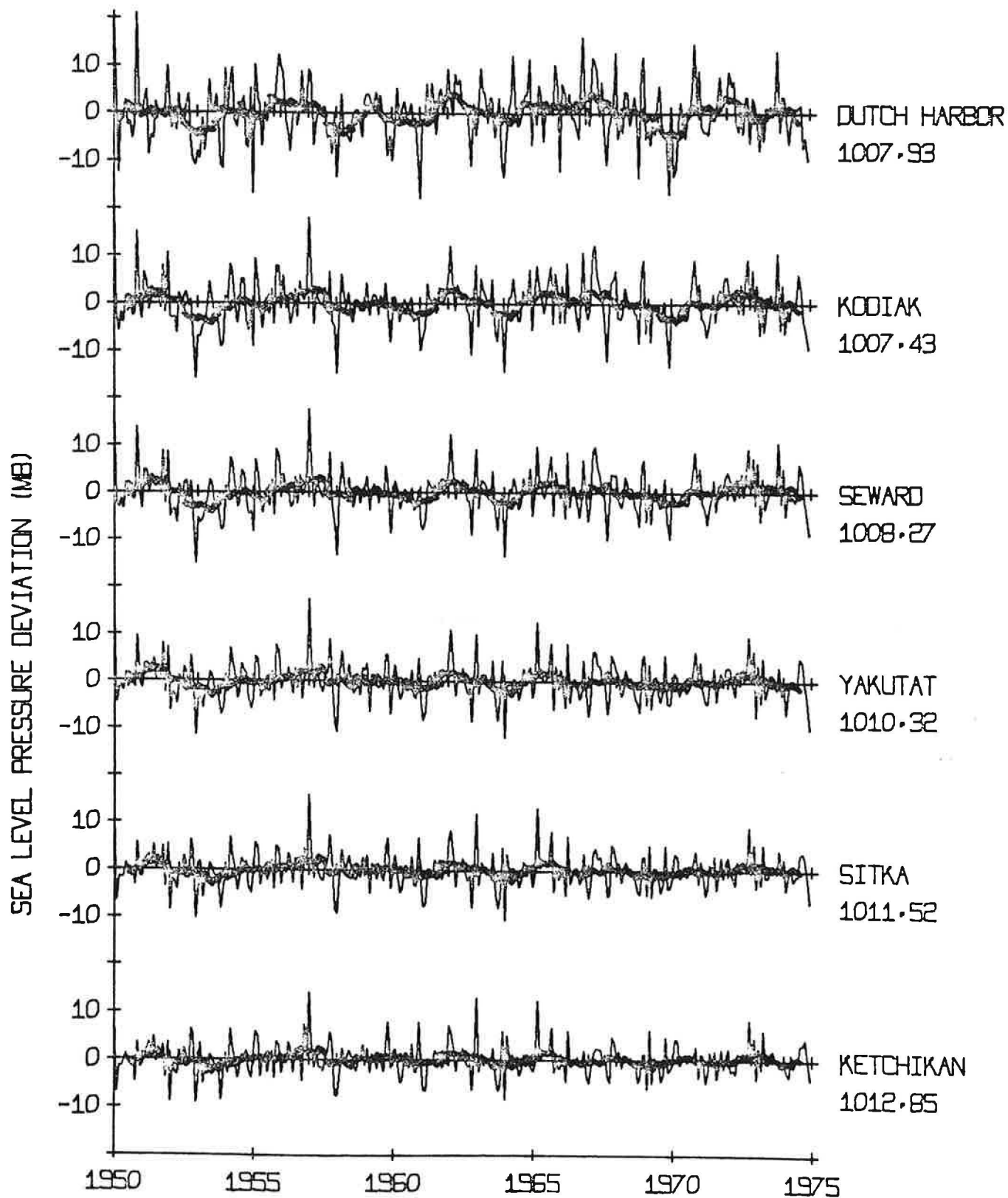


Figure 33. Deviations in sea level pressure (mb) from monthly mean (1950-74) values at the indicated coastal stations and 12-month running mean (dotted line).

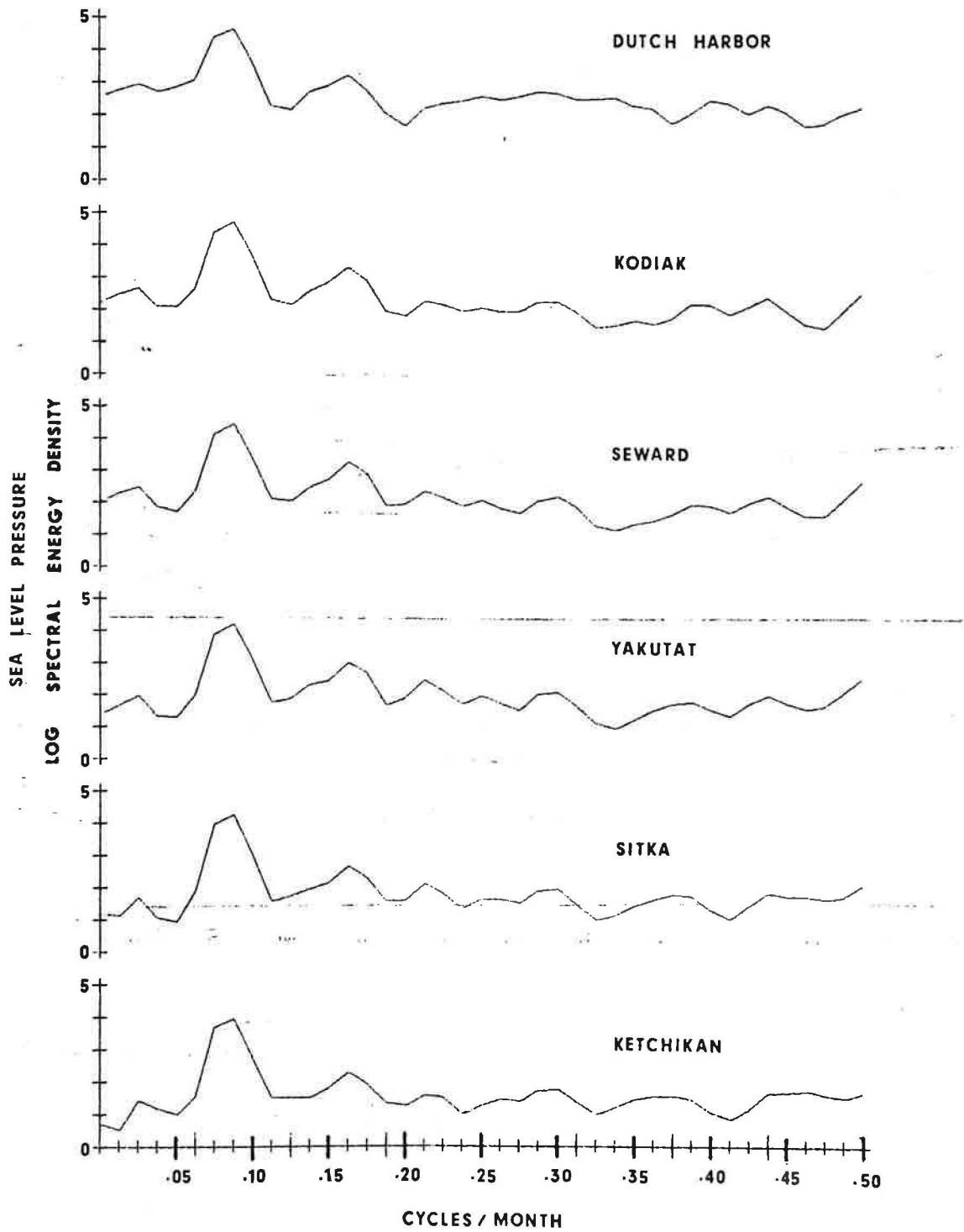


Figure 34. Spectral energy densities (40 lags) for sea level pressure at the indicated coastal stations indicating dominant annual cycle.

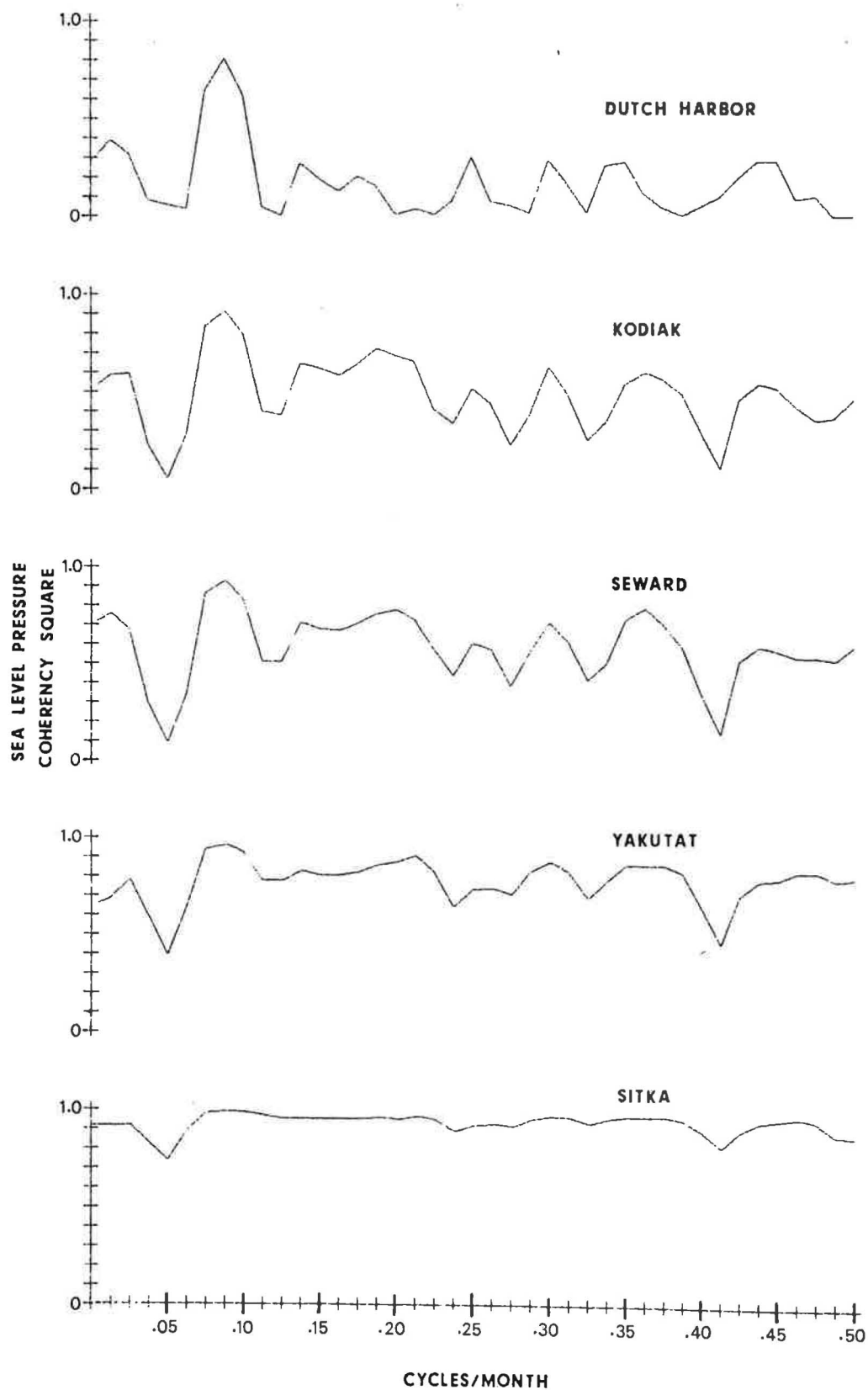


Figure 35. Coherence in sea level pressure at the indicated coastal stations, using Ketchikan as reference station, showing good coherence (>0.9) for annual cycle (.085 cy/mo).

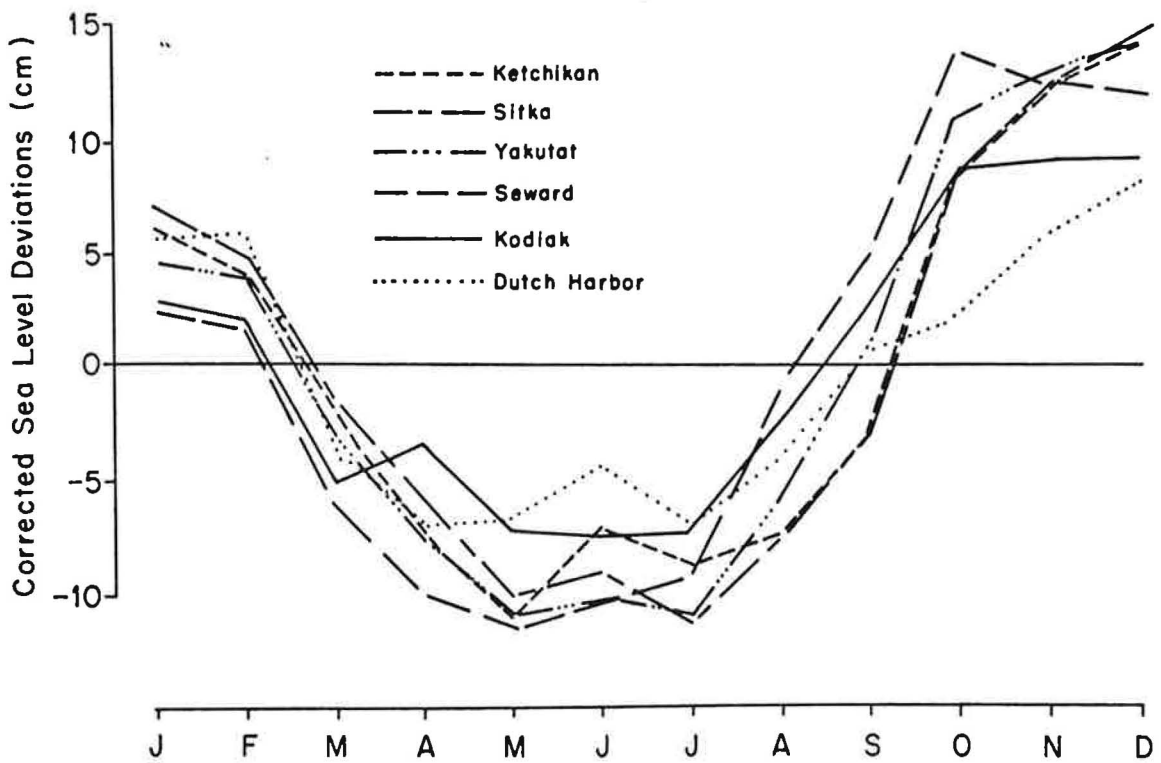


Figure 36. Deviations in monthly mean corrected (for atmospheric pressure) sea level (cm) from long term mean (1950-74) values at the indicated coastal stations showing increase in sea level in winter.

control between the various stations that would permit relating levels at the various sites to a common datum which would permit ascertaining relative levels. Deviations from monthly mean sea level for 1950-74 and 12-month running mean corrected sea level were compiled (Fig. 37). Here again there is continuity in short pulses (e.g. November 1952, January 1958, and others). However, positive and negative anomalies extend for longer periods up to 4 years. Well above normal sea level was evident at Dutch Harbor from 1957-61 and at Ketchikan from 1966-70. The apparent progressive lowering of sea level at Dutch Harbor from 1957 to 1974 is not evident at the other stations, but the below normal levels are evident from 1970 to 1974. These data can be grossly summarized for the area Sitka to Kodiak as follows: 1950-54 above normal, 1955-57 below normal, 1958-62 above normal, 1963 below normal, 1964-69 normal, 1970-74 below normal. As might be anticipated, power spectral analysis (40 lags) for corrected sea level at the coastal stations exhibits the 1 year frequency (Fig. 38). Data at Dutch Harbor, Seward, Yakutat and Ketchikan indicate significant energy densities at periods of less than one year and there is a high coherence ($>.9$) at this frequency at all stations compared to Ketchikan (Fig. 39). In contrast to sea level pressure, there is a marked coherence at 0.5 cy/mo. As before, the limited data points do not permit clear definition of periods greater than 1 year.

C. Relation to Transport

An increase in sea level normally signifies an increase in northward flow into the gulf. Such considerations can only be made when equivalent transport data are available. Obviously this cannot be obtained from

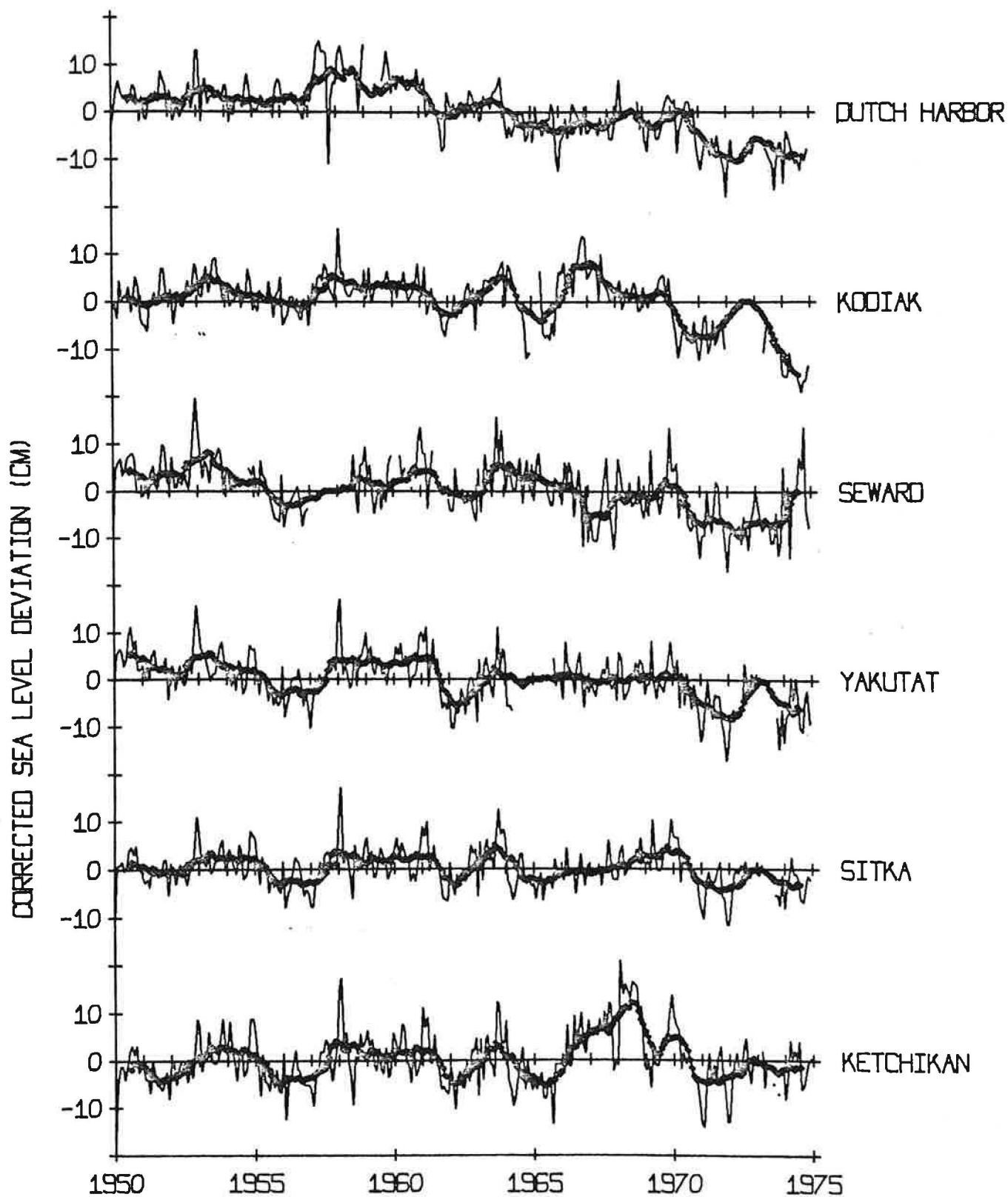


Figure 37. Deviations in corrected sea level (cm) from monthly mean (1950-74) values at the indicated coastal stations and 12-month running mean (dotted line).

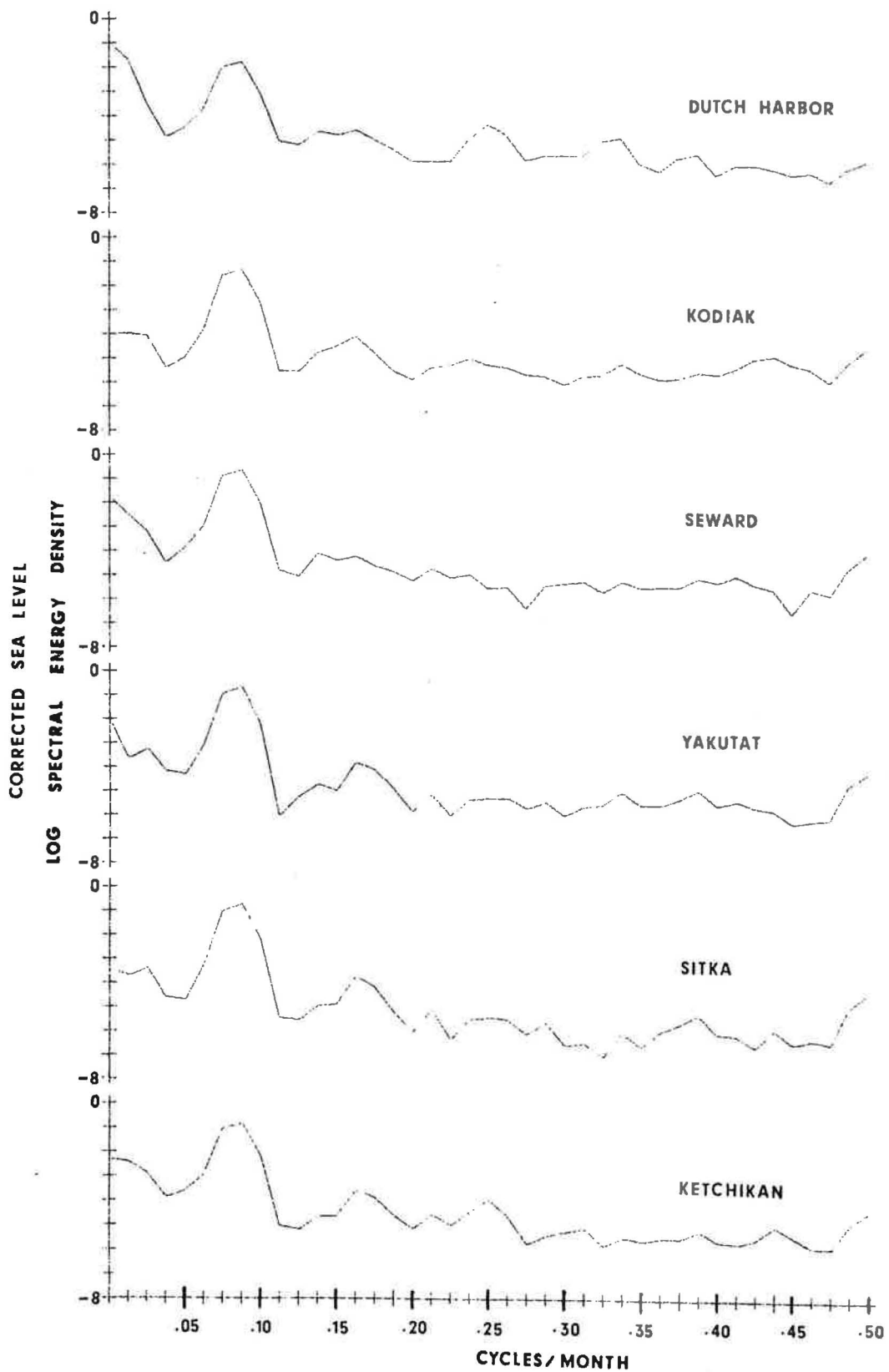


Figure 38. Spectral energy densities (40 lags) for corrected sea level at the indicated coastal stations showing the dominant 1 year cycle.

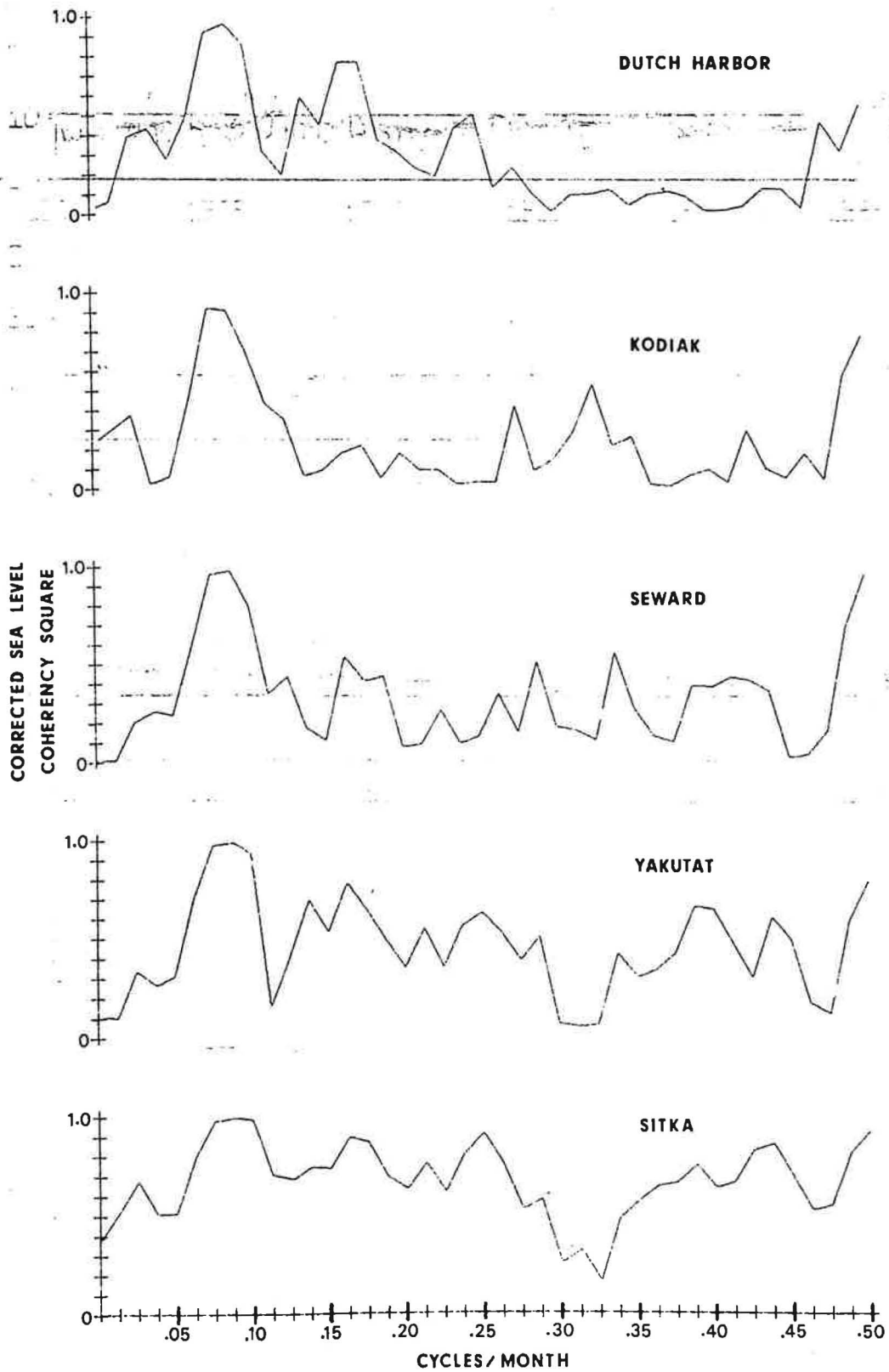


Figure 39. Coherence in corrected sea level at the indicated coastal stations, using Ketchikan as a reference station, showing good coherence (>0.9) for annual cycle.

station data which are available only for one or two months in a limited number of years. However, comparisons can be made with wind-stress transports. Monthly mean wind-stress transports across 55°N (+northward; -southward) computed for the years 1900-74 indicate a mean transport of 11.22 Sv (Fig. 40). There is a progressive increase in the 25-year mean values from 8.39 to 10.90 to 14.35 Sv that is probably primarily, if not almost entirely, due to progressively better definition of sea level pressure fields; thus, limited comparisons between past and more recent data can be made. Further, the high monthly mean wind-stresses in winter are not of sufficient duration for the calculated transports to become established, but the presence of additional energy is indicated.

The individual monthly mean transports in 1950-74 have a greater range (~ 80 Sv) than in the previous two 25-year periods (~ 60 Sv). The following winters stand out as having high northward transport: 1908-09, 1949-50, 1955-56, 1958-59 and 1965-66. Anomalous southward transports are indicated in: fall 1900, winter 1920, winter 1929, fall 1930, summer 1936, summer 1958 and fall 1965.

Transport ranges reflected in the 12-month running means are quite similar (~ 12 Sv) for the three 25-year periods. Except for the years 1950-1965 when there is evidence of an approximate 3-year cycle there is no immediately apparent suggestion of any other periodicities. The long data record (900 data points) provides the first substantial look at periods greater than one year and spectral analyses using 80 and 160 lags substantiate the peak near 3 years.

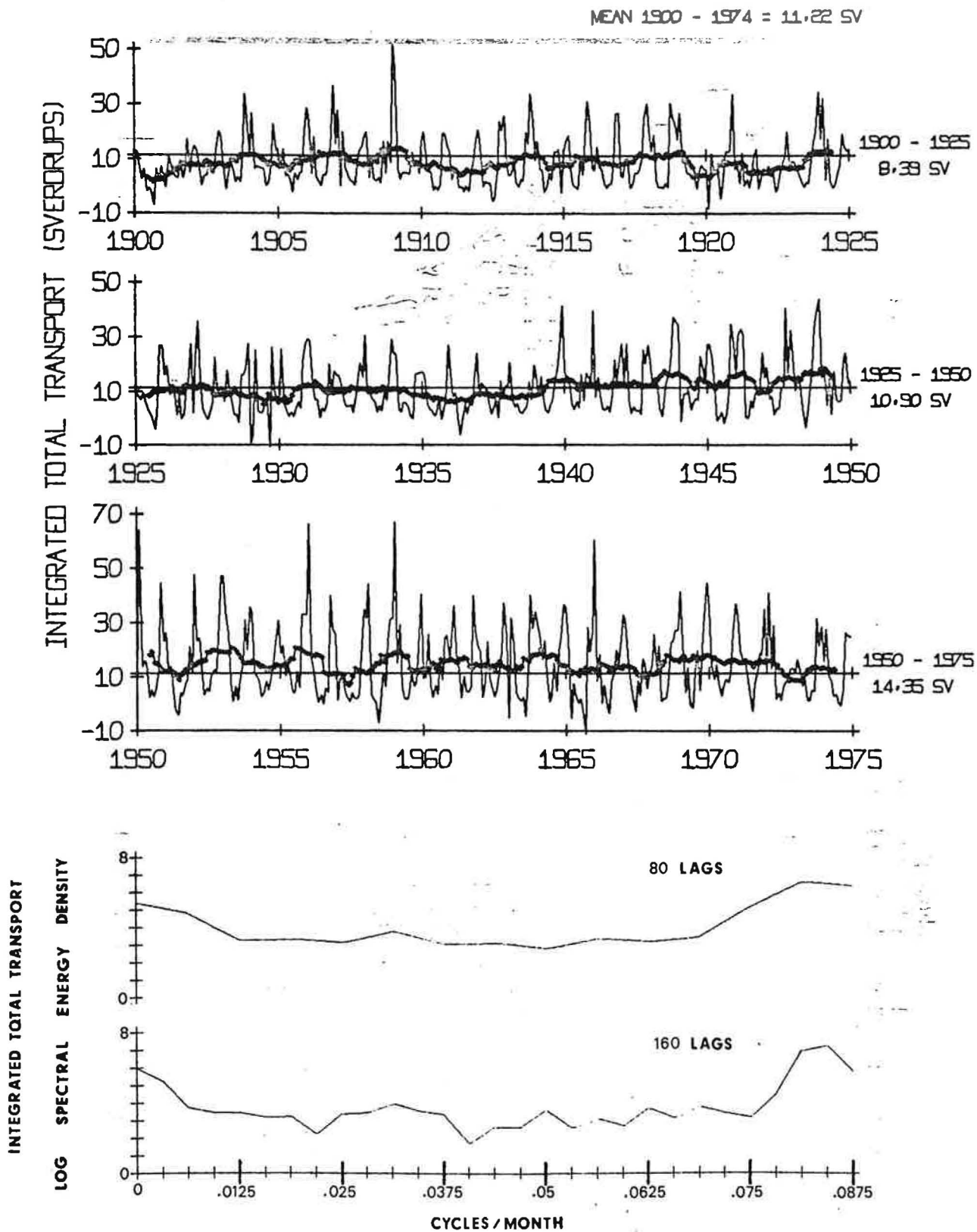


Figure 40. Monthly integrated total transports (Sv) across 55°N (+northward, -southward) 1900-74, 12-month running mean (dotted line), and spectral energy density (80 and 160 lags).

VI. SURFACE CONVERGENCE AND DIVERGENCE

The surface wind drift, i.e. the water carried along in the very surface layer of the ocean under the direct action of the wind, usually contributes only slightly to the surface velocity field, and because of its limited vertical extent is nearly always negligible in terms of total mass transport. However, the surface drift field can contain very large convergences and divergences, which may fluctuate rapidly, both in pattern and intensity. These convergences and divergences create pressure gradients and redistributions of mass which alter the underlying geostrophic currents. Because it is likely that these alterations are highly important on the scales of interest to OCSEAP field programs, a rather detailed study of the convergence-divergence pattern in the surface waters of the Gulf of Alaska has been made.

The energetic winter season dominates the annual cycle. Typically, positive wind stress curl associated with an atmospheric low pressure system induces divergent surface drift. Where the coastal boundary of the Gulf presents a barrier to this drift, convergence and intense downwelling result (Bakun, 1975). Such a situation would act to intensify the characteristic ridging of the density structure in the interior of the Gulf and to steepen the plunge of the isopycnals toward the coast. This "pumping" between the coastal and offshore areas would tend to build up baroclinicity through the winter season, which apparently would dissipate during the more relaxed portion of the year.

In order to investigate the coupled system, indices of divergence of wind-induced surface flow at 6-hourly intervals from January, 1967 through December 1975 were generated at 15 locations indicated in Figure 41. The surface flow field is approximated as Ekman Transport and an

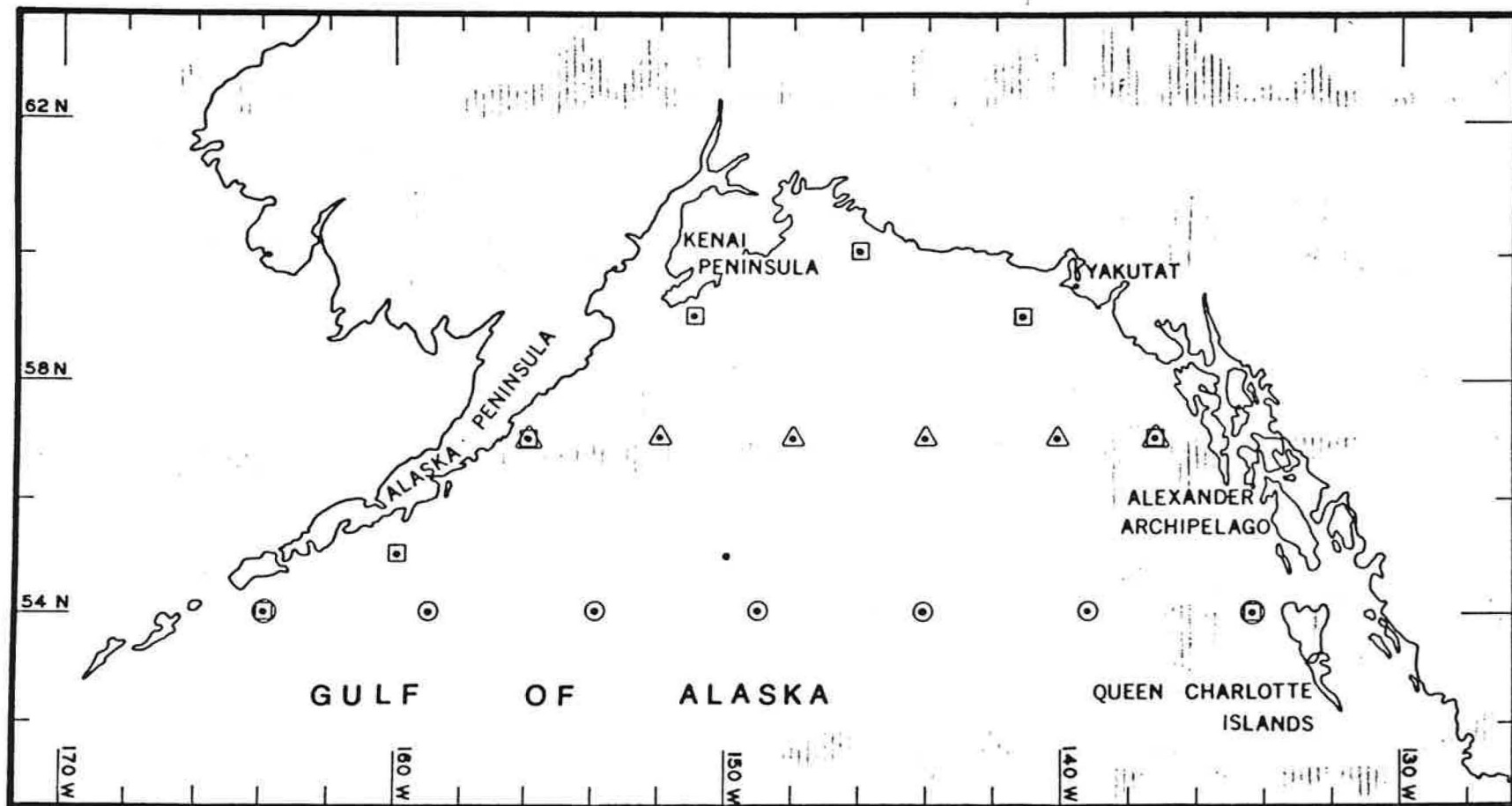


Figure 41 - Chart of the Gulf of Alaska region, showing locations at which time series of surface convergence-divergence indices were computed.

example segment of the time series at one location is shown (Fig. 42).

In the previous sections data fields averaged over a month or longer have been discussed. This is because attention has been focused on lower frequency, relatively slowly changing components of the variations, either because we are not equipped to deal with the shorter term variability or because sparsity of data requires that we collect observations over some time interval in order to get an adequate sample. Now an attempt will be made to deal with the synoptic scale. Such an approach is called for in this case because the extremely large variance of the surface divergence field on short time scales requires that proper interpretation of even the longer period variations be made within the framework of the process as it is actually occurring on the synoptic scale.

On this scale attention shifts from such mean pressure features as the Aleutian Low, or a Continental High, to individual traveling storm systems. Major winter storm tracks cut directly across the gulf from the southwest toward the northeast. Mean speeds of storm movement along these tracks are of the order of 25 knots (Klein, 1957). During the summer a larger proportion of storms turn northward through the Bering Sea and so are not felt with full intensity in the Gulf of Alaska. In addition, the summer storms are normally much less intense than the winter storms. The available reports of wind speed and direction for an area such as the gulf tend to be sparse and unevenly distributed. Example distributions of reports (Fig. 43) show that major fraction of available reports come from shore stations which, being subject to topographical influences, may not be completely representative of conditions offshore. The distribution of the observations taken at sea changes continually, and for any single observation, random errors in measurement or position may introduce

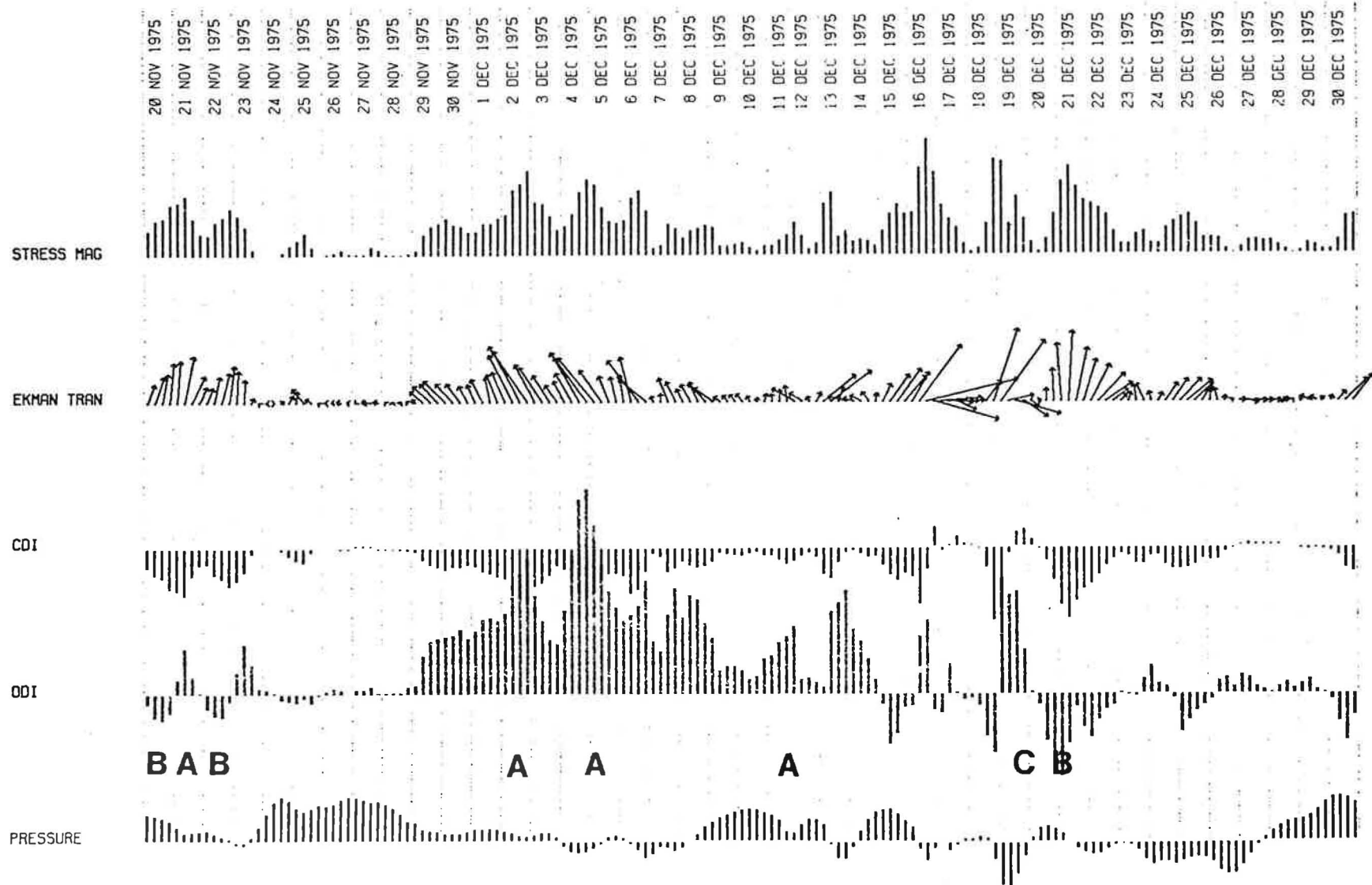


Figure 42 - Example time series segment (60°N , 146°W , Nov. 20, 1975 - Dec. 30, 1975). Upper graph indicates the stress magnitude at each 6-hourly synoptic sampling. Second graph indicates the magnitude and direction of Ekman transport; north is toward the top, etc. Third graph indicates the coastal divergence index (CDI). Fourth graph indicates the offshore divergence index (ODI). Large letters refer to type of event according to classification of Fig. 44.

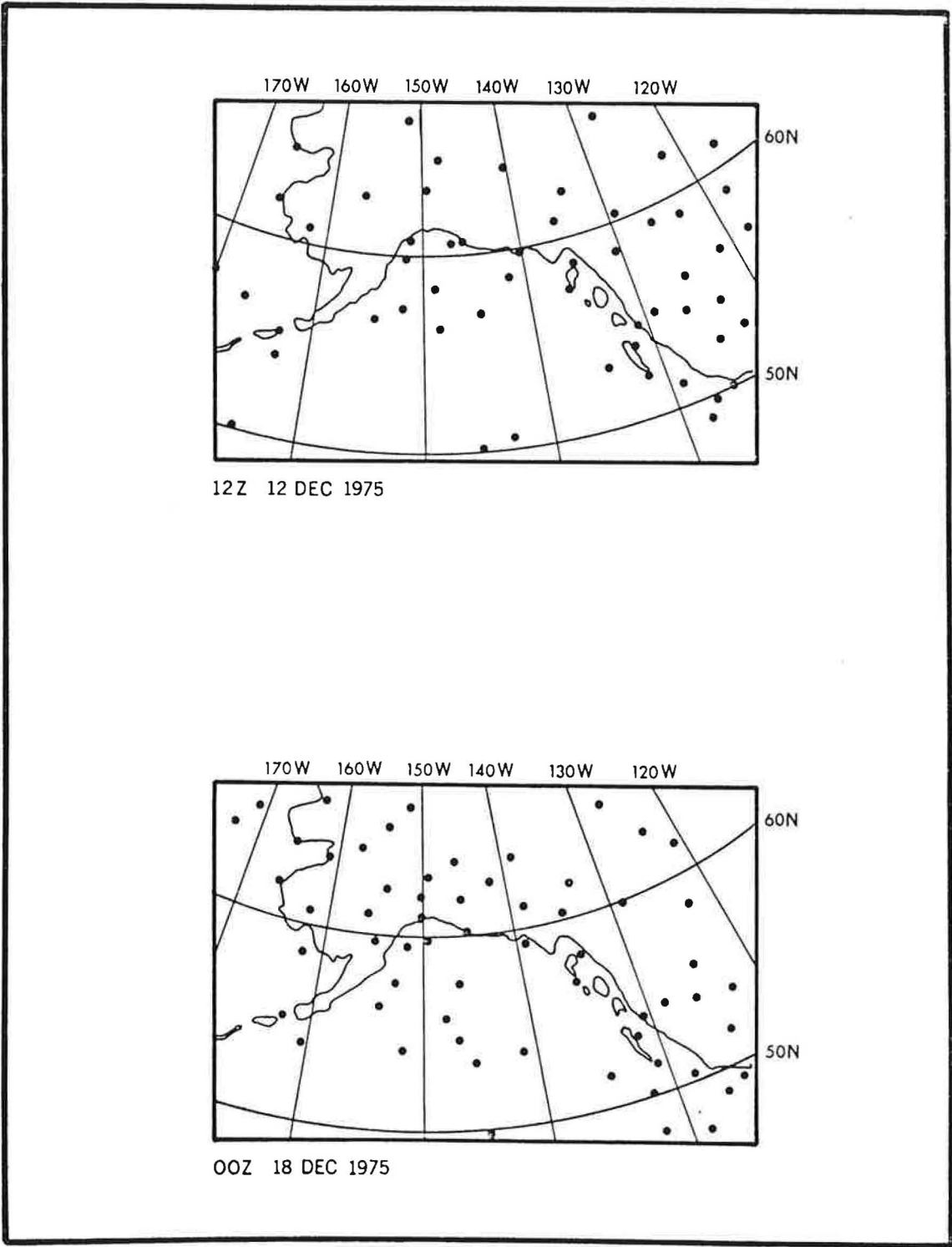


Figure 43 - Example distributions of synoptic reports which arrived at Fleet Numerical Weather Central in time for incorporation in the operational surface pressure analysis.

variability which is greater than the variability in the process itself (Nelson, 1974).

One way to arrive at a fairly consistent time series is to make use of analysed products produced by meteorological agencies. For this portion of the study 6-hourly synoptic surface atmospheric pressure analyses produced by Fleet Numerical Weather Central (FNWC) have been used. These analyses incorporate all available wind reports in the form of equivalent pressure gradients. The use of the pressure reports, which are linked to the wind field through well-known relationships, effectively increases the data base.

The method of atmospheric pressure analysis presently in use at FNWC is described by Holl and Mendenhall (1972). The basic steps in the analysis are as follows:

- Preparation of "first guess" field: The pressure analysis for the previous synoptic sampling, 6 hours earlier, is extrapolated forward using a computation of 6-hour upper air movement and a 6-hour surface forecast using the FNWC primitive equation computer forecast model.
- Assembly of new information: new reports are compared to the first guess field, subjected to a gross error check, and assigned a reliability value; surface wind reports are assembled in a gradient field.
- Blending for pressure: a blending equation of 61 terms which take into account the pressure, gradient, second-differences, cross differences, and Laplacians, plus the reliability value of each of these, is used to assemble a "best fit" pressure field.

- , Computation of reliability field: depending on the amount and reliability of information available, each grid-point value is assigned a reliability.
- Reevaluation and lateral rejection: reports are again compared to blended pressure field and reliability field and assigned new reliability values; those failing to meet criteria are rejected.
- Recycling: a new assembly is made according to the new first guess field and assigned reliabilities. The whole process is then repeated a third time to gain further accuracy.

In order to produce the computed indices discussed in this section pressure data from FNWC fields archived on magnetic tape were arranged on a 3-degree computational grid and the curl of the wind stress, $\nabla \times \vec{\tau}$ derived as shown in equations 5-20, except that constant drag coefficient of 0.0013, appropriate for synoptic rather than mean data, was used.

The Ekman transport, \vec{E} , is derived as

$$\vec{E} = \frac{1}{f} \vec{\tau} \times \vec{k} \quad (25)$$

where \vec{k} is a unit vector directed vertically upward.

The divergence of Ekman transport integrated over the width of the coastal upwelling-downwelling boundary zone, per unit length of coast, is given, to a high degree of approximation, by the offshore component. Bakun (1973) called this by the term upwelling index. In this report we refer to it as the coastal divergence index, abbreviated as CDI.

$$CDI = \vec{E} \cdot \vec{n} \quad (26)$$

where \vec{n} is a unit vector normal to the coast. Units used are metric tons per second per 100-meter length of coast.

Away from the boundary zone the divergence of Ekman transport is computed as

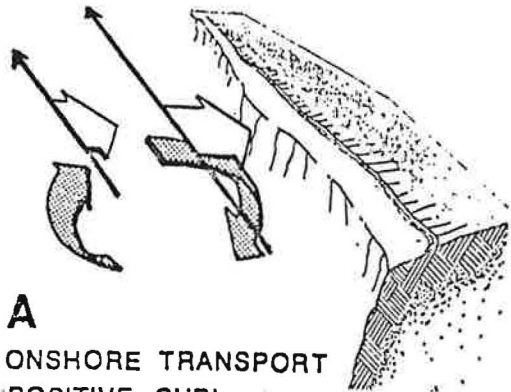
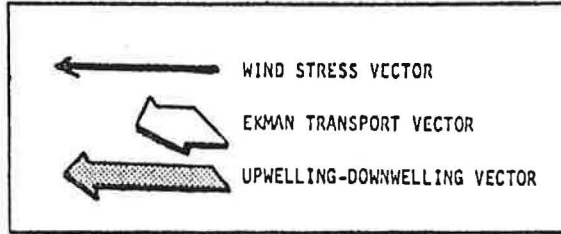
$$ODI = \nabla \cdot \vec{E} = \frac{1}{f} \nabla \times \vec{\tau} - \frac{\beta}{f} \vec{E} \cdot \vec{j} \quad (27)$$

where β indicates the meridional derivative of f . ODI stands for offshore divergence index. The values presented in this report are in terms of vertical velocity (millimeters per day) through the bottom of the Ekman layer required to balance the computed divergence.

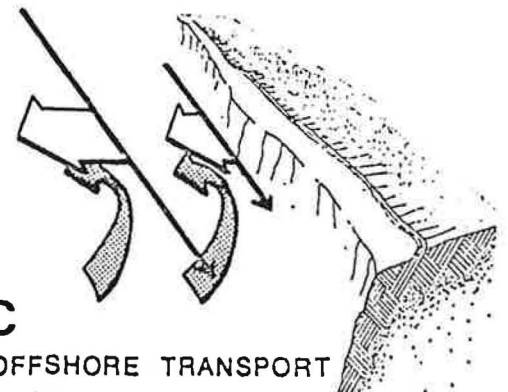
A. Vicinity of the coastal boundary

Various combinations of coastal and offshore convergence or divergence occur near the coastal boundary (Fig. 44). Both types A and B are characterized by coastal convergence (negative CDI) in the coastal boundary zone; surface water is piled up toward the coast with a resulting depression of the isopycnals, tending to intensify counter-clockwise flow along the border of the gulf. In the case of type A, divergence immediately offshore of the boundary zone (positive ODI) would favor confinement of the intensification to a narrow zone next to the coast. In the type B situation continued convergence offshore of the boundary zone (negative ODI) would spread the effect toward the interior of the Gulf.

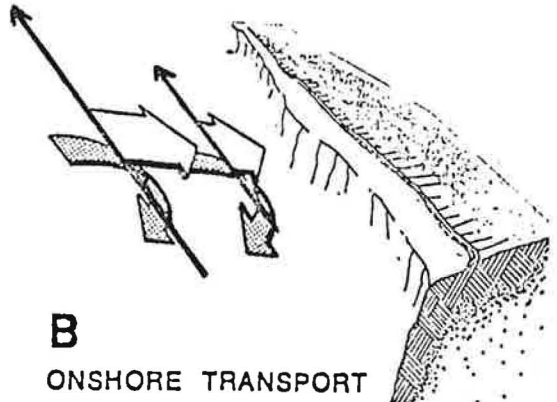
Under situations C and D, coastal divergence (positive CDI) would favor clockwise circulation along the boundary of the Gulf (or deceleration of counter-clockwise flow, etc.). Correspondingly, type C (positive ODI) would tend to spread the effect, while type D (negative ODI) would tend to confine it to the immediate boundary zone.



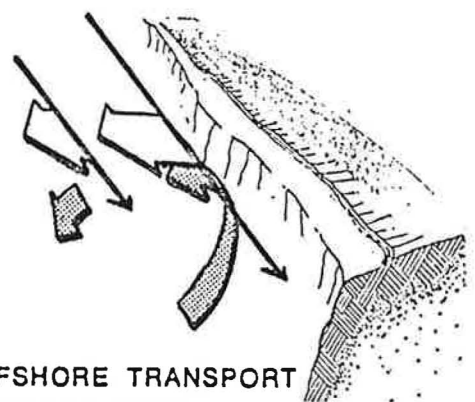
A
 ONSHORE TRANSPORT
 POSITIVE CURL
 (-CDI, +ODI)



C
 OFFSHORE TRANSPORT
 POSITIVE CURL
 (+CDI, +ODI)



B
 ONSHORE TRANSPORT
 NEGATIVE CURL
 (-CDI, -ODI)



D
 OFFSHORE TRANSPORT
 NEGATIVE CURL
 (+CDI, -ODI)

Figure 44 - Classification of indicated events according to combination of coastal and offshore convergence or divergence. A. Onshore Ekman transport and positive wind stress curl; convergence and downwelling at the coast, divergence and upwelling offshore. B. Onshore Ekman transport and negative wind stress curl; convergence and downwelling at the coast, continued convergence offshore. C. Offshore Ekman transport and positive wind stress curl; divergence and upwelling at the coast, continued divergence offshore. D. Offshore Ekman transport and negative wind stress curl; divergence and upwelling at the coast, convergence offshore.

The monthly frequency distributions of coastal divergence indices (CDI), at the near coastal locations (surrounded by squares in Fig. 41) show strongly negative mean values during the winter, indicating convergence and resulting downwelling at the coast (Fig. 45). The area of greatest intensity extends from the Kenai Peninsula (59°N, 151W) to the Alexander Archipelago (57N, 137W), reaching a maximum near Yakutat (59N, 141W). This situation relaxes during the remainder of the year; coastal divergence (positive CDI) is indicated on average over much of the gulf during summer. This "summer upwelling season" is longest in the southwest portion, extending from April to December near the extremity of the Alaska Peninsula and exhibiting three separate maxima (April, August, and November). The season of mean upwelling becomes progressively shorter and less intense with distance clockwise around the gulf, lasting three months off the Kenai Peninsula and essentially vanishing off the Alexander Archipelago.

The maximum variance corresponds in season and location to maximum absolute values of the mean. Standard deviations are larger than the means. Thus the winter season is characterized by highly energetic pulsations and relaxations of coastal convergence. In other seasons, the general trend is for the variance to decrease with the mean. The most stable situation appears to be the summer season in the northern gulf (59N, 151W; 60N, 146W; 59N, 141W). The three separate maxima exhibiting fairly similar mean positive CDI values off the lower Alaska Peninsula (54N, 164W; 55N, 160W) appear quite distinct in terms of variance. The August maximum in the mean shows the lowest variance, whereas, the November maximum exhibits standard deviations nearly three times those of August. Thus, the mean

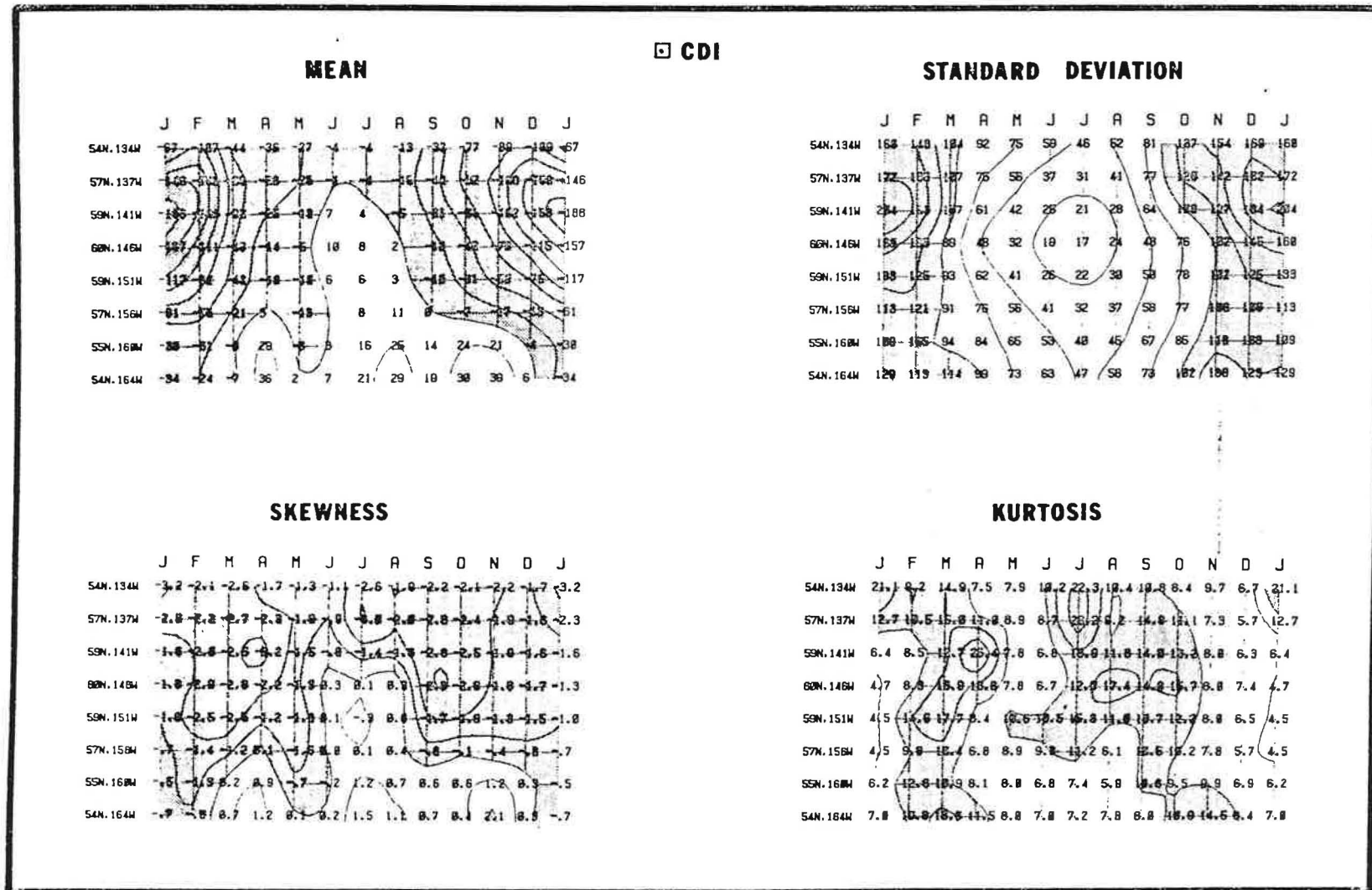


Figure 45 - Moments of the frequency distributions of coastal divergence indices (CDI) grouped by month at the near-coastal locations indicated by triangles in Fig. 41. Mean: units are cubic meters per second transported off each 100-meter width of coast; contour interval is 25. Standard Deviation: units and contour interval are the same as for the mean. Skewness: contour interval is one normalized unit. Kurtosis: contour interval is 5 normalized units.

upwelling indicated for November represents an energetic mix of upwelling and downwelling events, with the balance tipped slightly toward upwelling.

The skewness tends to have the same sign as the mean; i.e. extreme events during downwelling seasons tend to be downwelling events, and those during upwelling seasons to be upwelling events. Some modification of this general pattern appears in the northern gulf where the distribution of skewness shows a tendency to be more negative than the mean (i.e. a considerable contribution from relatively extreme downwelling events even during seasons of mean upwelling). Off the lower Alaska Peninsula an expansion of the period of positive skewness beyond that of positive mean value indicates relative importance of extreme upwelling events, most probably related to very intense storms centered north of the Alaska Peninsula.

In all months and locations the kurtosis is larger than 3.0 indicating that there appears to be a much larger contribution of extreme events than would be the case in a Gaussian process. The details of the distribution of kurtosis are controlled to some extent by the fact that the kurtosis is normalized against the variance; thus, the winter season exhibits relatively low kurtosis because the variance is high (i.e. events which would be "extreme" at other seasons are the norm during winter). When a winter-type storm appears in the spring, for example, it contributes to a higher kurtosis because the general level of activity is lower. The relatively high kurtosis during the summer season indicates that the generally stable situation is interrupted only infrequently. Large contributions to the variance from extreme events are indicated for the lower Alaska Peninsula area during the fall season.

The monthly frequency distributions of offshore divergence indices (ODI) at the near coastal locations (Fig. 46) have mean values which are positive, indicating divergence on the average offshore of the coastal upwelling-downwelling zone, except during January in the southwestern Gulf and during the summer from the Kenai Peninsula eastward. Strongest divergence on average occurs near Yakutat during winter, corresponding in season and location to the maximum negative CDI values.

The ODI variance is largest in winter, but rather than corresponding in location to the mean as was the case for the CDI values, there is a double maximum (59N, 151W; 57N, 137W) with a relative minimum in the area of the maximum mean values. In the southwestern Gulf the period of maximum variance shifts to the fall.

The skewness of the monthly ODI distributions tends to be positive; extreme events are characterized by divergent surface drift associated with cyclonic storms. Some of the monthly distributions in the northern and eastern gulf exhibit a slight negative skewness in the spring or summer. The kurtosis indicates major contributions to the variance from infrequent, extreme events.

Comparison of mean CDI and ODI values confirms that, in a mean sense, the preeminent situation along the coastal boundary of Gulf is type "A" (see Fig. 44). The extreme energy of the downwelling at the coast and divergence offshore associated with winter storm systems completely dominates the annual cycle. Table 2 lists the "types" corresponding to the monthly mean situation at the various locations. Type D is restricted to the extremely low-energy summer situation in the northern gulf. The

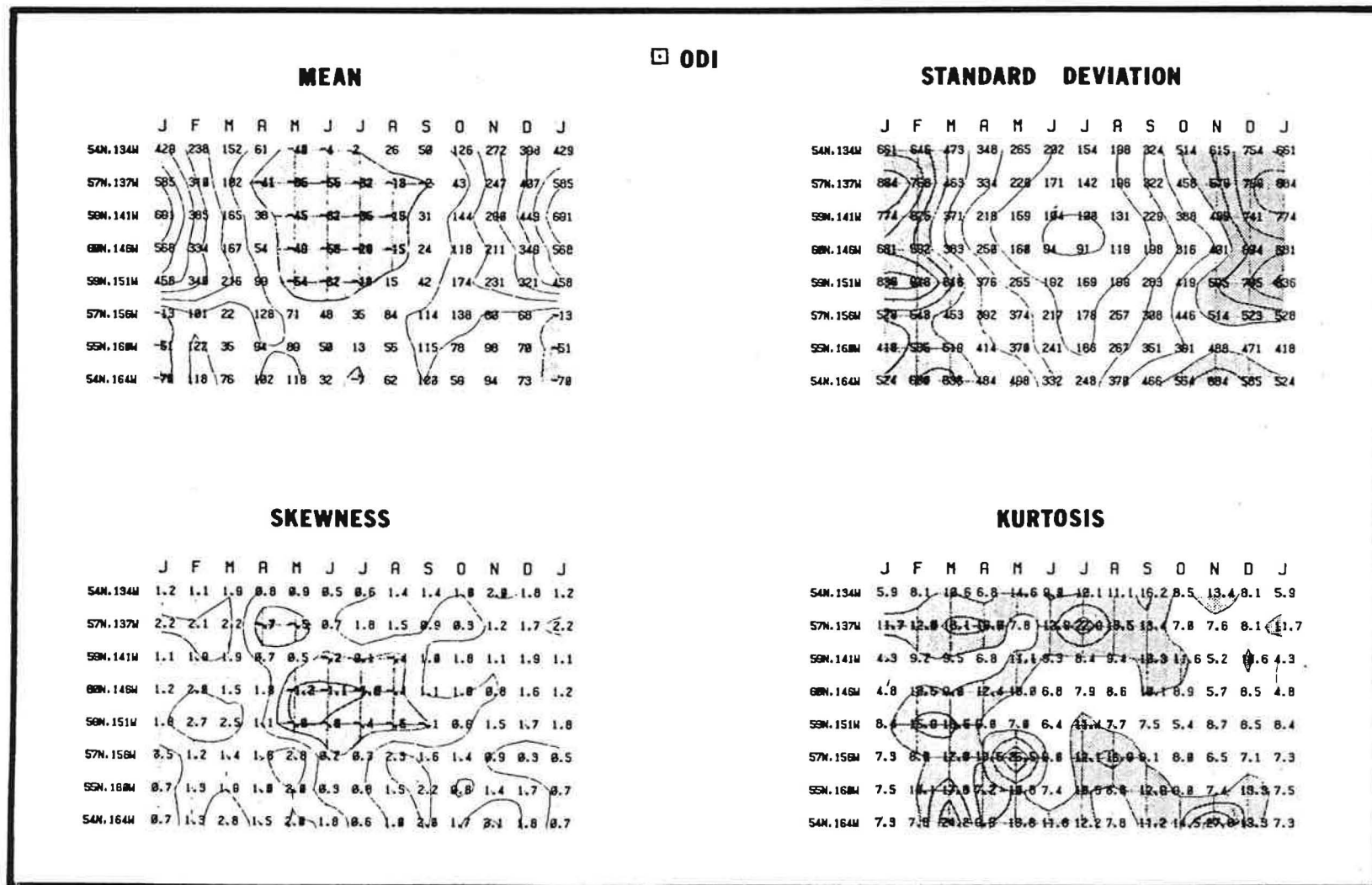


Figure 46 - Moments of the frequency distributions of offshore divergence indices (ODI) grouped by month at the near-coastal locations indicated by squares in Fig. 41. Mean: units are millimeters per day upward velocity through the bottom of the Ekman layer required to balance the indicated divergence; contour interval is 100. Standard deviation: units and contour interval is one normalized unit. Kurtosis: contour interval is 5 normalized units.

TABLE 2 - Monthly mean "types" of convergence-divergence couple, according to the classification of Figure 44, characterizing the near-coastal locations indicated by squares in Figure 41.

	Jan	Feb	Mar	Apr	May	Jun	Jul	Aug	Sep	Oct	Nov	Dec
54N, 164W	B	A	A	C	C	C	C	C	C	C	C	C
55N, 160W	B	A	A	C	A	C	C	C	C	C	C	A
57N, 156W	B	A	A	C	A	C	C	C	C	A	A	A
59N, 151W	A	A	A	A	B	D	D	C	A	A	A	A
60N, 146W	A	A	A	A	B	D	D	D	A	A	A	A
59N, 141W	A	A	A	A	B	D	D	B	A	A	A	A
57N, 137W	A	A	A	B	B	B	B	B	B	A	A	A
54N, 134W	A	A	A	A	B	B	A	A	A	A	A	A

coastal area of the lower Alaska Peninsula is, on average, under a type C situation over much of the year; considering this surface drift effect alone, the net tendency would seem to be to break down some of the baroclinicity built up in the type A situation further east.

The fraction of 6-hourly samplings during each month characterized by the various event types are summarized for several locations (Fig. 47). The seasonal shift from type A to type D at 59N, 141W is well illustrated. In this presentation, all periods, even where the index values were so small as to be negligibly different from zero, were included in calculating the percentages. When the weaker events are excluded the percentage of the dominant event type increases. By progressively increasing the required intensity the percentages of the less common types would eventually approach zero.

In order to perform spectral analysis on seasonal time series of substantial length, we have constructed composite winter and summer time series of the indices at each location. For example, winter time series were formed of all values within weeks of which the first day falls within the months of December, January, or February. Thus, the first week of December, 1974 follows directly after the last week in February, 1973. Summer series were similarly formed from values within weeks which begin in June, July, or August, etc. This procedure affects only the longer period spectral estimates which tend to be lost in the unresolvable seasonal and climatic scale energy. The results effectively summarize the features observed from analysis of the various short, properly continuous, seasonal segments of the time series.

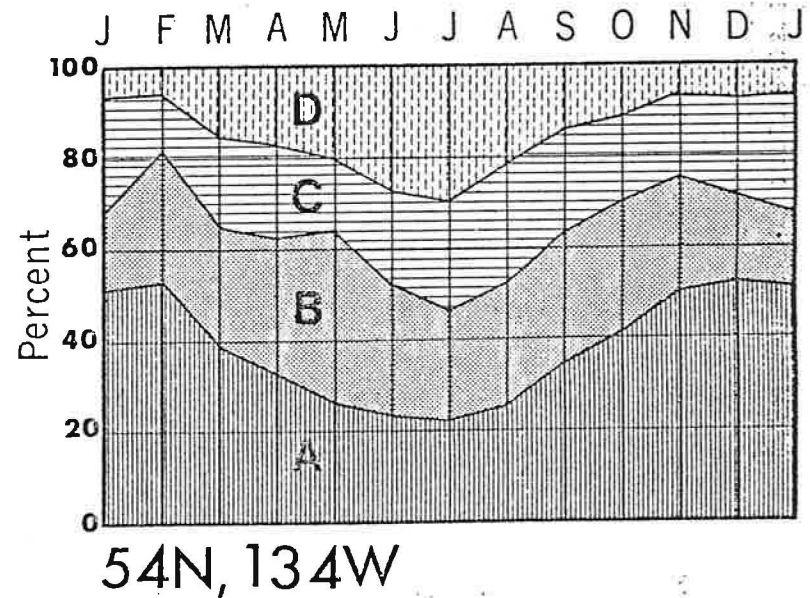
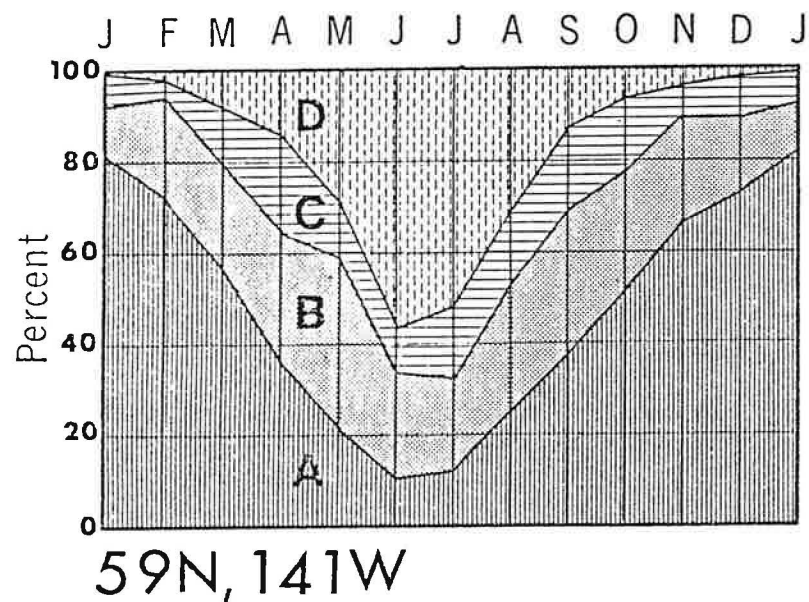
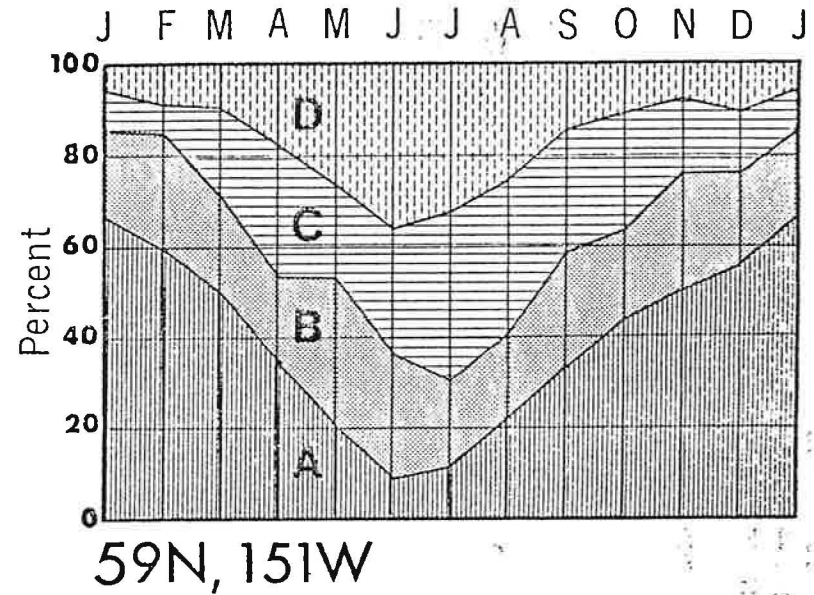
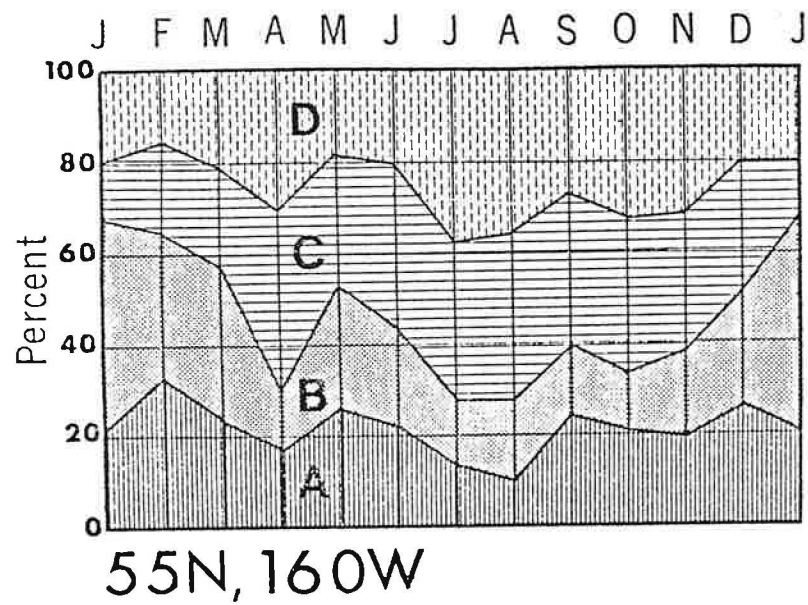


Figure 47 - Percentages, by month, of 6-hourly synoptic samplings characterized by each of the "event types" classified in Fig. 44.

Autocorrelation functions were computed from the CDI series (Fig. 48) and from the ODI series (Fig. 49). In all cases autocorrelation drops off rapidly within the first several days; time scales of individual events are characteristically short. A diurnal fluctuation, most marked in the CDI series, is apparent during summer (and less markedly in spring) at near-coastal locations in the northern and eastern Gulf. A somewhat lower frequency oscillation, indicating the "event" scale, is visible in many of the functions.

Examples of cross correlations between the CDI indices and ODI indices at the same location (Fig. 50) show that cross correlation tends to be negative for short lag periods, most markedly in the winter in the northeastern Gulf where the type A situation (negative CDI, positive ODI) predominates. Indications of negative cross correlations during summer in the same area are related to the predominance of Type D. Off the Alaska Peninsula cross correlation is low, indicating a rather complex mixture of event types and intensities.

Power spectra corresponding to the autocorrelation functions (see Figs. 48 and 49) have been constructed (Figs. 51 and 52) based on 100 lags of seasonal data series containing over 3000 data points each. This translates to about 66 degrees of freedom, representing considerable stability in the resulting spectral estimates. The spectra are similar in general form, resembling "red noise" spectra. Such spectra, which are characterized by a general decrease in energy from lower to higher frequencies, are indicative of temporal persistence within the series.

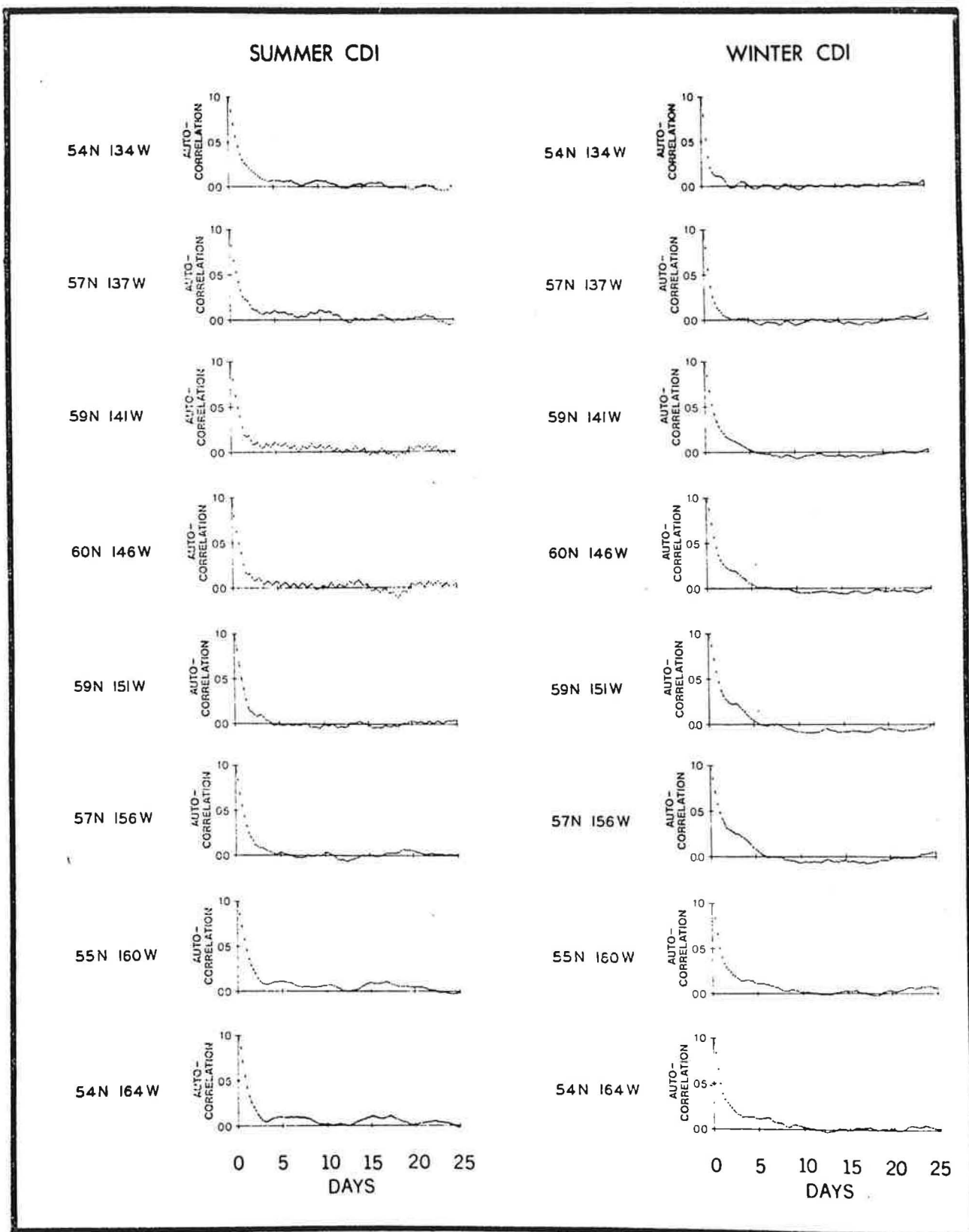


Figure 48 - Autocorrelation functions for coastal divergence indices (CDI) at the near-coastal locations.

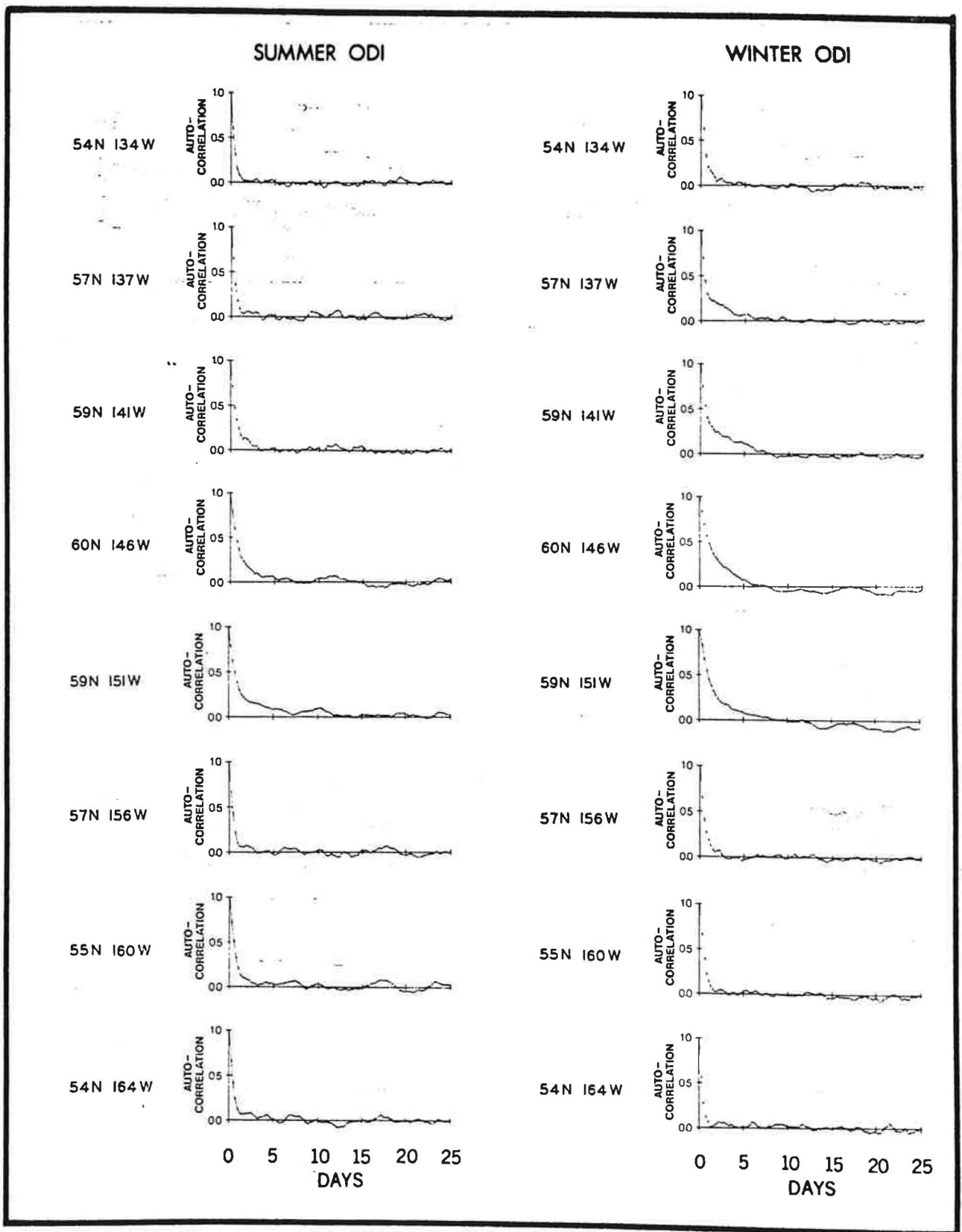


Figure 49 - Autocorrelation functions for offshore divergence indices (ODI) at the near-coastal locations.

CDI VS. ODI

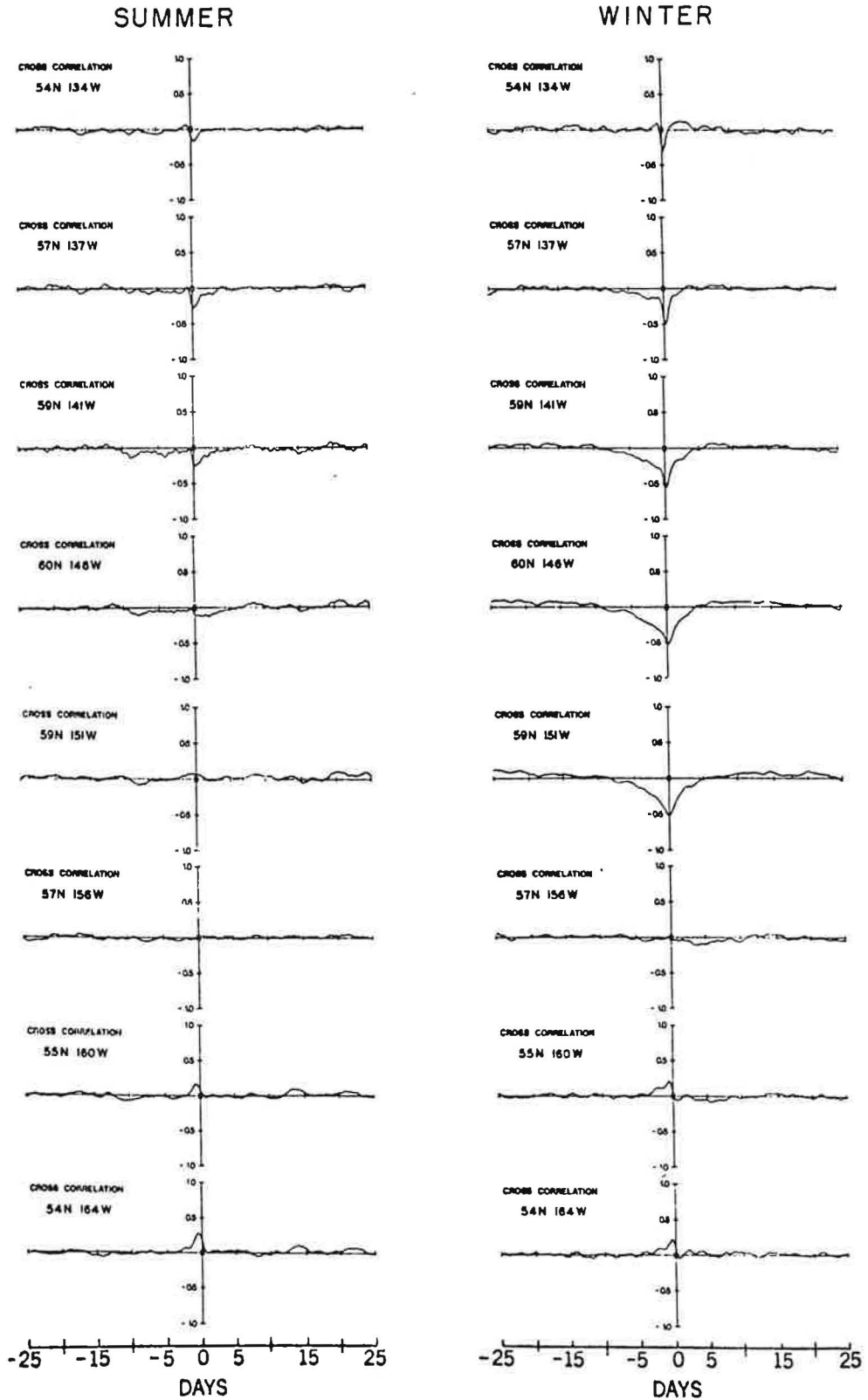


Figure 50 - Cross correlation functions for coastal divergence indices (CDI) v.s. offshore divergence indices at the near-coastal locations. Summer functions are on the left; winter functions on the right.

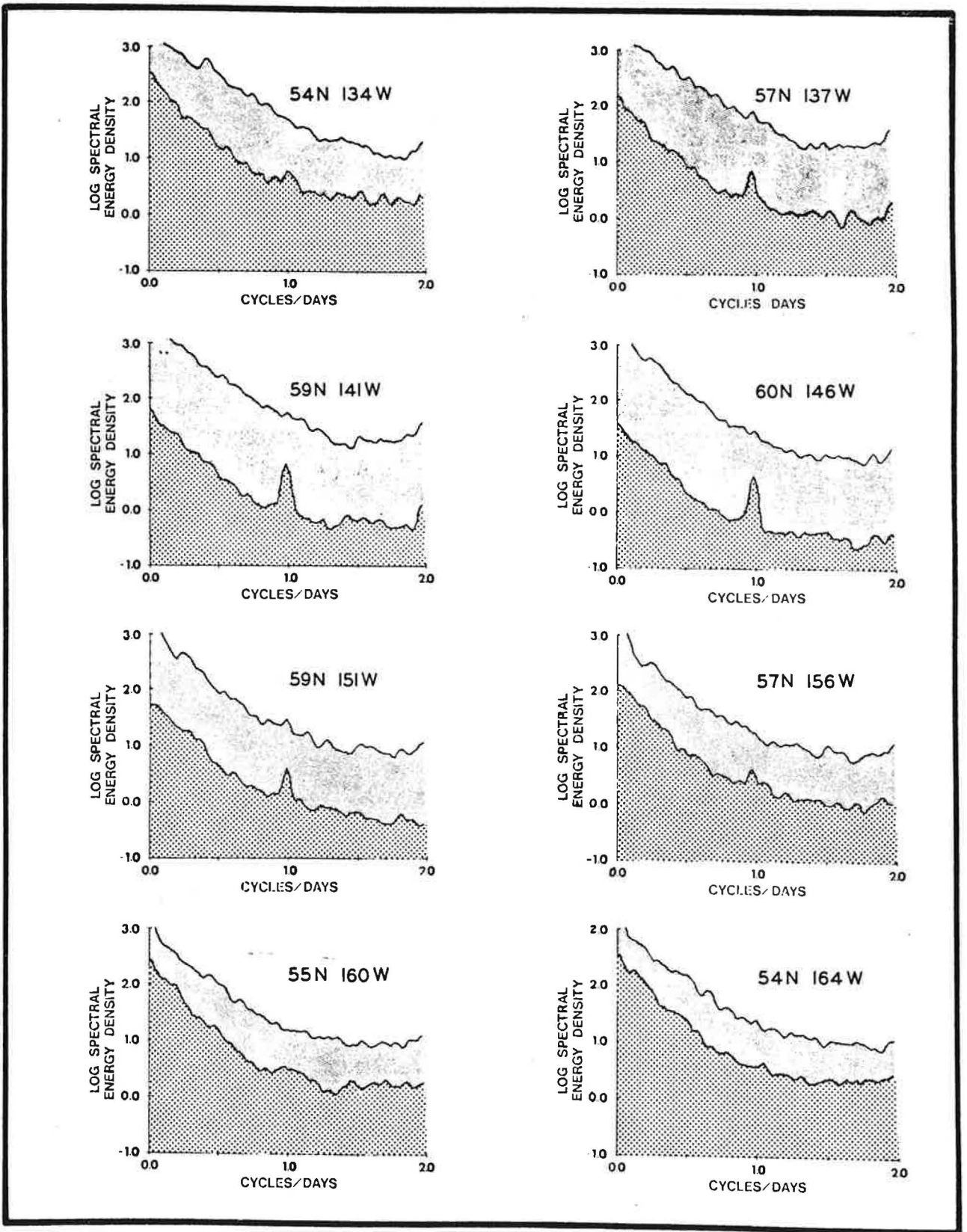


Figure 51 - Power spectra for coastal divergence indices (CDI). Winter and summer spectra at each location are superimposed. Higher energy (upper) trace plots the winter spectrum.

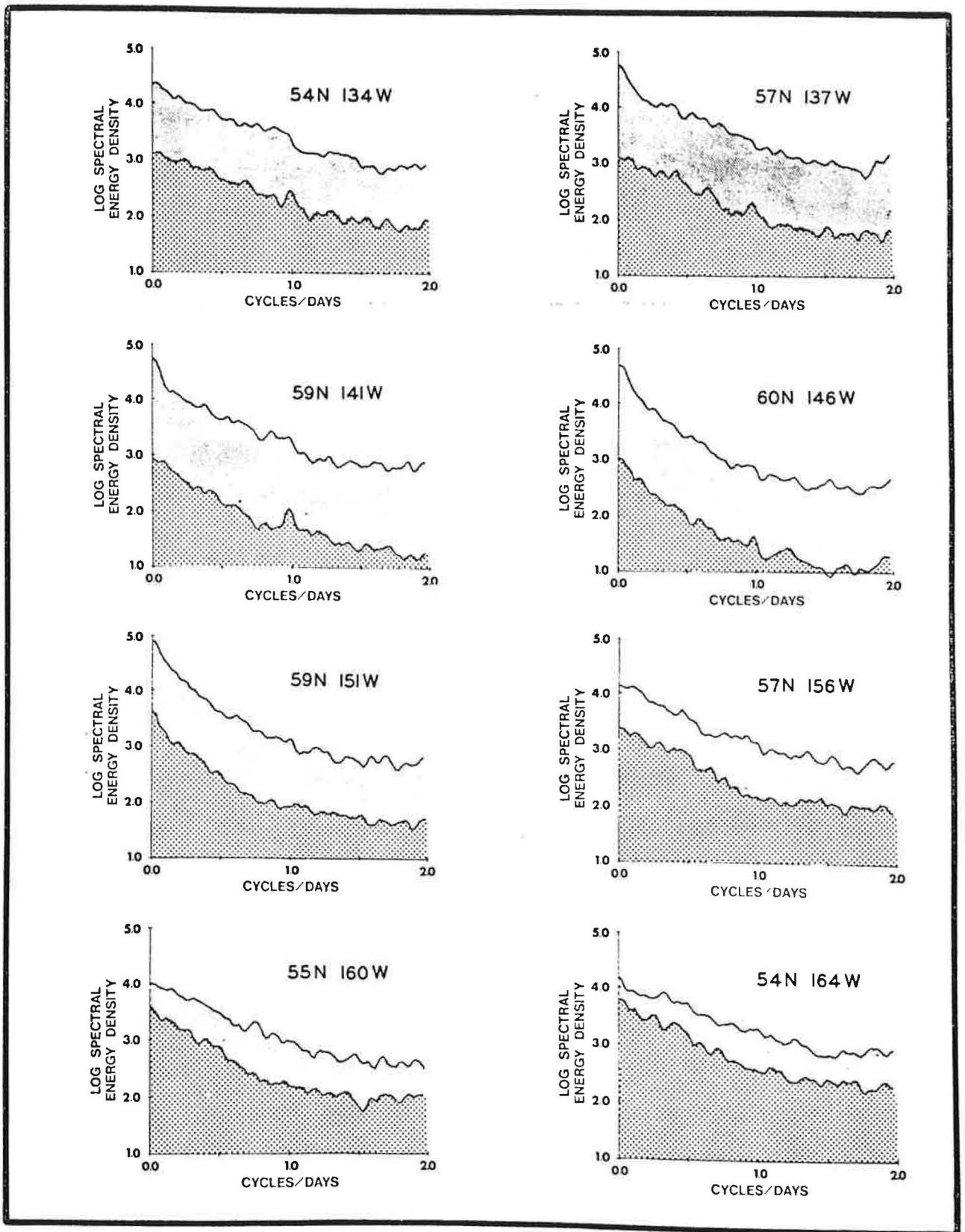


Figure 52 - Power spectra for offshore divergence indices (ODI) at near-coastal locations. Winter and summer spectra at each location are superimposed. Higher energy (upper) trace plots the winter spectrum.

Superimposed are several other features of interest. Considerable energy is spread over the "event scale" of periods of somewhat greater than a day to a week or more. In certain of the series this stands out as a broad hump representing a quasi-periodicity, that is a definite rhythm, albeit somewhat irregular. The only true periodicity is the diurnal fluctuation which stands out as a definite spike in the spring and summer spectra at locations in the northern and eastern gulf. The smaller spike at the semi-diurnal frequency appears merely because the diurnal variation is not perfectly sinusoidal, the morning to afternoon intensification being generally more rapid than the evening to morning relaxation.

Coherence functions for the CDI v.s. the ODI winter series (Fig. 53) indicate maximum coherence at the "event" and longer frequency bands in the "type A" area in the northern and eastern Gulf. Coherence is progressively less toward the southwest. During the summer coherence is minimal except at the diurnal frequency. In general, coherence between the CDI and ODI series at the same location is small compared to, for example, the coherence between series of the same type of index at adjacent locations (Fig. 54). The indication is that the CDI and ODI signals act as semi-independent variables, less so in the fairly well defined "type A" situation of cyclonic winter storms moving through the northern and eastern Gulf, and more so in the Alaska Peninsula area where the various combinations of angle of storm movement in relation to the coast, position of storm center north or south of the coastal boundary, etc., introduces a much larger degree of randomness.

60N 146W vs. 59N 141W

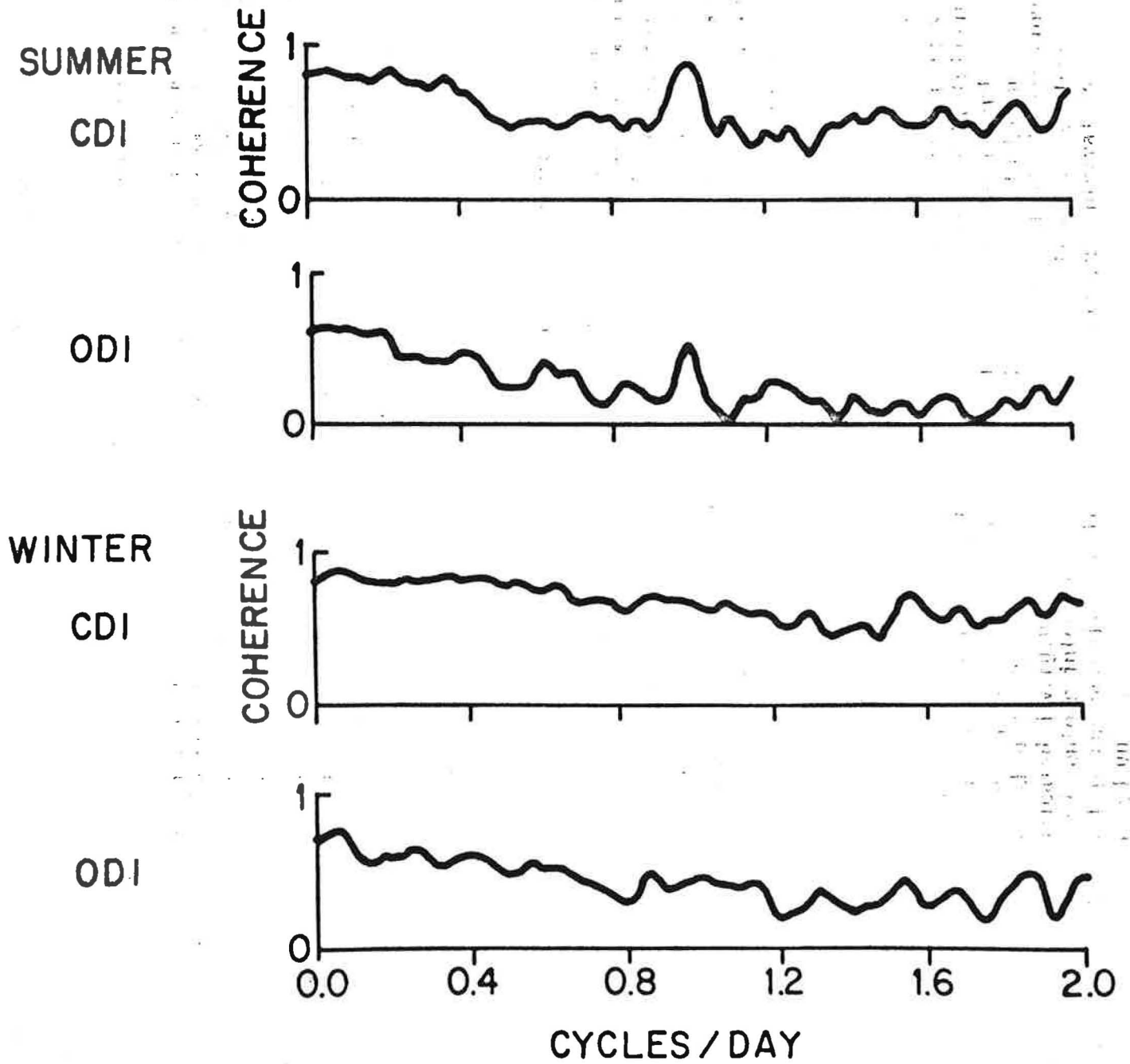


Figure 54 - Coherence functions between index series at adjacent locations: 60N, 146W v.s. 59N, 141W.

B. Interior of the Gulf

Away from the influence of the coastal boundary the CDI computations are, of course, not applicable; the distribution of surface divergence is indicated by the ODI series. The monthly frequency distributions of ODI series along 57°N (Fig. 55) and along 54°N (Fig. 56) show strongly positive mean ODI values during winter in the eastern portion of the gulf, reaching a maximum at 57N, 140W. This location thus appears as the point of maximum intensity of winter divergence. Intensity decreases from this location in all directions, but least rapidly to the north where the intersection of the lobe of intense divergence with the coast results in the maximum type A offshore divergence - coastal downwelling couple at 59N, 141W, described in the previous section. The mean intensities along 54N are much lower than at 57N.

The maximum mean negative values during the summer are likewise at 57N, 140W. The period of mean summer convergence (negative ODI values) which lasts from May through August along the coast in the northern and eastern Gulf (see Fig. 46) becomes progressively shorter westward along 57N, finally disappearing near 150W longitude. Along 57N mean convergence appears only during May and June at the near coastal location, 54N, 134W (Fig. 57).

The series at 57N, 140W also exhibits the greatest variance (see Fig. 56) during winter of any of the locations studied. Thus this location appears to mark a region of "maximum energy" in the surface divergence field of the Gulf of Alaska, both in the sense of amplitude of the seasonal mean signal and in the "spectral energy" sense of

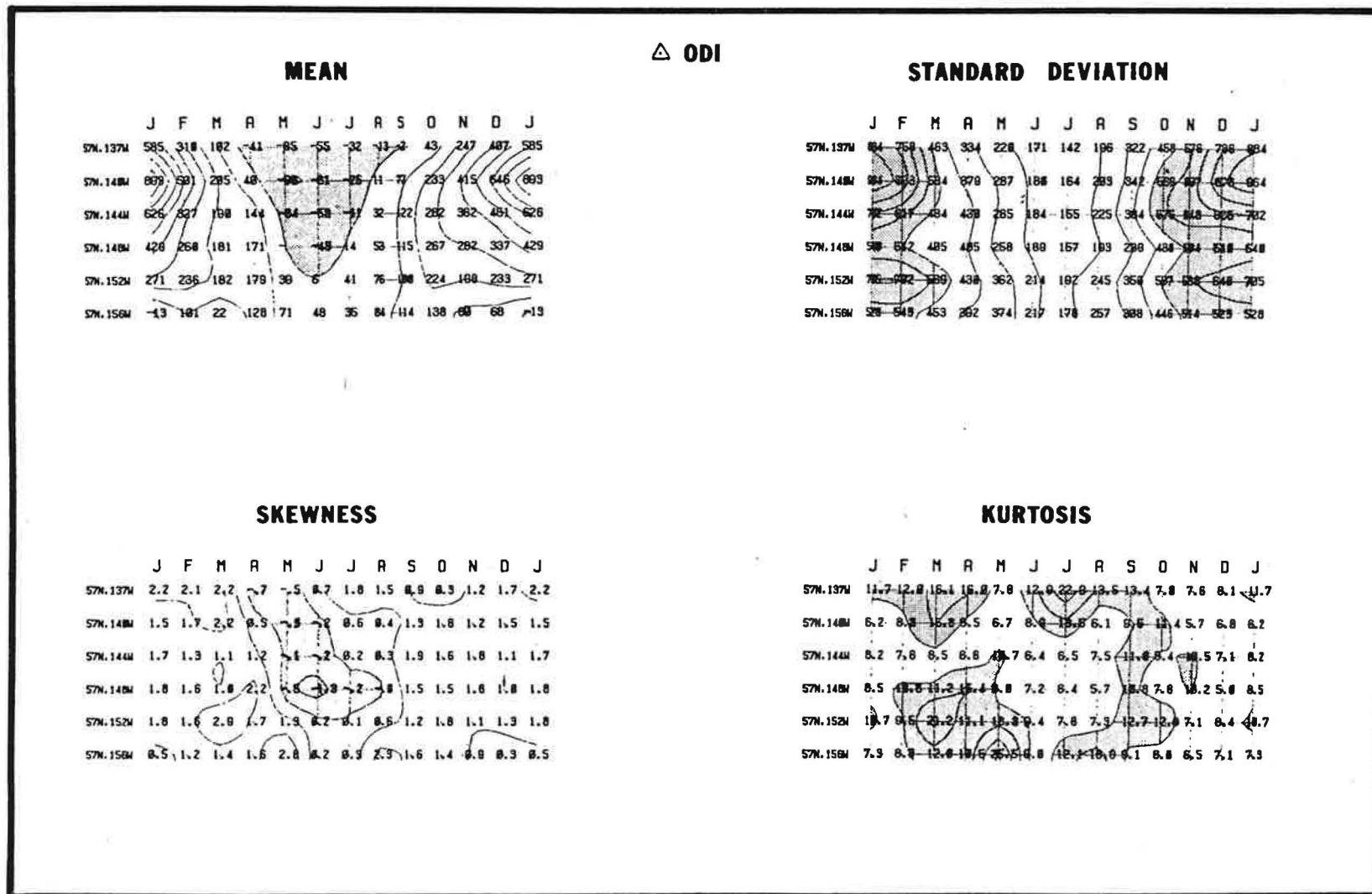


Figure 55 - Moments of the frequency distributions of offshore divergence indices (ODI) grouped by month at the locations along 57N indicated by triangle symbols in Fig. 41. Mean: units are millimeters per day upward velocity through the bottom of the Ekman layer required to balance the indicated divergence; contour interval is 100. Standard deviation: units and contour interval are as for the mean. Skewness: contour interval is one normalized unit. Kurtosis: contour interval is 5 normalized units.

⊙ ODI

MEAN

	J	F	M	A	M	J	J	A	S	O	N	D	J
54N.134M	429	238	152	81	48	4	2	26	58	126	272	368	429
54N.139M	248	188	115	88	4	14	17	38	32	120	210	247	249
54N.144M	157	165	126	206	129	65	62	102	117	227	221	281	157
54N.149M	65	189	88	165	181	63	61	97	113	204	171	124	65
54N.154M	12	128	36	132	131	88	51	66	84	139	65	81	12
54N.159M	48	21	8	87	66	57	18	58	109	78	65	78	43
54N.164M	78	118	76	182	118	32	4	62	108	58	94	73	78

STANDARD DEVIATION

	J	F	M	A	M	J	J	A	S	O	N	D	J
54N.134M	661	645	473	348	285	282	154	188	324	514	616	754	661
54N.139M	588	500	377	363	312	256	186	218	304	461	488	688	588
54N.144M	518	677	448	461	363	283	281	274	363	648	689	685	518
54N.149M	483	629	438	411	345	253	182	268	371	648	682	618	488
54N.154M	588	644	459	369	436	296	188	278	371	468	648	617	583
54N.159M	548	682	677	582	682	347	246	368	476	614	688	661	541
54N.164M	624	688	686	484	488	332	248	378	468	664	686	686	624

SKEWNESS

	J	F	M	A	M	J	J	A	S	O	N	D	J
54N.134M	1.2	1.1	1.8	0.8	0.8	0.5	0.6	1.4	1.4	1.8	2.8	1.8	1.2
54N.139M	2.6	2.8	1.4	1.1	0.7	2.9	2.6	2.1	1.8	1.8	1.4	1.2	2.6
54N.144M	1.6	1.6	2.1	1.5	1.1	1.8	1.6	1.2	2.7	2.2	2.9	1.1	1.5
54N.149M	0.8	1.3	1.8	2.8	1.4	0.8	1.3	1.6	2.2	2.4	2.8	1.8	0.8
54N.154M	0.6	1.3	1.6	1.1	2.1	0.8	0.8	0.8	1.5	1.6	1.2	0.7	0.6
54N.159M	0.6	0.8	0.6	0.5	1.8	0.2	0.2	1.4	2.8	0.5	0.9	0.8	0.6
54N.164M	0.7	1.3	2.8	1.5	2.8	1.8	0.6	1.8	2.8	1.7	0.1	1.8	0.7

KURTOSIS

	J	F	M	A	M	J	J	A	S	O	N	D	J
54N.134M	5.9	8.1	19.6	6.8	14.6	8.8	12.1	11.1	15.2	8.5	13.4	8.1	5.9
54N.139M	17.4	11.6	9.7	7.2	8.2	15.7	24.9	15.6	9.2	7.2	9.8	6.7	17.4
54N.144M	18.8	8.6	18.4	7.4	8.2	7.3	18.8	9.8	19.8	11.8	12.8	7.2	18.8
54N.149M	6.2	9.8	12.8	11.2	7.5	7.5	8.1	9.2	12.8	17.8	15.8	7.7	6.2
54N.154M	7.7	9.8	14.1	8.1	18.8	6.8	8.7	7.8	8.5	18.8	11.8	6.9	7.7
54N.159M	6.1	8.1	8.3	7.8	18.1	8.4	8.9	7.9	14.5	7.9	7.8	8.9	6.1
54N.164M	7.3	7.8	24.2	8.5	18.8	11.8	12.2	7.8	11.2	11.6	20.8	18.8	7.3

Figure 56 - Moments of the frequency distributions of offshore divergence indices (ODI) grouped by month at the locations along 54N indicated by circle symbols in Fig. 41. Mean: units are millimeters per day upward velocity through the bottom of the Ekman layer required to balance the indicated divergence; contour interval is 100. Standard deviation: units and contour interval are as for the mean. Skewness: contour interval is one normalized unit. Kurtosis: contour interval is 5 normalized units.

extremely rapid and strong pulsations. A lesser maxima in variance at 57N, 152W is apparently connected to the maxima along the coast at 59N, 151W (Fig. 46).

The skewness is negative along 54N latitude (Fig. 56) and, except for a limited period during the summer convergence season, along 57N latitude (see Fig. 55). Extreme events are usually divergent. The kurtosis as before, indicates major importance of rather infrequent, very intense events.

Power spectra for summer and winter ODI series at locations along 57N (Fig. 57) and at locations along 54N (Fig. 58) indicate that winter energy tends to be greatest to the north and east and summer energy is greatest to the south and west. The spike indicating the diurnal periodicity during summer is most prominent near the point of "maximum energy" at 57N, 140W. To the west and south the diurnal spike disappears.

Examples of cross correlations between the "maximum energy" locations at 57N, 140W and several surrounding locations (Fig. 59) indicate that correlation is highest at zero lag between 57N, 140W and the point of maximum winter "type A" coastal situation at 59N, 141W. A suggestion of higher correlation at positive lags between 57N, 140W and 57N, 137W and at negative lags between 57N, 140W and 57N, 144W illustrates the general eastward progression of the signal. Correlation with a location to the south, 54N, 139W, is considerably lower and is highest at a negative lag of one 6-hour period, even though the southern location is one degree further east. This indicates the northward progression of the signal which added to the eastward progression matches the general northeastward trend of the storm tracks. Correlation with the point at

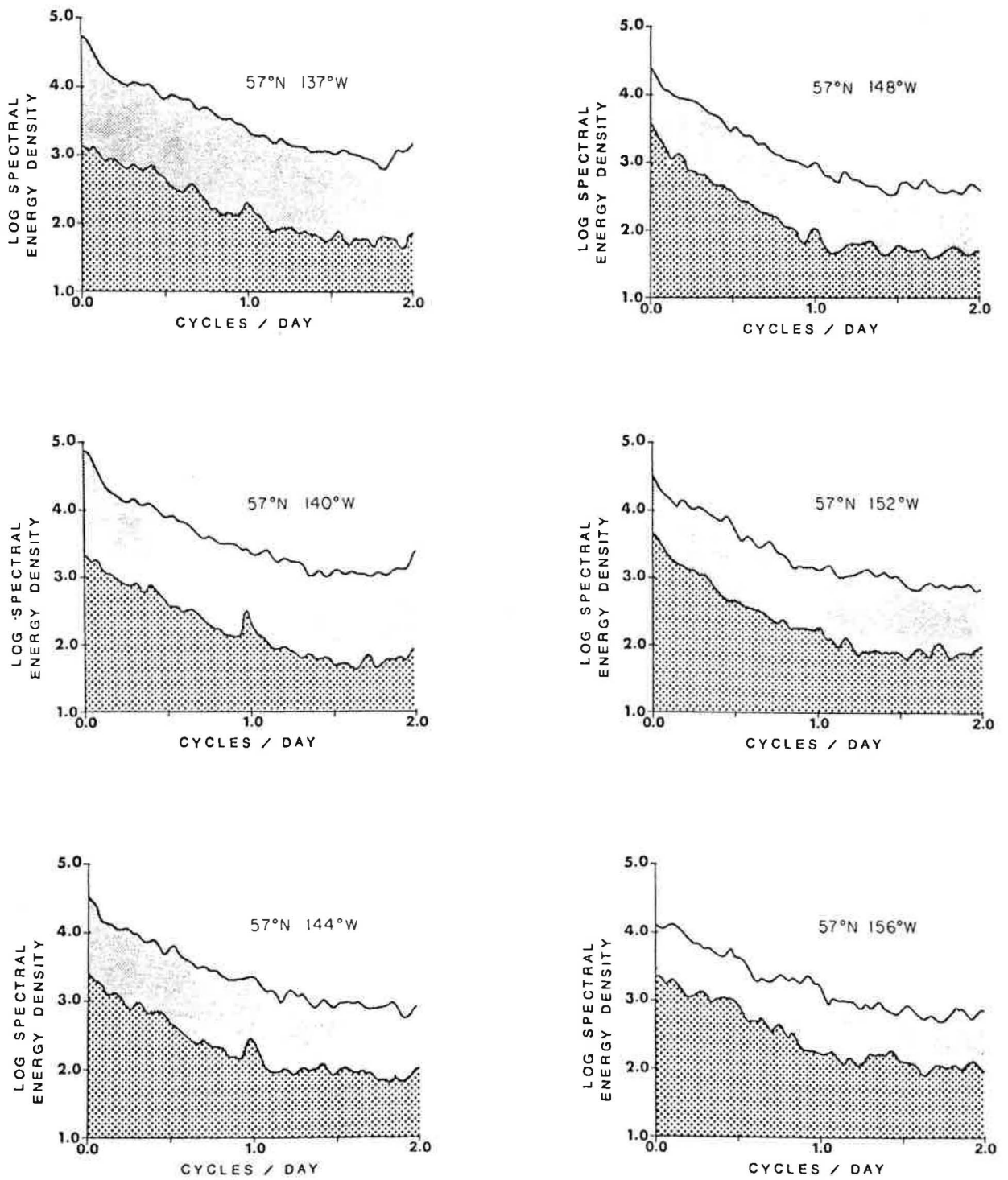


Figure 57 - Power spectra for offshore divergence indices (ODI) at locations along 57N latitude (locations indicated by squares in Fig. 41.) Winter and summer spectra at each location are superimposed. Higher energy (upper) trace plots the winter spectrum.

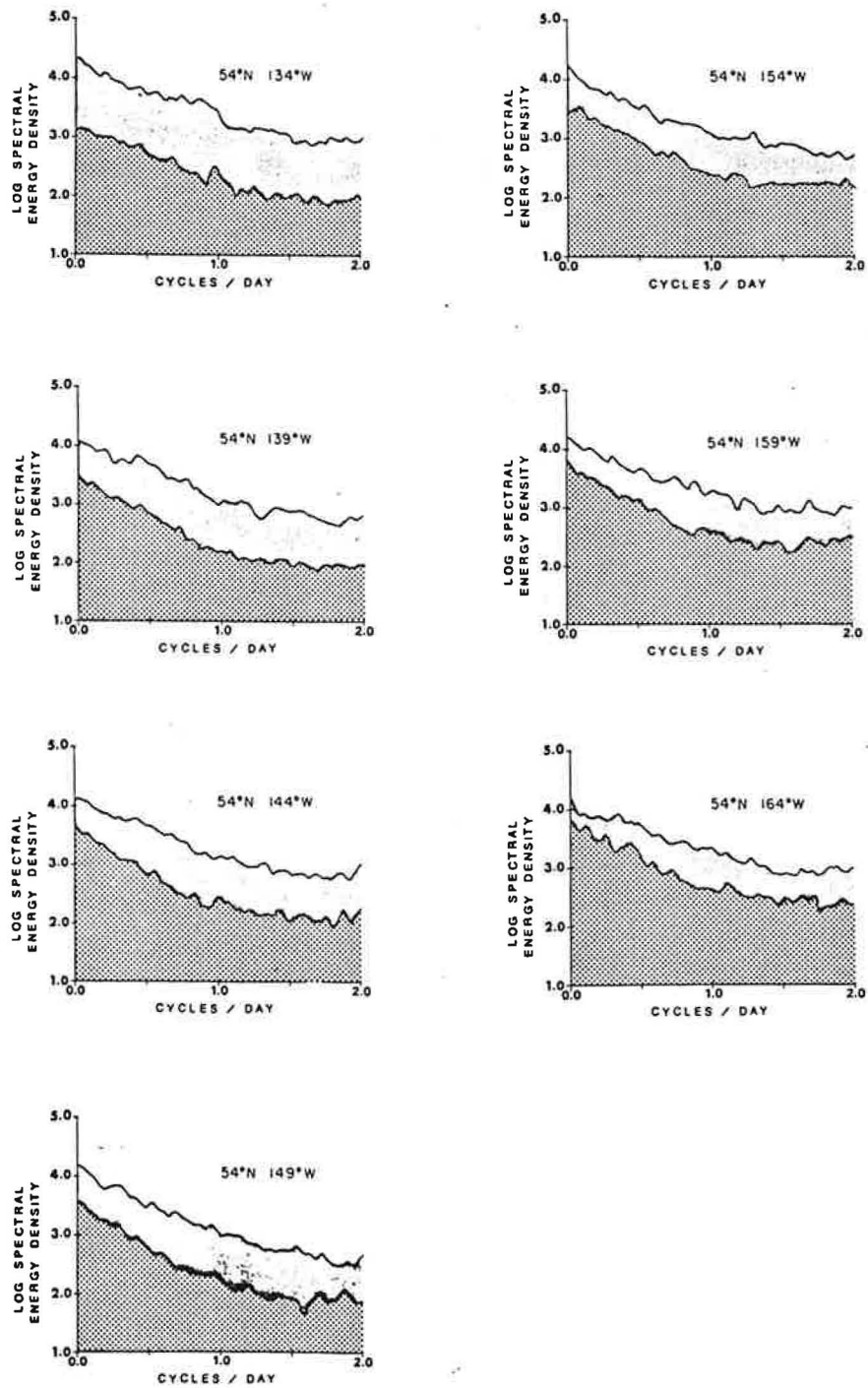


Figure 58 - Power spectra for offshore divergence indices (ODI) at locations along 54N latitude (locations indicated by circles in Fig. 41.) Winter and summer spectra at each location are superimposed. Higher energy (upper) trace plots the winter spectrum.

CROSS CORRELATION

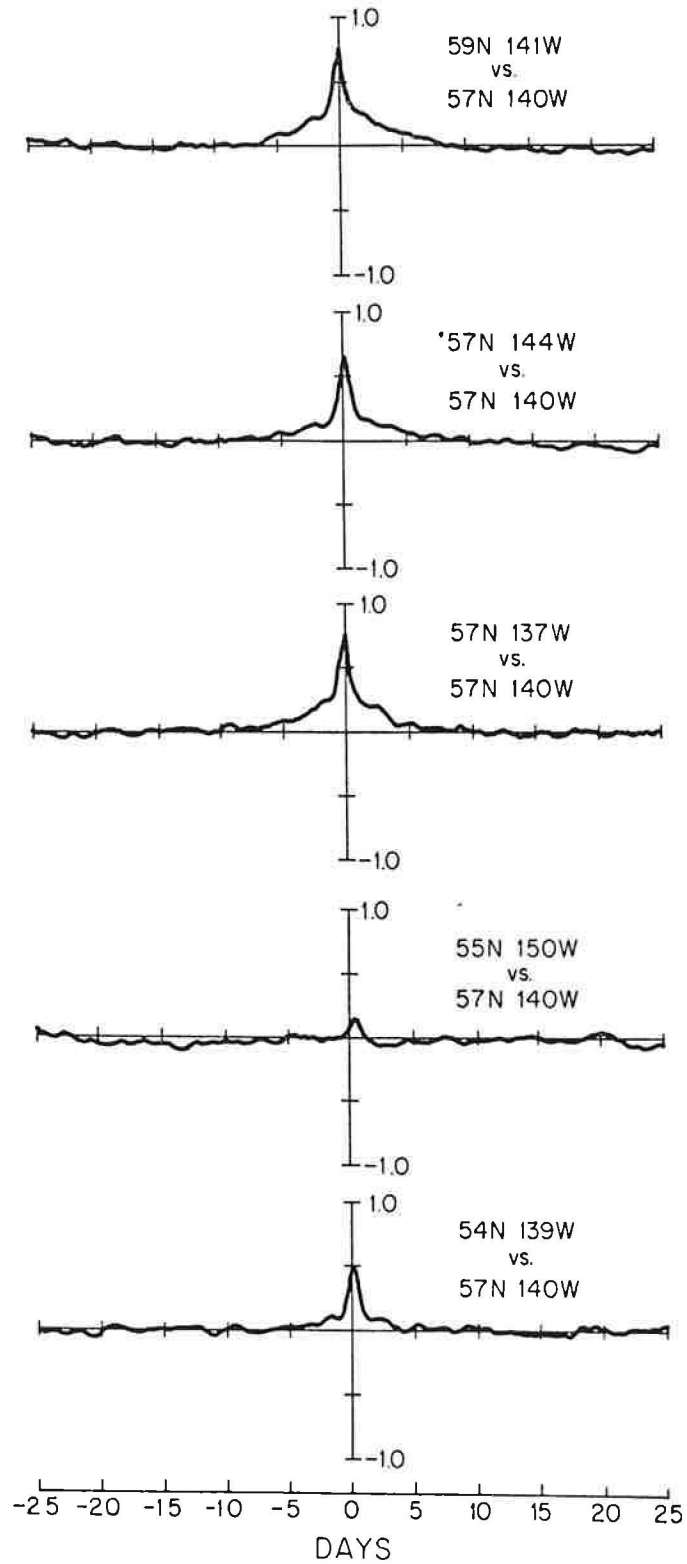


Figure 59 - Cross correlation functions for the winter ODI series at 57N, 140W v.s. winter ODI series at several surrounding locations.

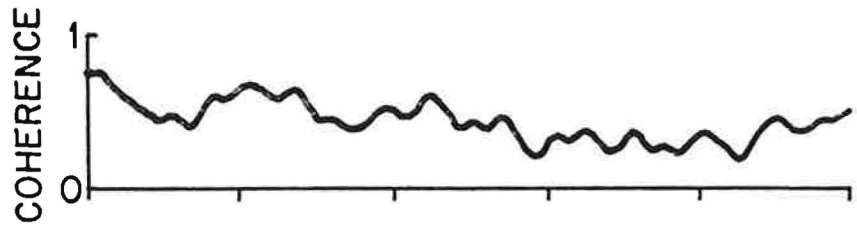
55N, 150W is quite low, reaching its greatest value at negative lags of two 6-hour periods in the winter and three six hour periods in the summer; the progression is slower in the summer than in the winter.

Coherence functions corresponding to the cross-correlation functions of Fig. 59 indicate that the signal at 59N, 141W appears strongly related to that at 57N, 140W (Fig. 60). The adjacent points along 57N are likewise quite strongly related, particularly in the "event" frequency range. However, the coherence with the location to the south, 54N, 139W, is considerably less. Coherence with the signal at 55N, 150W, although on the line of general storm progression, is so low that it is not possible to prove statistically the signals are even related. This indicates considerable modification of the storm systems as they move across the gulf, consistent with its description as a region of strong atmospheric cyclogenesis.

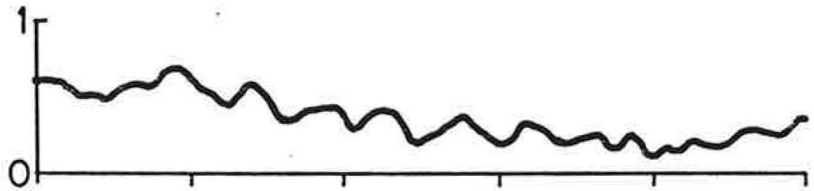
C. Conditions - 1973, 1974 and 1975

The monthly mean CDI and ODI values at the near-coastal locations and the monthly mean ODI values at locations along 57N for the individual years 1973, 1974, and 1975 (Fig. 61) show distributions which are rather complicated in detail. However, it may be useful to delineate certain major features which may have had important effects on the ocean environment during these most recent years of increased field studies. In early 1973, maximum magnitudes of both the ODI and CDI indices appeared during January at 57N, 151W; apparently, the maximum strength of the winter "type A" couple was located in the northwestern Gulf, rather than in its "usual" position in the northeastern Gulf as indicated by the

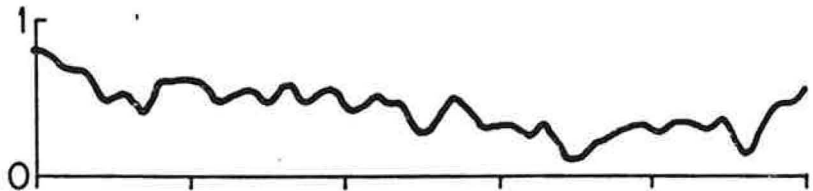
59N 141W
vs.
57N 140W



57N 144W
vs.
57N 140W



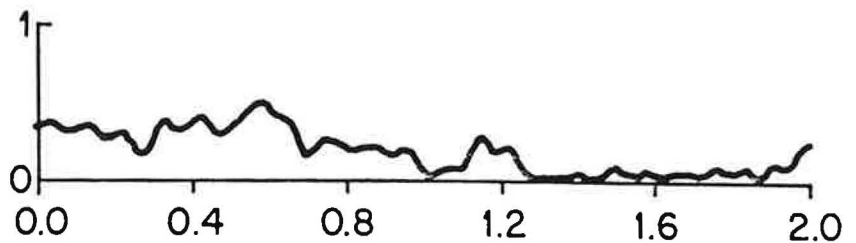
57N 137W
vs.
57N 140W



55N 150W
vs.
57N 140W



54N 139W
vs.
57N 140W



CYCLES/DAY

Figure 60 - Coherence functions for the winter ODI series at 57N, 140W v.s. winter ODI series at several surrounding locations.

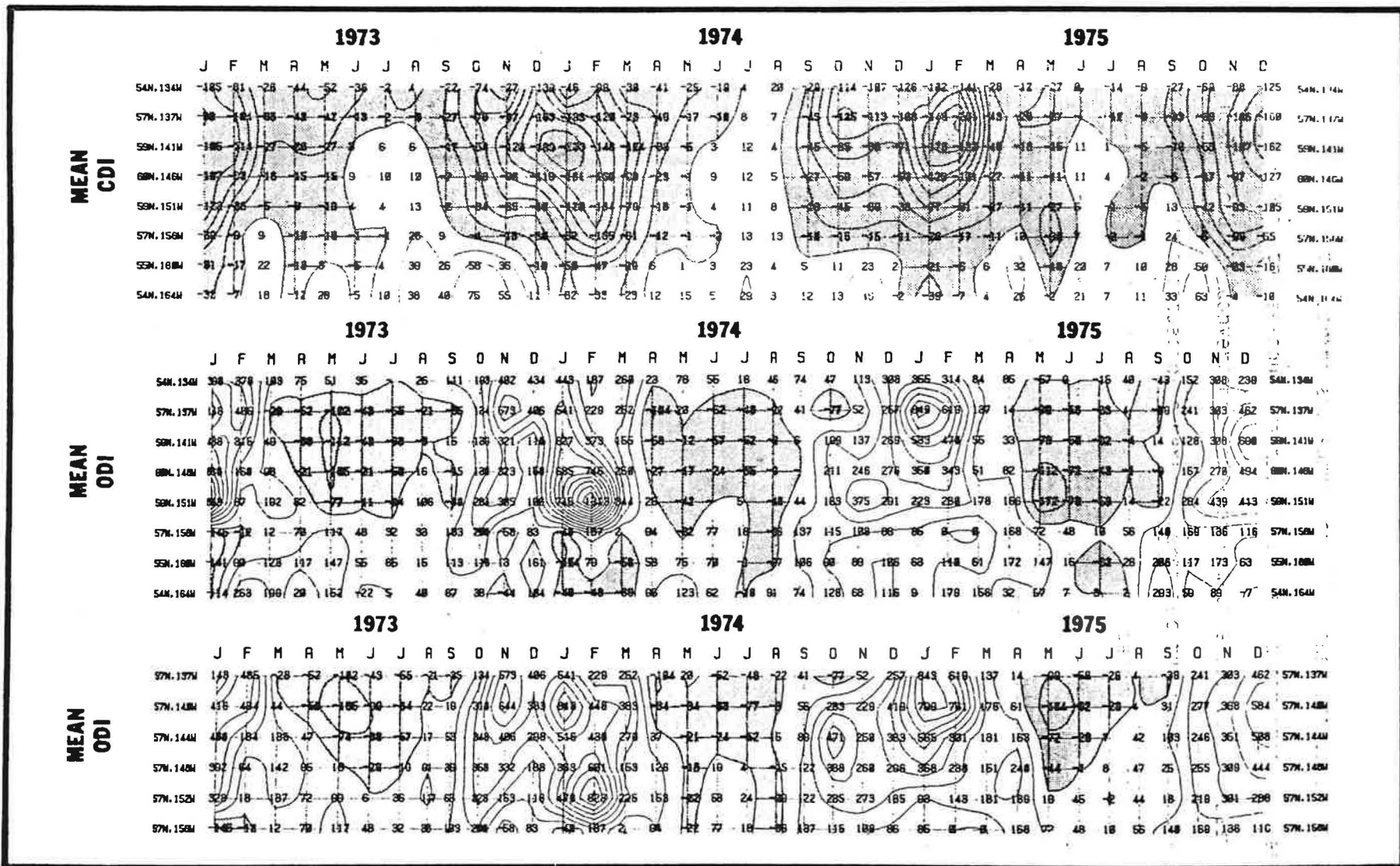


Figure 61 - Monthly means of index series for the years 1973, 1974, and 1975. Top figure: CDI series at near-coastal locations; units are cubic meters per second transported off each 100-meter width of coast. Middle figure: ODI series at near coastal locations; units are millimeters per day upward velocity through the bottom of the Ekman layer required to balance the indicated divergence. Bottom figure: ODI series at locations along 57N latitude; units, etc., are same as for middle figure.

nine-year composite mean monthly distributions (see Figs. 45 and 46). Lower than normal magnitudes of both types of indices during February and March throughout the northern Gulf point to an unusually rapid relaxation of the winter situation. For example, an early transition to a "type C" couple is indicated off the Alaskan Peninsula during March, where normally the transition occurs in April (Table 2). The trend toward less positive than normal ODI values in the northern Gulf continued through the spring to considerably stronger than normal negative values in May, representing quite energetic downward pumping in the offshore area, particularly in the northeastern Gulf. The last quarter of 1973 featured a strong predominance of coastal upwelling along the outer Alaskan Peninsula.

During the first quarter of 1974, stronger than normal convergence (negative CDI values) is indicated along the coast of the Gulf of Alaska, except in the extreme east. Maximum offshore divergence (positive ODI values) appeared, as in the previous year, in the northwestern Gulf. An extremely large mean ODI value was computed for February at 59N, 151W. Actually, anomalously large values appeared during all of the first three months of 1974 at both 59N, 151W, and 60N, 146W. The values at 59N, 141W, the normal maximum along the coast, although much smaller than those further east, were near the 9-year mean values for that location. The result is an extremely strong "type A" couple for the northern Gulf during early 1974. The implication is that dramatically increased baroclinicity in the ocean structure may have had an important effect on the dynamics of the area for some period to follow.

During the spring and summer of 1974, the indices tended to have values near the seasonal means, but by fall a situation of weaker than normal coastal convergence (smaller negative CDI values) seems to have set in. This situation generally persisted through the whole winter over much of the Gulf and was coupled with generally weaker than normal divergence offshore during December and January. An exception was the eastern Gulf where a reasonably strong "type A" couple is indicated for January and February. In total, the winter of 1974-75 appears to have been one of less energetic "type A" pumping than seems to be normal. Certainly the situation contrasts highly with the very energetic situation of the previous winter.

VII. SUMMARY AND CONCLUSIONS

Our knowledge of the physical oceanography of the Gulf of Alaska is quite inadequate to forecast flow. This stems largely from the lack of a persistent, challenging oceanographic program that permits progressive advances based on acquired knowledge. The focus of attention has been not only limited, but intermittent, however, this has not been due to a lack of interest on the part of the oceanographer, rather because of lack of funds, equipment, and adequate theory. Thus, a normal advance from the descriptive phases of presenting observed and steady-state conditions to the analytical phases of understanding processes and forecasting various time-dependent phenomena has not taken place.

There have been several periods of rather extensive research activity: in the late 19th century by the U.S. Bureau of Fisheries, the late 1920's and early 1930's by the International Fish Commission, the mid 1950's to the early 1970's by the International North Pacific Fisheries Commission, and in recent years by the Institute of Marine Science of the University of Alaska.^{6/} The interval between periods of activity has gradually decreased from about 50 years to the order of 5 years or less, and hopefully the instigation of the OCSEAP studies will result in the continuing research effort required to obtain adequate knowledge concerning flow.

The dominant physical phenomena in the Gulf of Alaska is the Aleutian low pressure system whose center moves anti-cyclonically out of the northern Bering Sea in early autumn, crosses the Alaska Peninsula and attains a mean position of about 55°N, 155°W in the gulf in late fall and early winter. During winter it moves southwestward to about

^{6/} See Rosenberg (1972).

50°N, 175°E before returning northward into the western Bering Sea in late winter and early spring. The cyclogenesis and cold air advection in the gulf associated with the mean position of the low pressure center in fall and winter determines the extent and intensity of winter overturn and vertical divergence, as well as, the containment of precipitation, in the form of ice and snow along the coast and in the snowshed ringing the gulf which determines to a great extent the amount of dilution in coastal waters in spring and summer. Station data are marginally adequate in period 1955-62 to show considerable differences between the upper layer temperature distributions in 1956 and 1958, and between the surface salinity distributions in 1957 and 1958, but these are certainly not extreme conditions. Approximate ranges for temperatures in coastal waters are $-1.8 - 18^{\circ}\text{C}$, and in the central part of the gulf, $1 - 14^{\circ}\text{C}$; approximate ranges of salinity in coastal waters are several parts per thousand to 32.6 ‰ and in the central part of the gulf, $32.2 - 33.0 \text{ ‰}$. At depth, below the effects of seasonal influences, conditions are somewhat in a steady-state condition, this makes it difficult to trace anomalous intrusions, or percentage of flow attributed to various sources without extensive data, but there is evidence in the temperature fields that significant changes can occur over periods of several years and certainly longer trends must also exist. Temperature data in the gulf are considered too fragmentary to show the rather consistent 2-3 year variations of $\pm 1-2^{\circ}\text{C}$ detected in the central and western parts of the Pacific Ocean by Favorite and McLain (1973).

In regard to surface flow, drift bottle studies have shown that the source of surface flow into the gulf is not from the Kuroshio but largely from the Oyashio and its extension the Subarctic Current, and there is a well documented coastal flow northward along the west coasts of the United States and Canada that also extends into the gulf. Studies have shown that the nature of the separation of the Subarctic Current off the coast is quite variable and complex and, thus, the effect of the northern branch of this flow, which penetrates into the gulf, is equally variable and complex. There is an indisputable onshore component of surface flow around the gulf. But it is not known whether the drifting objects are transported around the gulf largely seaward of the continental shelf and only when they are carried out of the oceanic flow and over the shelf are they trapped in a coastal regime and carried directly ashore, or whether, in spite of tidal currents and increased frictional effects, there is continuity in northward flow in offshore and onshore areas that results in a gradual dispersal of floating objects on the coast as the flow sweeps around the gulf. Nevertheless, it is apparent that floating objects released over the continental shelf at the eastern part of the gulf drift into coastal embayments such as Prince William Sound and Cook Inlet, and move southwestward on either side of Kodiak Island. Further, there is evidence that floating objects in the northern part of the gulf have a potential for wide dispersal: northward into Bering Sea, westward out along the Aleutian Islands, eastward in the Subarctic Current to the coast of Southeastern Alaska, the west

coasts of British Columbia, Washington, Oregon and California, and westward again to the central Pacific Islands and the Asian coast.

Geostrophic currents are somewhat of a dilemma. First, closely spaced data suggest that the broad sweep of cyclonic flow around the gulf, generally shown in atlases or summaries of widely spaced data, is actually a highly turbulent regime composed of eddies of various dimensions. There is a frequent suggestion of a large perturbation at the eastern side of the gulf whose dimensions and configuration do not suggest a shelf wave phenomenon, but rather the possibility that at times some of the northward flow funneling into the eastern side of the gulf is unable to move westward across the head of the gulf and is found to turn back on itself. Second, although geostrophic currents clearly reflect the area of divergence, the Ridge Domain, a dominant oceanographic feature in the gulf, there are no direct measurements that permit ascertaining to what extent this feature is governed by (1) Ekman transport (2) a normal internal readjustment of mass between two opposing flows, and (3) a vertical movement of northward flowing deep water, caused by the effect of the land barrier imposed by the gulf. Third, the high velocity cyclonic flow at the edge of the continental shelf is also a dominant feature and an inshore countercurrent is usually detected in geostrophic computations. At this time it is not clear whether this is an aspirative phenomenon not uncommon under such circumstances, whether it is merely an error caused by inadequacies in this method in the presence of physical boundaries, or whether it is largely the effect of eddies or shelf waves along the edge of the

continental shelf. Finally, there is the large variability in transport computed from the sporadic cruise data in one instance (1960) a 50% increase in mean flow, and a 100% increase over low flows, but there is no consistent evidence of winter intensification in flow expected as a result of increased wind-stress during that period. However, increases in sea levels at coastal stations in winter suggest that there is at least a barotropic response. Thus, it would appear that winter intensification of flow does occur but the pulses of winter wind-stress are of too short a duration for the distribution of mass to adjust to the actual flow regime; however, over decades and centuries the calculated geostrophic regime appears to have adjusted to an integrated, quasi-steady state between the effects of winter intensification and summer relaxation. Thus, there may be an inherent under-estimation of actual flow in summer when using the wind-stress transport method. The long data record of sea level pressures provides a qualitative indication of transport variability. Spectral energy densities indicate a dominant annual period and a suggestion of an approximate 3-year period. The latter is evident primarily in the decade 1950-59 and does not appear to be a dependable forecasting index. Although monthly transports occasionally show totally unrealistic values, quarterly means and 12-month running means indicate a relatively ordered system (within limits) with no apparent indices to forecast anomalous events.

Of course, wind-stress estimates are merely that, estimates, and so are the outputs of model studies whose results are largely

dependent on wind-stress inputs. It should also be obvious that fluctuations in conditions in the gulf are also influenced by various external and internal forces throughout the Pacific Ocean. Nevertheless, considerable advances in our knowledge of the physical oceanography of the gulf will come from short-period monitoring of actual conditions and extensive direct current measurements, not only across the shelf, but also across the slope and in the Ridge Domain. OCSEAP studies are beginning to provide such data.

Studies of surface divergence indices show the extreme variability in direction and intensity of wind-stress in time and space around the gulf, as well as insight into mechanisms that essentially pump water in contact with the shelf shoreward in summer and seaward in winter. The eastern side of the gulf has been shown to be the most energetic in regard to these processes and considerable variability is apparent. An attractive feature of the ODI and CDI computations is their basis in data fields that are routinely prepared and made available in real-time by meteorological agencies; in fact the fields are forecast over periods up to 72 hours or more. Thus, there is a potential for a very inexpensive, real-time monitoring of conditions affecting the flow field in the gulf. Hopefully the OCSEAP studies now underway will help to establish the quantitative linkages required to translate such information into a practical tool for marine environmental management.

VIII. ACKNOWLEDGMENTS

We thank J. H. Johnson (PEG) and J. R. Hastings (NWFC) for assistance, comments and suggestions.

LITERATURE CITED

- Bakun, Andrew
1973. Coastal upwelling indices, west coast of North America. U.S. Dep. Commer. Natl. Oceanic Atmos. Admin., Tech. Rep. NMFS SSRF-671. 103 p.
- Bakun, Andrew
1975. Daily and weekly upwelling indices, west coast of North America, 1967-73. U.S. Dep. Commer., Natl. Oceanic Atmos. Admin., Tech. Rep. NMFS SSRF-693. 114 p.
- Barkley, Richard A.
1968. Oceanographic atlas of the Pacific Ocean. Univ. Hawaii Press, Honolulu. 20 p., 156 figs.
- Bennett, E. B.
1959. Some oceanographic features of the northeast Pacific Ocean during August 1955. J. Fish. Res. Bd. Canada 16(5):565-633.
- Bogdanov, K.
1961. (Water circulation in the Gulf of Alaska and its seasonal variability). Okeanologiya 1(5):815-824. In Russian. (Transl. in Deep-Sea Res., 1963, 10(4):479-487.)
- Burt, Wayne V., and Bruce Wyatt.
1964. Drift bottle observations of the Davidson current off Oregon, p. 156-165. In: Kozo Yoshida (ed.), Studies on oceanography. Univ. Tokyo Press.
- Dall, W. H.
1879. Meteorology, Appendix 1. In: Pacific Coast Pilot, coasts and island of Alaska, 2nd ser. 375 p. Gov. Print. Off., Washington, D.C.
- Dall, W. H.
1882. Report on the currents and temperatures of Bering Sea and the adjacent waters. U.S. Coast and Geodetic Survey, Report 1880, app. 16:297-340, pl. 80.
- Dall, W. H.
1899. The mollusk fauna of the Pribilof Islands. In: U.S. Treasury Dept. Committee on Fur-seal Invest., The fur seals and sea-islands of the North Pacific Ocean, pt. 3, p. 539-545, chart. Washington, Govt. Print. Off.
- Dodimead, A. J., F. Favorite, and T. Hirano
1963. Salmon of the North Pacific Ocean--Part II. Review of oceanography of the Subarctic Pacific Region. Int. North Pac. Fish. Comm., Bull. 13. 195 p.

- Dodimead, A. J., and H. J. Hollister.
 1962. Canadian drift bottle releases in the North Pacific Ocean. Fish. Res. Board Can., Manuscr. Rep. Ser. (Oceanogr. Limnol.) 141. 64 p. + 44 figs. (Processed.)
- Doe, L. A. E.
 1955. Offshore waters of the Canadian Pacific coast. J. Fish. Res. Board Can. 12(1):1-34.
- Favorite, Felix.
 1964. Drift bottle experiments in the northern North Pacific Ocean, 1962-1964. J. Oceanogr. Soc. Japan 20(4):160-167.
- Favorite, Felix.
 1974. On flow into Bering Sea through Aleutian Islands passes p. 3-37. In: D. W. Hood and E. J. Kelley (eds.), Oceanography of the Bering Sea. Inst. Mar. Sci. Occas. Publ. No. 2, Univ. Alaska, Fairbanks.
- Favorite, Felix.
 1975. The physical environment of biological systems in the Gulf of Alaska. Proceedings, Arctic Institute of North America symposium on science and natural resources in the Gulf of Alaska. Oct. 16-17, 1975, Anchorage (In Press).
- Favorite, F., A. J. Dodimead, and K. Nasu.
 1976. Oceanography of the Subarctic Pacific Region 1960-72. Int. North Pac. Fish. Comm., Bull. 33 (In Press).
- Favorite, F., and W. J. Ingraham, Jr.
 (1976a). On flow in the northwestern Gulf of Alaska May 1972. J. Oceanogr. Soc. Japan.
- Favorite, F., and W. J. Ingraham, Jr.
 (1976b). Sunspot activity and oceanic conditions in the northeastern North Pacific Ocean. NMFS Status of the Environment Report, 1975 (in preparation).
- Favorite, Felix, and Douglas R. McLain.
 1973. Coherence in transpacific movements of positive and negative anomalies of sea surface temperature, 1953-60. Nature (London) 244(5412): 139-143.
- Filatova, Z. A. (ed.).
 1973. Kompleksnye issledovaniya materikovogo sklona v raione zaliva Alyaska (multidisciplinary investigations of the continental slope in the Gulf of Alaska area). IV. Inst. Okeanol. 91. 260 p. (Transl., Fish. Res. Board Can., 1974, Transl. Ser. 3204.)
- Fisk, Donald M.
 1971. Recoveries from 1964 through 1968 of drift bottles released from a merchant vessel, S. S. Java Mail, en route Seattle to Yokohama, October 1964. Pac. Sci. 25(2):171-177

- Fofonoff, N. P.
1962. Machine computations of mass transport in the North Pacific Ocean. J. Fish. Res. Board Can. 19(6): 1121-1141.
- Fofonoff, N. P., and S. Tabata.
1966. Variability of oceanographic conditions between Ocean Station "P" and Swiftsure Bank off the Pacific coast of Canada. J. Fish. Res. Board Can. 23(6): 825-868.
- Fleming, R. H.
1955. Review of oceanography of the northern Pacific. Int. North Pac. Fish. Comm., Bull. 2. 43 p.
- Fomin, L. M.
1964. The dynamic method in oceanography. Elsevier Publ. Co., New York. 212 p.
- Galt, J. A.
1973. A numerical investigation of Arctic Ocean dynamics. J. Phys. Oceanog. 3(4): 379-396.
- Giovando, L. F., and Margaret K. Robinson.
1965. Characteristics of the surface layer in the northeast Pacific Ocean. Fish. Res. Board Can., Manuscr. Rep. Ser. (Oceanogr. Limnol.) 205. 13 p., 2 tables, 28 figs.
- Holl, M. M. and B. R. Mendenhall.
1972. Fields by information blending, sea-level pressure version. (U.S.) Fleet Numer. Weather Central, Monterey, Calif., FNWC Tech. Note 72-2. 66 p.
- Ingraham, W. James, Jr., and F. Favorite.
1968. The Alaskan Stream south of Adak Island. Deep-Sea Res. 15(4): 493-496.
- Ingraham, W. James, Jr., and James R. Hastings.
1974. Seabed drifters used to study bottom currents off Kodiak Island. Mar. Fish. Rev. 36(8): 39-41.
- Jacobs, Woodrow C.
1939. Sea level departures on the California coast as related to the dynamics of the atmosphere over the North Pacific Ocean. J. Mar. Res. 2: 181-193.
- Jacobs, Woodrow C.
1951. The energy exchange between sea and atmosphere and some of its consequences. Bull. Scripps Inst. Oceanogr. 6: 27-122.
- Klein, W. H.
1957. Principal tracks and mean frequencies of cyclones and anti-cyclones in the northern hemisphere. U.S. Dep. Commer., Weather Bur. Res. Paper 40. 60 p.

- LaViolette, Paul E., and Sandra E. Seim.
1969. Monthly charts mean minimum and maximum sea surface temperature of the North Pacific Ocean. (U.S.) Naval Oceanogr. Office, Spec. Publ. 123. 58 p.
- McEwen, George F., Thomas G. Thompson, and Richard Van Cleve.
1930. Hydrographic sections and calculated currents in the Gulf of Alaska, 1927 to 1928. Rep. Int. Fish. Comm. 4. 36 p.
- Moiseev, P. A. (ed.)
1963-1970. Sovetskie rybokhozyaistvennye issledovaniya v severo-vostochnoi chasti Tikhogo okeana (Soviet fisheries investigations in the Northeastern Pacific). In 5 parts. Pt. 1 - Tr. Vses. Nauchno-issled. Inst. Morsk. Rybn. Khoz. Okeanogr. (VNIRO) 48 (also Isv. Tikhookean. Nauchnoissled. Inst. Morsk. Rybn. Khoz. Okeanogr. (TINRO) 50), 1963, 316 p.; Pt. 2 - Tr. VNIRO 49 (Izv. TINRO 51), 1964, 272 p.; Pt. 3-Tr. VNIRO 53 (Izv. TINRO 52), 1964, 341 p.; Pt. 4-Tr. VNIRO 58 (Izv. TINRO 53), 1965, 345 p.; Pt. 5-Tr. VNIRO 70 (Izv. TINRO 72), 1970, 454 p. (Complete transl. of all 5 parts avail. Natl. Tech. Inf. Serv., Springfield, Va.--Pt. 1, 1968, 333 p., TT 67-51203; Pt. 2, 1968, 289 p., TT 67-51204; Pt. 3, 1968, 338 p., TT 67-51205; Pt. 4, 1968, 375 p., TT 67-51206; Pt. 5, 1972, 462 p., TT 71-50127.)
- Muench, Robin D. and C. Michael Schmidt.
1975. Variations in the hydrographic structure of Prince William Sound. Inst. Mar. Sci. Rep. R75-1. Univ. Alaska, Anchorage. 135 p.
- Muromtsev, A. M.
1958. Osnovnye cherty gidrologii Tikhogo okeana (Principal hydrological features of the Pacific Ocean). Gidrometerol. Izd., Leningrad. 631 p.; App. 2, Atlas of vertical profiles and maps indicating temperature, salinity, density and oxygen content. 124 p. (Transl. 1963, Natl. Tech. Inf. Serv., Springfield, Va., TT 63-11065.)
- Nelson, C. S.
1974. Wind stress climatology off the west coast of North America (abst) (0-2). AGU Fall Annu. Meet. EOS, Trans. Am. Geophys. Union 56(12): 1132.
- Pattullo, June G.
1960. Seasonal variation in sea level in the Pacific Ocean during the International Geophysical Year, 1957-1958. J. Mar. Res. 18: 168-184.
- Pattullo, June, Walter Munk, Roger Revelle and Elizabeth Strong.
1955. The seasonal oscillation in sea level. J. Mar. Res. 14: 88-156.

- Plakhotnik, A. F.
 1962. *Gidrologiya severo-vostochnoi chasti Tikhogo Okeana (obzor literaturnykh istochnikov)*. (Hydrology of the northeastern Pacific Ocean - review of literature sources). *Tr. Vses. Nauch.-issled. Inst. Morsk. Rybn. Khoz. Okeanogr.* 46: 190-201.
- Reid, J. L., and A. W. Mantyla.
 1976. On the seasonal variation of sea elevations along the coast of the northern North Pacific Ocean. *AGU Fall Annu. Meet., Trans. Am. Geophys. Union* 56(12): 1009.
- Reid, Joseph L., Jr., Gunnar I. Roden, and John G. Wyllie.
 1958. Studies of the California Current system. *Prog. Rep. Calif. Coop. Oceanic Fish. Invest.*, 1 July 1956 - 1 Jan. 1958: 28-56.
- Robinson, Margaret K.
 1957. Sea temperature in the Gulf of Alaska and in the northeast Pacific Ocean, 1941-1952. *Bull. Scripps Inst. Oceanogr.* 7(1): 1-98, 61 figs.
- Robinson, Margaret K., and Roger A. Bauer.
 1971. Atlas of monthly mean surface and subsurface temperature and depth of the top of the thermocline, North Pacific Ocean. (U.S.) Fleet Numer. Weather Central, Monterey, Calif. 24 p. + 72 figs. (Processed.)
- Roden, Gunnar I.
 1960. On the nonseasonal variations in sea level along west coast of North America. *J. Geophys. Res.* 65: 2809-2826.
- Roden, Gunnar I.
 1969. Winter circulation in the Gulf of Alaska. *J. Geophys. Res.* 74(18): 4523-4534.
- Rosenberg, Donald H. (ed.)
 1972. A review of the oceanography and renewable resources of the northern Gulf of Alaska. Univ. Alaska, Fairbanks, Inst. Mar. Sci., IMS Rep. R72-23. 690 p.
- Saur, J. F. T.
 1962. The variability of monthly mean sea level at six stations in the eastern North Pacific Ocean. *J. Geophys. Res.* 67: 2781-2790.
- Schulz, Bruno.
 1911. Die stromungen und die temperaturverhaltnisse des Stillen Ozeans nordlich von 40° N-Br. einschliesslich des Bering-meeres. *Ann. Hydrogr. Marit. Meteorol.* 39: 177-190, 242-264.
- Sverdrup, H. U.
 1947. Wind-driven currents in a baroclinic ocean; with applications to the equatorial currents of the Eastern Pacific. *Proc. Natl. Acad. Sci.* 33: 318-326.

- Sverdrup, H. U., M. S. Johnson, and R. H. Fleming.
 1942. The oceans: their physics, chemistry and general biology. Prentice-Hall, Inc., New York. 1087 p.
- Tabata, Susumu.
 1965. Variability of oceanographic conditions at Ocean Station "P" in the northeast Pacific Ocean. Trans. Royal Soc. Can. 3, Ser. 4, Sect. 3: 367-418.
- Thompson, Thomas G., George F. McEwen, and Richard Van Cleve.
 1936. Hydrographic sections and calculated currents in the Gulf of Alaska 1929. Rep. Int. Fish. Comm. 10. 32 p.
- Thompson, William F., and Richard Van Cleve.
 1936. Life history of the Pacific halibut. (2) Distribution and early life history. Rep. Int. Fish. Comm. 9. 184 p.
- Thomson, Richard E.
 1972. On the Alaskan Stream. J. Phys. Oceanogr. 2(4): 363-371.
- Tully, J. P., and F. G. Barber.
 1960. An estuarine analogy in the subarctic Pacific Ocean. J. Fish. Res. Board Can. 17(1): 91-112.
- Welander, Pierre.
 1959. On the vertically integrated mass transport in the oceans. P. 95-101. In: B. Bolin (ed.), The atmosphere and the sea in motion. Rockefeller Inst. Press in association with Oxford Univ. Press, New York.
- Wild, John James.
 1877. Thalassa, an essay on the depth, temperature, and currents of the ocean. Marcus Ward & Co., London. 140 p.
- Wyrтки, Klaus.
 1964. Total integrated mass transports and actual circulation in the eastern South Pacific Ocean, p. 47-52. In: K. Yoshida (ed.), Studies on oceanography. Univ. Wash., Seattle.